TESIS DE LA UNIVERSIDAD DE ZARAGOZA

2016

96

Emanuele Cozzo

Multiplex Networks Structure and Dynamics

Departamento
Física Teórica

Director/es
Moreno Vega, Yamir

ISSN 2254-7606

Prensas de la Universidad
Universidad Zaragoza

ISSN 2254-7606

Universidad Zaragoza
1542

Tesis Doctoral

MULTIPLEX NETWORKS STRUCTURE AND DYNAMICS

Autor

Emanuele Cozzo

Director/es

Moreno Vega, Yamir

UNIVERSIDAD DE ZARAGOZA

Física Teórica

2016

Multiplex Networks
Structure and Dynamics

Emanuele Cozzo
Departamento de Física Teórica
Universidad de Zaragoza

Tesis Doctoral
Director
Yamir Moreno

2015

Contents

List of Figures

Introduction

The complex networks view of complex system

In the beginning were networks, and networks were everywhere
The concept of network served for a long time as a metaphor supporting a *structural approach*, i.e., an approach that puts the accent on the relations among the constituents of a given system, in a wide range of scientific fields, from biology to sociology, and spanning organizational levels from sub-cellular organization to social organization. In all those fields we can observe a shift from the use of the concept of network as a metaphor to a more substantial notion [99, 50, 19], which has led to what is now known as complex networks science.

The science of complex networks provides an interdisciplinary point of view for the study of complex systems, as it constitutes a unifying language that permits to abstract from the specific details of a system to focus on its structure of interactions. The result of this operation of abstraction is a graph model of the system. On its turn, a graph is a specific mathematical object, and a plethora of mathematical tools has been developed to deal with it. Admittedly, the real power of representing a complex system through a graph lies in the hypothesis that the structure and function of the system under study are intimately related to one another. Paraphrasing Wellman [99]: *It is a comprehensive paradigmatic way of taking structure seriously by studying directly how patterns of ties determine the functioning of a system.*

Now, we understand a *complex network* as a system whose patterns of interactions can not be described by a random graph model with a Poissonian distribution of the connections. From the point of view of a physicist, complex networks are systems that display a strong disorder with large fluctuations of the structural characteristics. As such, the tools developed in condensed matter theory and in statistical physics revealed to be well suited to study the architecture of complex networks [30]. While

statistical physics provides complex networks science with a set of tools, graph theory stands at its basis providing a formal language. The first step in complex network research is to represent the structure of the system under study as a graph, followed by an analysis of the topological features of the obtained representation through a set of informative measurements. This first step can be understood as the *formal representation* of the system, while the second one can be seen as the *topological characterization* of the system's structure [23].

Both the peculiar nature of complex networks as topological structures (in comparison, for example, with a lattice) and the particular nature of the system under study push the need for the definition of structural metrics. The *degree distribution* is the most simple example of a structural metric needed for a gross characterization of the inhomogeneity of a networked system. The degree of a node in a network is the number of connections it has to other nodes and the degree distribution is the probability distribution of these degrees over the whole network. While it is really uninformative in a homogeneous system (a lattice, a random regular network or a poisson random graph), it gives a basic understanding of the degree of the disorder in the case of complex networks. So much so, that the discovery that many networked system has power law degree distributions set the start of the current interest in complex networks science.

On the other hand, the needs of each particular field of research serve as a guide for the definition of particular structural metrics that quantify some relational concepts developed in that field. This is the case of the plethora of centrality measures defined to capture the relation of power in social network analysis [33]. The topological characterization of a complex network also implicitly allows for classifications, either of the constituents of the system, or when comparing different systems. However, *understanding* the structure of a complex network means, roughly speaking, to comprenhend what is informative, and what is the result of chance (or of structural constrains). Therefore, a third step in complex network investigation is its statistical characterization, that is, the quantification of the statistical significance of network properties and their dependencies. Crucial in this step is the generation of appropriate null models since once a structural property is recognized as statistically significant, a mechanism for the emergence of such a property could be proposed and further investigated [69].

Finally, the core hypothesis that the structure and the function are intimately related to one another returns. The forth step is then the functional characterization. The study of the relations between the structure and the dynamics (as a proxy of the function). From a physicist point of view, the interest is in studying the critical properties of dynamical processes defined on complex networks, as models of real process and emergent functions. The crucial point is that many of the peculiar critical effects showed by processes defined on complex networks are closely related and universal for different models, basically reinforcing the hypothesis of the relation between the structure and the function, together with the "statistical physical" approach [30]. On the other hand, when a particular system is under study, this part of the investigation deals with the task of finding the structural properties that may explain the observed phenomena.

In summary, schematically, an investigation in complex networks science goes trough the following cycle

Step 1: formal representation

Step 2: topological characterization

Step 3: statistical characterization

Step 4: functional characterization.

Interestingly enough, one can also link the historical development of complex networks science according to those 4 schematic step, being the formalization at its origin, the topological and statistical characterization of empirical systems its phase of statement, and the functional characterization its current mature stage as a science.

From simple networks to multiplex networks

The concept of multiplex networks may be anchored in communication media or in the multiplicity of roles and milieux. When focusing on the former aspect, one realizes that the constituents of a complex system continuously switch among a variety of media to make the system perform properly. On the other hand, focusing on the latter, one takes into account the fact that interactions are always context dependent as well as integrated through different contexts.

The term *multiplexity* was coined in early 1962 in the social anthropology framework by Max Gluckman (in [36]) to denote "the coexistence of different normative elements in a social relationship", i.e., the co-existence of distinct roles in a social relationship. While this first definition focus on context and roles, Kapferer offered a second definition based on the overlap of different activities and/or exchanges in relationships, focusing on the social relationship as a medium for the exchanges of different types of information [45]. The duality between media and roles in founding the multiplexity of social relations is still present in the contemporary debate, with authors such as David Bolter and Richard Gusin [9] advocating the former, and others like Lee Rainie and Barry Wellman the latter [77]. However, whether defined by roles or media, multiplexity always refers to "multiple bases for interaction" in a network [93].

It is indubitable that new push for the formal and quantitative research in multiplex networks comes from the social and technological revolution brought by the Internet and mobile connections. Chats, on-line social networks, and a plethora of other human-to-human machine mediated channels of communications, together with the possibility of being always on-line (hyperconnectivity [98]), have accelerated the proliferation of layers that makes "the sociality". Although it has a longer history in the field of social sciences, the concept of multiplexity, and consequently of multiplex networks, is not restricted to them. For example, it is gaining an important role in contemporary Biology, where we can observe the same shift from its use as a metaphor to a more substantial notion of the concept of multiplex networks. In particular, it is associated to the method of integration of multiple set of omic data (data from genomis, proteomics, and metabolomics) on the same population; as well as to the case of metagenomic networks where the dynamical interactions between the genome of the host and that of the microbes living in it, the cross-talk being mediated by chemical and ecological interactions. As with the case of social multiplex networks, also in biology the origin of the renovated interest in multiplex networks is largely due to a technological jump that has made it possible the availability of large and diverse amounts of data coming from very different experimental settings.

Also in the traditional field of transportation networks, the notions of multiplexity and multiplex networks have a natural translation in different modes of transportations connecting the same physical location in a city, a country, or on the globe.

Finally, in the field of engineering and critical infrastructures, the concept of multiplexity applies to the interdependence of different lifelines[21]. Even if the notion of multiplexity was introduced years ago, the discussions included few analytical tools to accompany them. This situation arose for a simple reason: although many aspects of single-layer networks are well understood, it is challenging to properly generalize even the simplest concept to multiplex networks. Theoretical developments on multilayer networks in general, and on multiplex networks in particular, have gained steam only in the last few years, for different reasons, among which surely stands the technological revolution represented by the digitalization and the social transformations that has accompanied it, as we have mentioned before.

Now, we understand multiplex networks as a non-linear superposition of complex networks, where components, being them social actors, genes, devices, or physical locations, interacts through a variety of different relationships and communication channels, which we conceptualize as different layers of the multiplex network. This conceptualization of a multiplex network posesses a number of challenges to the science of complex networks: from the formal description of a complex network (starting from the fact that a constituent of a networked system, represented by a node in a traditional single layer network, is no more an "elementary" unit, indeed it has an internal - possibly complex - structure that must be formally represented), to the ultimate goal of understanding how this new level of structural complexity represented by the interaction of different layers reveals itself in the functioning of the system.

Structure of the thesis

Following the 4-step schematic representation given above, this thesis is organized as follows. In Chapter 1 we deal with the representation of multiplex networks in terms of graphs and matrices. In this chapter, we basically face the problem of setting a formal language that includes the new level of complexity represented by the superposition of different layers of interaction. We give there the basic definitions that underpin the notion of multiplex networks.

In Chapter 2 we deal with the problem of characterizing the topology of a multiplex network within the formalism developed in Chapter 1. In particular, we generalize the definition of the clustering coefficient and that of subgraph centrality to multiplex networks. We will show that generalizing traditional metrics to multiplex networks

"the naive way" usually leads to blurred results, while constructing on first principles leads to well-defined metrics that may unveil "how multiplexity works". This is the case, for example, of our definition of clustering coefficients for multiplex networks, which enlightens the context dependent nature of social relations.

In Chapter 3 we continue to address the problem of the structural characterization of a multiplex network by means of its spectral properties, both using perturbative approaches and the analytical relations existing between some natural coarse-grained representations of the network formalisms introduced in Chapter 1 and the original multiplex network.

In Chapter **??** the structural transitions that a multiplex network may undergo are studied by means of its spectral properties. The core question in multiplex network theory is whether or not they are "substantially" different form a traditional single layer network, for example in the critical properties of a dynamics occuring on top of it. We will address this problem by studying the dominating topological scale that appears and disappears in a multiplex network while a parameter controlling the level of coupling between the layers is changed. This is done by studying the Laplacian spectrum of multiplex networks.

Finally, in Chapter 5 we develop a model of social contagion taking place on a multiplex network. We will study the critical properties of such a model, relating them to the structural characteristics of the multiplex networks via its spectrum.

Chapter 1

Multiplex Networks: basic definition and formalism

In this chapter we present the notion of multiplex networks as it will be used in this thesis. It is common to introduce multiplex networks as a particular specification of the more general notion of multilayer networks [1], conversely, we prefer to have the former as a primary object.
We then show how this structure can be represented by adjacency matrices, introducing the notion of "supra-adjacency" matrix. A different algebraic representation of multiplex networks is possible by means of higher order tensors[27]. Even if the tensorial formalism is not discussed here, it is worth noting that supra-adjacency matrices could be obtained as a particular flattening of an adjacency tensor representing the multiplex network.
This introductory chapter represents an effort to set a formal language in this area intended to be general and complete enough as to deal with the most diverse cases. Although it might seem pedantic, setting a rigorous algebraic formalism is crucial to make possible and, in a certain sense, automatic further more complex reasonings, as well as to design data structures and algorithms.

1.1 Graph representation

A networked system $\mathbf{N}$ is naturally represented by a graph.
A graph is a tuple $G(V, E)$, where V is a set of nodes, and $E \subseteq V \times V$ is a set of edges that connects pair of nodes. Nodes represent the components of the system, while edges represent interactions or relations among them. If an edge exists in G between node u and node v, i.e. $(u, v) \in E$, they are said to be adjacent, and we indicate the

adjacency relation with the simbol $\sim$, i.e. we will write $u \sim v$ if $(u, v) \in E$.
In order to represent a networked system in which different types of relations or interactions exist between the components - a multiplex network -, the notion of layer must be introduced. Let $L = \{1, ..., m\}$ be an index set, which we call the layer set. A layer is an index that represents a particular type of interaction or relation. $\mid L \mid = m$ is the number of layers in the multiplex network. Consider now a set of nodes V, where nodes represent the components of the system, and let $G_P = (V, L, P)$ be a binary relation, where $P \subseteq V \times L$. The statement $(u, \alpha) \in P$, with $u \in V$, and $\alpha \in L$, is read *node u participates in layer* α. We call the ordered pair $(u, \alpha) \in P$ a node-layer pair and we say that the node-layer pair (u, α) is the representative of node u in layer α, thus P is the set of the node-layer pairs. In other words, we are attaching etiquettes to nodes that specify in which type of relations (layers) the node participates in.
$G_P = (V, L, P)$ can be interpreted as a (bipartite) graph where P is the edge set. $\mid P \mid = N$ is the number on node-layer pairs, while $\mid V \mid = n$ is the number of nodes. If each node $u \in V$ has a representative in each layer, i.e. $P = V \times L$, we call the multiplex a *node-aligned multiplex*, and we have that $\mid P \mid = mn$. As we shall see later, things are always simpler when the multiplex is node-aligned.
Now, each system of relations or interactions of different kind is naturally represented by a graph $G_\beta(V_\beta, E_\beta)$, where $V_\beta = \{(u, \alpha) \in P \mid \alpha = \beta\}$, that is V_β is a subset of P composed by all the node-layer pairs that has the particular index β as second element. In other words, it is the set of all the representatives of the node set in a particular layer. The set of edges $E_\beta \subseteq V_\beta \times V_\beta$ represents interactions or relations of a particular type between the components of the systems. We call $G_\beta(V_\beta, E_\beta)$ a *layer-graph* and we can consider the set of all layer-graphs $M = \{G_\alpha\}_{\alpha \in L}$. $\mid V_\beta \mid = n_\beta$ is the number of node-layer pairs in layer β. For node-aligned multiplex networks we have $n_\alpha = n \forall \alpha \in L$.
Finally, consider the graph G_C on P in which there is an edge between two node-layer pairs (u, α) and (v, β) if and only if $u = v$; that is, when the two edges in the graph G_P are incident on the same node $u \in V$, which means that the two node-layer pairs represent the same node in different layers. We call $G_C(P, E_C)$ the coupling graph. It is easy to realize that the coupling graph is formed by $n =\mid P \mid$ disconnected components that are complete graphs or isolated nodes. Each component is formed by all the representatives of a node in different layers, and we call the components of G_C *supra-nodes*.

We are now in the position to say that a multiplex network is represented by the quadruple $\mathcal{M} = (V, L, P, M)$:

- the node set V represents the components of the system
- the layer set L represents different types of relations or interactions in the system
- the participation graph G_P encodes the information about what node takes part in a particular type of relation and defines the representative of each component in each type of relation, i.e., the node-layer pair
- the layer-graphs M represent the networks of interactions of a particular type between the components, i.e., the networks of representatives of the components of the system.

Consider the union of all the layer-graphs, i.e. $G_l = \bigcup_\alpha G_\alpha$. We call such a graph the intra-layer graph. Note that, if each layer-graph is connected, this graph is formed by m disconnected components, one for each layer-graph.
Finally, we can define the graph $G_\mathcal{M} = G_l \cup G_C$, which we call the supra-graph. $G_\mathcal{M}$ is a synthetic representation of a multiplex network. Note that supra-nodes are cliques [1] of $G_\mathcal{M}$.

To summarize, up to now, we have two different entities representing the components of a multiplex network: nodes and node-layer pairs. A node corresponds to a 'physical object', while node-layer pairs are different instances of the same object. For instance a node could represent an on-line user, while node-layer pairs would represent different accounts of the same user in different on-line social networks; or a node could represent a social actor, while node-layer pairs would represent different social roles (friend, worker, family member) of the same social actor; or a node could stand for a location in a transportation network, while node-layer pairs would represent stations of different transportation modes.
The connection between nodes and node-layer pairs is given by the notion of supra-nodes: i.e., clique in the supra-graph formed by node-layer pairs that are instances of the same object. Moreover, for clarity, we denote nodes using the symbols u, v, w; for brevity we may indicate a node-layer pair with a single symbol instead of using the ordered pair (u, α), and we will use the symbols i, jh.
To round off the basic definitions used henceforth, let's also define $l(u) = (u, \alpha) \in P \mid \alpha \in L$

[1] A clique, C, in an undirected graph $G = (V, E)$ is a subset of the vertices, $C \subseteq V$, such that every two distinct vertices are adjacent.

to be the set of node-layer pairs that correspond to the same node u. Note that not every node has a representative in every layer, and $l(u)$ may have cardinality 1. We call $\kappa_u = |l(u)|$ the *multiplexity degree* of the node u, that is, the number of layers in which an instance of the same object u appears. We also define $l^{-1}(i)$ to be the unique node that corresponds to the node-layer pair i.
When it is clear from the context, we may refer to node-layer pairs simply as nodes.

1.2 Matrix representation

Given a graph $G(V, E)$, we can associate to it a matrix $\mathbf{A}$ whose elements $a_{uv} = 1_{u\sim v}$, where 1_x is the indicator function, i.e., it is equal to one if the x is true, otherwise it is zero. The matrix $\mathbf{A}$ is called the adjacency matrix of G, and by identifying a network $\mathbf{N}$ with its graph representation, we say that $\mathbf{A}$ is the adjacency matrix of $\mathbf{N}$.
We can consider the adjacency matrix of each of the graphs introduced in the previous section. The adjacency matrix of a layer graph G_α is a $n_\alpha \times n_\alpha$ symmetric matrix $\mathbf{A}^\alpha$, with $a^\alpha_{ij} = 1$ if and only if there is an edge between i and j in G^α. We call them layer adjacency matrices.
Likewise, the adjacency matrix of G_P is an $n \times m$ matrix $\mathbf{P}$, with $p_{u\alpha} = 1$ if and only if there is an edge between the node u and the layer α in the participation graph, i.e., only if node u participates in layer α. We call it the participation matrix. The adjacency matrix of the coupling graph G_C is an $N \times N$ matrix $\mathcal{C} = \{c_{ij}\}$, with $c_{ij} = 1$ if and only if there is an edge between node-layer pair i and j in G_C, i.e., if they are representatives of the same node in different layers. We can arrange the rows and the columns of $\mathcal{C}$ such that node-layer pairs of the same layer are contiguous. It results that $\mathcal{C}$ is a block matrix with zero diagonal blocks. Besides, rows and columns can be arranged in a way such that the off-diagonal blocks are diagonals. Thus, $c_{ij} = 1$, with $i, j = 1, \ldots, N$ represents an edge between a node-layer pair in layer 1 and a node-layer pair in layer 2 if $i < n_1$ and $n_1 < j < n_2$. We call this the standard labelling and we assume that node-layer pairs are always labelled this way. Note that this labelling also induces a labelling of node-layer pairs in single layer-graphs such that the same row and column in different layer adjacency matrices correspond to the representative of the same node in different layers.

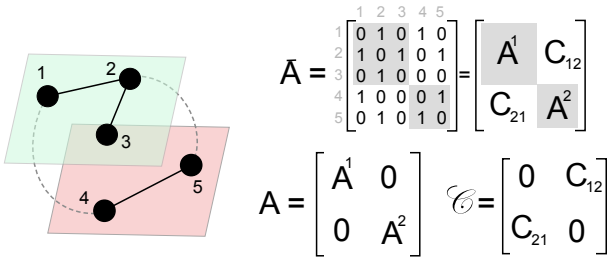

Figure 1.1: Example of a multiplex network. The structure of each layer is represented by an adjacency matrix $\mathcal{A}^i$, where i =1, 2. $\mathcal{C}_{lm}$ stores the connections between layers l and m. Note that the number of nodes in each layer is not the same.

1.2.1 The supra-adjacency matrix

The *supra-adjacency* matrix $\bar{\mathcal{A}}$ is the adjacency matrix of the supra-graph $G_{\mathcal{M}}$. Just as $G_{\mathcal{M}}$, $\bar{\mathcal{A}}$ is a synthetic representation of the whole multiplex $\mathcal{M}$. By definition, assuming the standard labelling, it can be obtained from the intra-layer adjacency matrices and the coupling matrix in the following way:

$$\bar{\mathcal{A}} = \bigoplus_{\alpha} \mathbf{A}^{\alpha} + \mathcal{C}. \tag{1.1}$$

We also define $\mathcal{A} = \bigoplus \mathbf{A}^{\alpha}$, and we call it the intra-layer adjacency matrix. By definition, $\mathcal{A}$ is the adjacency matrix of the intra-layer graph G_l. Figure 1.1 shows the supra-adjacency matrix, the intra-layer adjacency matrix, and the coupling matrix of a multiplex network.
$\bar{\mathcal{A}}$ takes a very simple form in the case of node-aligned multiplex networks, that is

$$\bar{\mathcal{A}} = \mathcal{A} + \mathbf{K}_m \otimes \mathbf{I}_n, \tag{1.2}$$

where $\mathbf{K}_m$ is the adjacency matrix of a complete graph on m nodes, and I_n is the $n \times n$ identity matrix.
It is even simpler when layer-graphs are identical:

$$\bar{\mathcal{A}} = \mathbf{I}_m \otimes \mathbf{A} + \mathbf{K}_m \otimes \mathbf{I}_n, \tag{1.3}$$

where $\mathbf{A}$ is the adjacency matrix of each identical layer graph.

Some basic metrics are easily calculated from the supra-adjacency matrix. The degree of a node-layer i is the number of node-layers connected to it by an edge in $G_{\mathcal{M}}$ and is given by

$$K_i = \sum_j \bar{\mathcal{A}}_{ij}. \tag{1.4}$$

Sometimes we write $i(\alpha)$ as an index, instead of simply i, to explicitly indicate that the node-layer i is in layer α even if the index i already uniquely indicates a node-layer

pair. Since $\bar{\mathcal{A}}$ can be read as a block matrix, with the $\mathbf{A}^\alpha$ on the diagonal blocks, the index $i(\alpha)$ can be interpreted as block index. It is also useful to define the following quantities

$$e_\alpha = \sum_{\beta<\alpha} n_\beta, \tag{1.5}$$

which we call the excess index of layer α. The layer-degree of a node-layer i, $k_{i(\alpha)}$, is the number of neighbors it has in G^α, i.e.,, $k_{i(\alpha)} = \sum_j a^\alpha_{ij}$. By definition of $\bar{\mathcal{A}}$

$$k_{i(\alpha)} = \sum_{j=1+e_\alpha}^{n_\alpha+e_\alpha} \bar{\mathcal{A}}_{ij}. \tag{1.6}$$

The coupling degree of a node-layer i, $c_{i(\alpha)}$, is the number of neighbors it has in the coupling graph, i.e.,, $c_{i(\alpha)} = \sum_j c_{ij}$. From $\bar{\mathcal{A}}$ we get

$$c_{i\alpha} = \sum_{\substack{j<e_\alpha,\\ j>n_\alpha+e_\alpha}} \bar{\mathcal{A}}_{ij}. \tag{1.7}$$

By definition

$$c_i = \kappa_{l^{-1}(i)} - 1. \tag{1.8}$$

Finally, we note that the degree of a node-layer can be expressed as

$$K_{i(\alpha)} = \sum_j \bar{\mathcal{A}}_{ij} = k_{i\alpha} + c_{i\alpha}. \tag{1.9}$$

Eq.(1.9) explicitly expresses the fact that the degree of a node-layer pair is the sum of its layer-degree plus its coupling-degree.

1.2.2 The supra-Laplacian matrix

Generally, the Laplacian matrix, or simply the Laplacian, of a graph with adjacency matrix $\mathbf{A}$ is given by

$$\mathbf{L} = \mathbf{D} - \mathbf{A} \tag{1.10}$$

where $\mathbf{D} = diag(k_1, k_2, \dots)$ is the degree matrix.
Thus, it is natural to define the *supra-Laplacian* matrix of a multiplex network as the Laplacian of its supra-graph

$$\bar{\mathcal{L}} = \bar{\mathcal{D}} - \bar{\mathcal{A}}, \tag{1.11}$$

where $\bar{\mathcal{D}} = diag(K_1, K_2, \ldots, K_N)$ is the degree matrix.
Besides, we can define the layer-Laplacian of each layer-graph G_α as

$$\mathbf{L}^\alpha = \mathbf{D}^\alpha - \mathbf{A}^\alpha, \tag{1.12}$$

and the Laplacian of the coupling graph

$$\mathcal{L}_C = \Delta - \mathcal{C} \tag{1.13}$$

where $\Delta = diag(c_1, c_2, \ldots, c_N)$ is the coupling-degree matrix.
By definition, we have

$$\bar{\mathcal{L}} = \bigoplus_\alpha \mathcal{L}^\alpha + \mathcal{L}_C. \tag{1.14}$$

As it was the case of the supra-adjacency matrix, Eq. (1.14) takes a very simple form in the case of a node-aligned multiplex, i.e.,

$$\bar{\mathcal{L}} = \bigoplus_\alpha (\mathbf{L}^\alpha + (m-1)I_N) - \mathbf{K}_m \otimes I_n, \tag{1.15}$$

and when layer-graphs are identical:

$$\bar{\mathcal{L}} = \mathbf{I}_m \otimes (\mathbf{L} + (m-1)I_n) - \mathbf{K}_m \otimes I_n, \tag{1.16}$$

where $\mathbf{L}$ is the Laplacian of each identical layer-graph.

1.2.3 Multiplex Walk Matrices

A walk on a graph is a sequence of adjacent vertices. The length of a walk is its number of edges. For a simple graph (which has no multiple edges), a walk may be specified completely by an ordered list of vertices [100].A step is the elementary component of a walk, i.e., two adjacent nodes.
We define a supra-walk as a walk on a multiplex network in which, either before or after each intra-layer step, a walk can either continue on the same layer or change to an adjacent layer. We represent this choice by the matrix:

$$\widehat{\mathcal{C}} = \beta\mathcal{I} + \gamma\mathcal{C} \tag{1.17}$$

the parameter β is a weight that accounts for the walk staying in the current layer, and γ is a weight that accounts for the walk stepping to another layer. In a supra-walk, a supra-step consists either of only a single intra-layer step or of a step that includes both an intra-layer step changing from one layer to another (either before or after having an intra-layer step). In the latter type of supra-step, note that we are

disallowing two consecutive inter-layer steps. In other words, supra-walks are walks on the supra-graph $G_{\mathcal{M}}$ with this latter prescription.
Roughly speaking, a *multiplex walk matrix* is a matrix that encodes the permissible steps in a multiplex network. The matrix $\mathcal{A}\widehat{\mathcal{C}}$ encodes the steps in which after each intra-layer step a walk can continue on the same layer. On the other hand, the matrix $\widehat{\mathcal{C}}\mathcal{A}$ encodes the steps in which after each intra-layer step a walk can continue on the same layer. Both matrices $\mathcal{A}\widehat{\mathcal{C}}$ and $\widehat{\mathcal{C}}\mathcal{A}$ can be interpreted as the adjacency matrix of a directed (possible weighted) graph. We call such graphs, auxiliary supra-graph.
In general, depending on the rules prescribed to walk the multiplex, one can define an auxiliary supra-graph G_M whose adjacency matrix is $\mathcal{M} = \mathcal{M}(\mathcal{A}, \mathcal{C})$. It should be noted that, by definition, the supra-adjacency matrix is also a walk matrix.
We introduce such matrices because, as we will see in the next chapter, often it is of interest to treat intra and inter-layer edges differently, where changing layer is an action of a different nature with respect to going from a node to another.

1.3 Coarse-graining representation of a multiplex network

Because of the structure of a multiplex network, it is natural to try to aggregate the interaction pattern of each layer in a single network somehow. An operation that we call *dimensionality reduction*, whereas the result of such operation leads to what we call an *aggregate network*.
Several candidates for the aggregate network have been proposed in the literature such as the average network [89], the overlapping network [8], the projected monoplex network or the overlay network [27]. We claim that the natural definition of an aggregate network is given by the notion of quotient network. In addiction, in the quotient network framework, we are able to introduce in a symmetric way another reduced network, the network of layers, that encodes the connectivity pattern between layers. In a sense that will be more clear in chapter 3, we say that the notion of quotient graph underpins the notion of multiplex network.

1.3.1 Mathematical Background

Let us first provide a brief, but self-contained description of network quotients.

1.3.1.1 Adjacency and Laplacian matrices

Suppose that $\{V_1, \ldots, V_m\}$ is a partition of the node set of a graph $G(V, E)$ with adjacency matrix $\mathbf{A} = (a_{ij})$, and write $n_i = |V_i|$.

The *quotient graph* $\mathcal{Q}$ of G is a coarsening of G with respect to the partition. It has one node per cluster V_i, and an edge from V_i to V_j weighted by an average connectivity from V_i to V_j

$$b_{ij} = \frac{1}{\sigma} \sum_{\substack{k \in V_i \\ l \in V_j}} a_{kl}, \tag{1.18}$$

where we have a choice for the size parameter σ: we will use either $\sigma_i = n_i$, or $\sigma_j = n_j$, or $\sigma_{ij} = \sqrt{n_i}\sqrt{n_j}$. We call the corresponding graph the *left quotient*, the *right quotient* and the *symmetric quotient* respectively. Fortunately, the matrix $\mathbf{B} = (b_{ij})$ has the same eigenvalues for the three choices of σ (see below). We refer by *quotient graph* to any of these three spectrally-equivalent graphs with adjacency matrix $\mathbf{B}$. Observe that the symmetric quotient is undirected, while the left and right quotients are not, unless all clusters have the same size, $n_i = n_j$ for all i, j.

The quotient formalism holds in more generality for any real symmetric matrix, as we explain here. Let $A = (a_{ij})$ be any real symmetric $n \times n$ matrix. Write $X = \{1, 2, \ldots, n\}$, let $\{X_1, \ldots, X_m\}$ be a partition of X, and let $n_i = |X_i|$. We write A_{ij} for the submatrix consisting of the intersection of the k-rows and l-columns of A such that $k \in X_i$ and $l \in X_j$. In particular, A_{ij} is an $n_i \times n_j$ matrix. Define b_{ij} as the average row sum of A_{ij},

$$b_{ij} = \frac{1}{n_i} \sum_{\substack{k \in X_i \\ l \in X_j}} a_{kl}. \tag{1.19}$$

The $m \times m$ matrix $Q_l(A) = (b_{ij})$ is called the *left quotient matrix of* A with respect to the partition $\{X_1, \ldots, X_m\}$.

We can express $Q_l(A)$ in matrix form, as follows. Let $S = (s_{ij})$ be the $n \times m$ *characteristic matrix* of the partition, that is, $s_{ij} = 1$ if $i \in X_j$, and 0 otherwise. Then $S^T AS$ is the matrix of coefficient sums of the submatrices A_{ij}, and, hence, $Q_l(A) = \Lambda^{-1} S^T AS$, where $\Lambda = \mathrm{diag}(n_1, \ldots, n_m)$.

There are two alternatives to $Q_l(A)$, called the *right quotient* and the *symmetric quotient*, written $Q_r(A)$ and $Q_s(A)$. They correspond to replacing $1/n_i$ in (1.19) by $1/n_j$ respectively $1/\sqrt{n_i}\sqrt{n_j}$. In matrix form, we have $Q_r(A) = S^T AS\Lambda^{-1}$ and $Q_s(A) = \Lambda^{-1/2} S^T AS\Lambda^{-1/2}$. Note that $Q_l(A)$ is the transpose of $Q_r(A)$, and they are not symmetric unless $n_i = n_j$ for all i, j.

Nevertheless, these three matrices have the same spectrum (the proof is straightforward):

Lemma. *Let X, D be $m \times m$ matrices, with D diagonal. Then the matrices DX, XD and $D^{1/2}XD^{1/2}$ have all the same spectrum.*

Summarising, the *left quotient*, the *right quotient* and the *symmetric quotient* graph of a graph G with adjacency matrix $\mathbf{A}$ is the graph $\mathcal{Q}$ with adjacency matrix $\mathbf{B} = Q_l(\mathbf{A})$, $\mathbf{B} = Q_r(\mathbf{A})$ and $\mathbf{B} = Q_s(\mathbf{A})$ respectively.
Consider the left quotient of $\mathbf{A}$ with respect to the partition. Observe that the row sums of $Q_l(A)$ are

$$\overline{d_i} = \frac{1}{n_i} \sum_{k \in V_i} d_k, \tag{1.20}$$

the average node degree in V_i. Let $\overline{\mathbf{D}}$ be the diagonal matrix of the average node degrees. Then we define the *quotient Laplacian* as the matrix

$$L_{\mathcal{Q}} = \overline{D} - Q_l(\mathbf{A}). \tag{1.21}$$

(See Chapter 3 for a full discussion on this choice.) Moreover, let $\widetilde{\mathcal{Q}}$ be the *loopless quotient* of G, that is, the quotient network $\mathcal{Q}$ with all the self-loops removed. As the quotient Laplacian ignores self-loops (See Chapter 3), we have $L_{\mathcal{Q}} = L_{\widetilde{\mathcal{Q}}}$.

1.3.1.2 Regular quotients

A partition of the node set $\{V_1, \ldots, V_m\}$ is called *equitable* if the number of edges (taking weights into account) from a node in V_i to any node in V_j is independent of the chosen node in V_i

$$\sum_{l \in V_j} a_{kl} = \sum_{l \in V_j} a_{k'l} \quad \text{for all } k, k' \in V_i, \tag{1.22}$$

for all i, j. This indicates a regularity condition on the connection pattern between (and within) clusters. If the partition is equitable, we call the quotient network *regular*. A source of regular quotients are network symmetries [58, 57]. We call a partition *almost equitable* if condition (1.22) is satisfied for all $i \neq j$ (but not necessarily for $i = j$), that is, if the regularity condition is satisfied after ignoring the intra-cluster edges. In this case, we call the quotient graph $\mathcal{Q}$ *almost regular*. Note that the quotient $\mathcal{Q}$ being almost regular is equivalent to the loopless quotient $\widetilde{\mathcal{Q}}$ being regular.

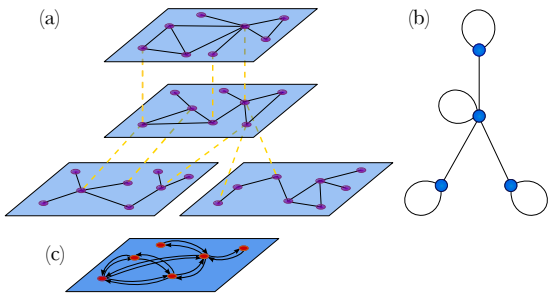

Figure 1.2: Schematic representation of a multiplex network with 4 layers and 8 nodes per layer (a), and its two quotients: the network of layers (b), and the aggregate network (c). In (a), dashed lines represent inter-layer edges. The quotient (b) is undirected, as all layers have the same number of nodes. The quotient (c) is only partially drawn, it is directed, and the edge thickness is proportional to the weight. The network of layers (b) corresponds to the layer interconnection structure, while the aggregate network (c) represents the superposition of all the layers onto one. In this sense, they can be thought of as 'horizontal' and 'vertical' quotients, as the figure suggests. Both quotients clearly represent a dimensionality reduction or coarsening of the original multilayer network.

1.3.2 The aggregate network

We define the node characteristic matrix $\mathbf{S}_n = (s_i u)$. $\mathbf{S}_n$ is an $N \times n$ matrix with $s_{iu} = 1$ if and only if the node-layer i is a representative of node u, i.e., it is in the connected component u of the graph G_C. We call it a characteristic matrix since nodes partition the node-layer set and $\mathbf{S}_n$ is the characteristic matrix of that partition. Then, the adjacency matrix of the aggregate network is given by:

$$\tilde{\mathbf{A}} = \Lambda^{-1}\mathbf{S}_n^T \bar{\mathcal{A}} \mathbf{S}_n, \tag{1.23}$$

where $\Lambda = diag\{\kappa_1, \ldots, \kappa_n\}$ is the multiplexity degree matrix.
We also define the *average connectivity* between nodes u and v as

$$d_{uv} = \frac{1}{\kappa_u} \sum_{\substack{i \in l(u) \\ j \in l(v9}} \bar{\mathcal{A}}_{ij}, \tag{1.24}$$

and write d_u for d_{uu}. In this way, in an aggregate network, each node has a self-loop weighted by d_u, and a directed edge from u to v weighted by d_{uv}. Note that in general the aggregate network is directed. It is not directed if the multiplex network is node-aligned.
We also define a loop-less aggregate network, that is just the aggregate network

without self-loops, i.e.,

$$\tilde{\mathbf{W}} = \tilde{A} - diag(\tilde{A}) \tag{1.25}$$

It is worth noting that

$$\tilde{\mathbf{W}} = \Lambda^{-1}\mathbf{S}_n^T \mathcal{A} \mathbf{S}_n. \tag{1.26}$$

Finally, we define the sum aggregate network as

$$\mathbf{W} = \mathbf{S}_n^T \mathcal{A} \mathbf{S}_n, \tag{1.27}$$

and note that for node-aligned multiplex networks we have

$$\mathbf{W} = m\tilde{\mathbf{W}}. \tag{1.28}$$

1.3.3 The network of layers

Likewise, we define the layer characteristic matrix $\mathbf{S}_l = \{s_{i\alpha}\}$ as an $N \times m$ matrix with $s_{i\alpha} = 1$ only if the node-layer i is in layer α, i.e., in the connected component α of the graph G_l. We call it a characteristic matrix since it is the characteristic matrix of the partition of the node-layer set induced by layers.
In the same way, the network of layers has adjacency matrix given by

$$\tilde{\mathbf{A}}_l = \Lambda^{-1}\mathbf{S}_l^T \bar{\mathcal{A}} \mathbf{S}_l, \tag{1.29}$$

where $\Lambda^{-1} = diag\{n_1, \ldots, n_m\}$.
Finally, we define the *average inter-layer degree* from α to β as

$$d^{\alpha\beta} = \frac{1}{n_\alpha} \sum_{\substack{i \in V_\alpha \\ j \in V_\beta}} a_{ij}\,. \tag{1.30}$$

This represents the average connectivity from a node in G_α to any node in G_β. If $\alpha = \beta$ we write d^α for $d^{\alpha\alpha}$, and call it the *average intra-layer degree*. Thus, each node corresponds to a layer, with a self loop weighted by the average intra-layer degree d^α, and there is a directed edge from layer α to layer β weighted by the average inter-layer degree $d^{\alpha\beta}$.

1.4 Supra-walk matrices and loopless aggregate network

In this section we will investigate the relation between the supra-walk representation of a multiplex and its loopless aggregate network, considering the case of node-aligned

multiplex networks.
We start with two basic observations:

$$\mathbf{S}_n^T \mathbf{S}_n = m\mathbf{I}_n$$
$$\mathbf{S}_n \mathbf{S}_n^T = I_N + C = \widehat{\mathcal{C}}(1,1). \tag{1.31}$$

Then, for a node-aligned multiplex network when changing layer has no cost we can write:

$$A\widehat{\mathcal{C}} = A\mathbf{S}_n\mathbf{S}_n^T. \tag{1.32}$$

Note that the second equation in 1.31 is true for a multiplex network with no switch cost even if it is not node-aligned, but the same does not hold for the first.
It then follows that

$$(A\widehat{C})^l = ASS^TASS^T \dots ASS^T = AS(S^TAS)^{l-1}S^T. \tag{1.33}$$

We can multiply both sides of 1.33 by $\mathbf{S}_n^T$ from the left and by $\mathbf{S}_n$ from the right, yielding

$$\mathbf{S}_n^T(A\widehat{C})^l\mathbf{S}_n = m^{l+1}\tilde{\mathbf{W}}^l = m^l\mathbf{W}^l. \tag{1.34}$$

In this way, we have obtained a relation between the powers of the supra-walk matrix $A\widehat{C}$ and the powers of the adjacency matrix of the loopless aggregate network, mediated by the supra-node characteristic matrix. Since powers of an adjacency matrix contain the number of walks between two nodes, we have a relation between the number of supra-walks in a multiplex network and the weight of weighted walks in its aggregate network when the multiplex is node-aligned and switching layer has no cost.
By writing 1.34 explicitly in terms of the elements of $\tilde{\mathbf{W}}$, this relation will be more explicit. Assuming summation over repeated indices, we have

$$m^{l+1}(\tilde{\mathbf{W}})_{uv} = s_{ui}(A\widehat{C})^l_{ij}s_{jv} = \sum_{i\in l(u)j\in l(v)} (A\widehat{C})^l_{ij}. \tag{1.35}$$

By construction, $m\tilde{\mathbf{W}} = \mathbf{W}$ is the adjacency matrix of a multigraph in which there is an edge between node u and node v for every edge that exists between each pair of representatives in every layer. The elements of $\mathbf{W}$ can be interpreted as number of edges or as weights. Thus, we have demonstrated that the number of supra-walks in the multiplex between every representative of two supra-nodes u and v is equal to

the number of walks in the multiedge aggregate network times the number of layers. It is also interesting to look at closed walks, i.e., cycles. We have

$$s_{ui}(A\widehat{C})^l_{ij}s_{ju} = \sum_{i\in l(u)j\in l(u)} (A\widehat{C})^l_{ij} = \sum_{i\in l(u)} (A\widehat{C})^l_{ii} + \sum_{i\in l(u)j\in l(u)i\neq j} (A\widehat{C})^l_{ij} \tag{1.36}$$

If we note that each block line of $A\widehat{C}$ has identical blocks, i.e., that

$$(A\widehat{C})^l_{ii} = (A\widehat{C})^l_{ij},\ \forall j \in l^{-1}(i),$$

we can write

$$\sum_{i\in l(u)} (A\widehat{C})^l_{ii} = m^l(\tilde{\mathbf{W}}^l)_{uu} = \mathbf{W}^l. \tag{1.37}$$

Thus, the number of closed supra-walks in the multiplex between every representative of two supra-nodes u and v is equal to the number of walks in the sum aggregate network.

This observation give us a hint on what happens when we transform a multiplex network that is not node-aligned into a node-aligned one, by adding spurious representatives of a node in layers where it has not. Essentially, this implies to magnify the number of walks existing between layers by adding *dead-ending* supra-walks.

To conclude, with these relations we can say that, when the multiplex is node-aligned, switching layers has no cost, and the separate identity of the representative of nodes in different layers is not informative, an aggregate representation of a multiplex network is equivalent to a supra-walk representation. In fact, the information about the identity of the representative of a node in different layers is the only we lose. The following observation make explicit the relation:

$$m^{-1}\mathbf{S}_n^T A\widehat{\mathcal{C}}\mathbf{S}_n = \mathbf{W} \tag{1.38}$$

i.e.,the sum aggregate network is the quotient of the supra-walk multiplex.

This relation holds true even for multiplex networks that are not node-aligned, but to prove whether this is true or not for other relations is not so straightforward in that case.

Chapter 2

Structural Metrics

A structural metric of a network is a measure of some property directly dependent on the system of relations between the components of the network, i.e.,by representing the network with a graph, a structural metric is a measure of a property that depends on the edge set. Since there is a correspondence between graph and adjacency matrix, a structural metric can be expressed as a function of the adjacency matrix, but it is not necessary. This fact differentiates between structural metrics and other kind of metrics, such as spectral metrics, that are defined only once an adjacency matrix is introduced.

Structural metrics can be local or global. A local metric p measures the property of a single node or pair of nodes, and we refer to the value of that metric on a node i or a pair of nodes i, j as p_i, p_{ij} respectively. The global version P of p measures the corresponding overall property of the network. In general, a global metric is defined as a mean of local ones.

An example of a structural metric is the connectivity k. As we have seen, the connectivity k_i of a node i is the number of neighbours the node i has. The global connectivity is defined as the mean connectivity $K = \frac{1}{N}\sum_i k_i$. The characteristic path length L is a global metric defined as $L = \frac{1}{n(n-1)}\sum_{i\neq j} l_{ij}$, where l_{ij} is the geodesic distance between the nodes i and j measured as the minimum number of edges connecting i and j.

Although in the two examples given above the global metric is simple the mean of the local one, it is not always the case, as for the clustering coefficient (see note 2 in section 2.1). The term local and global may have a different meaning in this context, in fact they may refer to the topological scale at which the system is considered. In this sense, the connectivity is a local measure since it takes into account only the first neighbours of a node, while the geodesic distance between two nodes is a global metric since it takes into account the whole network.

The quantitative description of structural network properties is a core task of complex network research. Firstly, it allows for the classification of different structures and the description of different categories. On the other hand, is the first step for the investigation of the relations between structure and function. Finally, it allows the construction of models that reproduce the structural features of an empiric system under study, as well as it allows to inquiry if a property of a system is the result of chance or if it reveals something on the particular way of evolving of the system. An example of the latter is the fact that, recognizing that the clustering coefficient of an empiric social network is on average greater than that of a random graph, allowed to propose the *triadic closure* as a crucial mechanism in the evolution of social networks. The other way around, the quantitative evaluation of the clustering coefficient between model networks and empirical ones allows the validation of the *triadic closure* hypothesis.
Thus, it is crucial to define a set of structural metrics for multiplex networks.
Here, we dare to suggests a list of requirement a structural metric should fulfil in order to be properly defined.
A structural metric for multiplex networks should

- reduce to the ordinary single-layer metric (if defined) when layers reduce to one
- be defined for node-layer pairs
- be defined for non-node-aligned multiplex networks

The first requirement refers to generalization of standard single-layer metrics to multiplex networks. It seems reasonable, although it is not trivial. In fact, usually generalizing "the naive way" leads to metrics that do not fulfil this requirement. We discuss this point in the next session in the particular case of the clustering coefficient.
The second requirement takes into account the fact that node-layer pairs are the basic objects that build up a multiplex network, thus, in general, to define a metric only on some version of the aggregate network is not enough.
The third requirement comes from the fact that, although it is easier to deal with node-aligned multiplex networks from an analytical point of view, real world multiplex networks in general are not node-aligned. Because of that, it is worth defining metrics for the general case, even when an analytic treatment is only possible in the node-aligned case.
An additional requirement is needed only in the case of intensive metrics:

- For a multiplex of identical layers when changing layer has no cost, an intensive structural metric should take the same value when measured on the multiplex network and on one layer taken as an isolated network.

This last requirement, that ask for a sort of "normalization", is needed in order to avoid spurious amplification of the value that a quantity takes just because of the number of layers. We will see this requirement at work in the case of sub-graphs centrality.
This *list of requirements* has not the pretension to be interpreted as a set of axioms and surely it is not definitive nor complete, but in our opinion it has the power to guide the generalization of standard single-layer metrics to multiplex networks in a systematic way, as well as to guide the theoretical development of new genuinely multiplex metrics.
In summary, we can recognize that it is insufficient to generalize existing diagnostics in a naïve manner and that one must instead construct their generalizations from first principles. In the following sections of this chapter, we will build on the basic notion of walks and cycles to properly generalize clustering coefficients and sub-graphs centrality to multiplex networks.

2.1 Structure of triadic relations in multiplex networks

In the present section, we focus on one of the most important structural properties of networks: triadic relations, which are used to describe the simplest and most fundamental type of transitivity in networks [55, 97, 95, 65, 47]. We develop multiplex generalizations of clustering coefficients, which can be done in myriad ways, and (as we will illustrate) the most appropriate generalization depends on the application under study.
There have been several attempts to define multiplex clustering coefficients [7, 16, 15, 24, 8], but there are significant shortcomings in these definitions. For example, some of them do not reduce to the standard single-layer clustering coefficient or are not properly normalized (see appendix A).
The fact that existing definitions of multiplex clustering coefficients are mostly *ad hoc* makes them difficult to interpret. In our definitions, we start from the basic concepts of walks and cycles to obtain a transparent and general definition of transitivity. This approach also guarantees that our clustering coefficients are always properly

normalized. It reduces to a weighted clustering coefficient [102] of an aggregated network for particular values of the parameters; this allows comparison with existing single-layer diagnostics. We also address two additional, very important issues: (1) Multiplex networks have many types of connections, and our multiplex clustering coefficients are (by construction) decomposable, so that the contribution of each type of connection is explicit; (2) because our notion of multiplex clustering coefficients builds on walks and cycles, we do not require every node to be present in all layers, which removes a major (and very unrealistic) simplification that is used in existing definitions.

The local clustering coefficient C_u of node u in an unweighted monoplex network is the number of triangles (i.e., triads) that include node u divided by the number of connected triples with node u in the center [97, 65]. The local clustering coefficient is a measure of transitivity [55], and it can be interpreted as the density of a focal node's neighborhood. For our purposes, it is convenient to define the local clustering coefficient C_u as the number of 3-cycles t_u that start and end at the focal node u divided by the number of 3-cycles d_u such that the second step of the cycle occurs in a complete graph (i.e., assuming that the neighborhood of the focal node is as dense as possible).[1] In mathematical terms, $t_u = (\mathbf{A}^3)_{uu}$ and $d_u = (\mathbf{AFA})_{uu}$, where $\mathbf{A}$ is the adjacency matrix of the graph and $\mathbf{F}$ is the adjacency matrix of a complete graph with no self-edges. (In other words, $\mathbf{F} = \mathbf{J} - \mathbf{I}$, where $\mathbf{J}$ is a complete square matrix of 1s and $\mathbf{I}$ is the identity matrix.)

The *local clustering coefficient* is thus given by the formulas $C_u = t_u/d_u$. This is equivalent to the usual definition of the local clustering coefficient: $C_u = t_u/(k_u(k_u - 1))$, where $k_u \geq 2$ is the degree of node u. (The local clustering coefficient is 0 for nodes of degree 0 and 1.) One can calculate a single global clustering coefficient for a monoplex network either by averaging C_u over all nodes or by computing $C = \frac{\sum_u t_u}{\sum_u d_u}$. Henceforth, we will use the term *global clustering coefficient* for the latter quantity.[2] In the following we will define clustering coefficients for multiplex networks, in D we use a simple example to illustrate the differences between the various notions.

[1] Note that we use the term "cycle" to refer to a walk that starts and ends at the same physical node u. It is permissible (and relevant) to return to the same node via a different layer from the one that was used originally to leave the node.

[2] The definition we adopt for the global clustering coefficient is an example of a global structural metric that is not defined as the mean value over all the nodes of its local version. Actually, it is defined as the ratio between the mean number of closed triple and the mean number of open triples.

2.1.1 Triads on Multiplex Networks

In addition to 3-cycles (i.e., triads) that occur within a single layer, multiplex networks also contain cycles that can traverse different additional layers but still have 3 intra-layer steps. Such cycles are important for the analysis of transitivity in multiplex networks. In social networks, for example, transitivity involves social ties across multiple social environments [95, 91]. In transportation networks, there typically exist several means of transport to return to one's starting location, and different combinations of transportation modes are important in different cities [35]. For dynamical processes on multiplex networks, it is important to consider 3-cycles that traverse different numbers of layers, so one needs to take them into account when defining a multiplex clustering coefficient. For this reasons, we build the clustering coefficient on the notion of supra-walk. Thus, the number of 3-cycles for node i is then

$$t_{M,i} = [(\mathcal{A}\widehat{\mathcal{C}})^3 + (\widehat{\mathcal{C}}\mathcal{A})^3]_{ii}\,, \tag{2.1}$$

where the first term corresponds to cycles in which the inter-layer step is taken after an intra-layer one and the second term corresponds to cycles in which the inter-layer step is taken before an intra-layer one. The subscript M refers to the particular way that we define a supra-walk in a multiplex network through the multiplex walk matrices $\mathcal{A}\widehat{\mathcal{C}}$ and $\widehat{\mathcal{C}}\mathcal{A}$. However, one can also use other types of supra-walks (see ref B), and we will use different subscripts when we refer to them. We can simplify Eq. 2.1 by exploiting the fact that both $\mathcal{A}$ and $\widehat{\mathcal{C}}$ are symmetric. This yields

$$t_{M,i} = 2[(\mathcal{A}\widehat{\mathcal{C}})^3]_{ii}\,. \tag{2.2}$$

It is useful to decompose multiplex clustering coefficients that are defined in terms of multilayer cycles into so-called *elementary cycles* by expanding Eq. 2.2 and writing it in terms of the matrices $\mathcal{A}$ and $\mathcal{C}$. That is, we write $t_{M,i} = \sum_{\mathcal{E}\in\mathscr{E}} w_{\mathcal{E}}(\mathcal{E})_{ii}$, where $\mathscr{E}$ denotes the set of elementary cycles and $w_{\mathcal{E}}$ are weights of different elementary cycles. We can use symmetries in our definition of cycles and thereby express all of the elementary cycles in a standard form with terms from the set $\mathscr{E} = \{\mathcal{AAA}, \mathcal{AAC}\mathcal{AC}, \mathcal{AC}\mathcal{AAC}, \mathcal{AC}\mathcal{AC}\mathcal{A}, \mathcal{AC}\mathcal{AC}\mathcal{AC}\}$. See Fig. 2.1 for an illustration of elementary cycles and 2.1.2 for details on deriving the elementary cycles. Note that some of the alternatives definition of a 3-cycle—which we discuss in B— lead to more elementary cycles than the ones that we just enumerated.

To define multiplex clustering coefficients, we need both the number $t_{*,i}$ of cycles and a normalization $d_{*,i}$. The symbol $*$ stands for any type of cycle: the 3-cycle

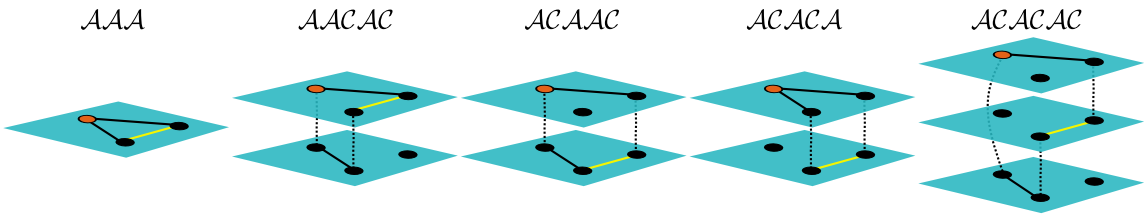

Figure 2.1: Sketch of the elementary cycles $\mathcal{AAA}$, $\mathcal{AACAC}$, $\mathcal{ACAAC}$, $\mathcal{ACACA}$, and $\mathcal{ACACAC}$. The orange node is the starting point of the cycle. The intra-layer edges are the solid lines, and the intra-layer edges are the dotted curves. In each case, the yellow line represents the second intra-layer step.

that we define in the main text, an elementary cycle, or the alternatives definition of 3-cycles that we give in B. Choosing a particular definition coincides to a given way to calculate the associated expression for $t_{*,i}$. To determine the normalization, it is natural to follow the same procedure as with monoplex clustering coefficients and use a complete multiplex network $\mathcal{F} = \bigoplus_\alpha \mathbf{F}^{(\alpha)}$, where $\mathbf{F}^{(\alpha)} = \mathbf{J}^{(\alpha)} - \mathbf{I}^{(\alpha)}$ is the adjacency matrix for a complete graph on layer α. We can then proceed from any definition of $t_{*,i}$ to $d_{*,i}$ by replacing the second intra-layer step with a step in the complete multiplex network. For example, we obtain $d_{M,i} = 2(\mathcal{A}\widehat{\mathcal{C}}\mathcal{F}\widehat{\mathcal{C}}\mathcal{A}\widehat{\mathcal{C}})_{ii}$ for $t_{M,i} = 2[(\mathcal{A}\widehat{\mathcal{C}})^3]_{ii}$. Similarly, one can use any other definition of a cycle (e.g., any of the elementary cycles or the cycles that we discuss in B) as a starting point for defining a multiplex clustering coefficient.

The above formulation allows us to define local and global clustering coefficients for multiplex networks analogously to monoplex networks. We can calculate a natural multiplex analog to the usual monoplex local clustering coefficient for any node i of the supra-graph. Additionally, in a multiplex network, a node u of an intra-layer network allows an intermediate description for clustering between local and the global clustering coefficients. We define

$$c_{*,i} = \frac{t_{*,i}}{d_{*,i}}\,, \tag{2.3}$$

$$C_{*,u} = \frac{\sum_{i\in l(u)} t_{*,i}}{\sum_{i\in l(u)} d_{*,i}}\,, \tag{2.4}$$

$$C_{*} = \frac{\sum_{i} t_{*,i}}{\sum_{i} d_{*,i}}\,, \tag{2.5}$$

where $l(u)$ is as defined before.

We can decompose the expression in Eq. 2.5 in terms of the contributions from

cycles that traverse exactly one, two, and three layers (i.e., for $m = 1, 2, 3$) to give

$$t_{*,i} = t_{*,1,i}\beta^3 + t_{*,2,i}\beta\gamma^2 + t_{*,3,i}\gamma^3\,, \tag{2.6}$$

$$d_{*,i} = d_{*,1,i}\beta^3 + d_{*,2,i}\beta\gamma^2 + d_{*,3,i}\gamma^3\,, \tag{2.7}$$

$$C_*^{(m)} = \frac{\sum_i t_{*,m,i}}{\sum_i d_{*,m,i}}\,. \tag{2.8}$$

We can similarly decompose Eqs. 2.3 and 2.4. Using the decomposition in Eq. 2.6 yields an alternative way to average over contributions from the three types of cycles:

$$C_*(\omega_1, \omega_2, \omega_3) = \sum_m^3 \omega_m C_*^{(m)}\,, \tag{2.9}$$

where $\vec{\omega}$ is a vector that gives the relative weights of the different contributions. We use the term *layer-decomposed clustering coefficients* for $C_*^{(1)}$, $C_*^{(2)}$, and $C_*^{(3)}$. There are also analogs of Eq. 2.9 for the clustering coefficients defined in Eqs. 2.3 and 2.4. Each of the clustering coefficients in Eqs. 2.3–2.5 depends on the values of the parameters β and γ, but the dependence vanishes if $\beta = \gamma$. Unless we explicitly indicate otherwise, we assume in our calculations that $\beta = \gamma$.

2.1.2 Expressing Clustering Coefficients Using Elementary 3-Cycles

We now give a detailed explanation of the process of decomposing any of our walk-based clustering coefficients into elementary cycles. An elementary cycle is a term that consists of products of the matrices $\mathcal{A}$ and $\mathcal{C}$ (i.e., there are no sums) after one expands the expression for a cycle (which is a weighted sum of such terms). Because we are only interested in the diagonal elements of the terms and we consider only undirected intra-layer supra-graphs and coupling supra-graphs, we can transpose the terms and still write them in terms of the matrices $\mathcal{A}$ and $\mathcal{C}$ rather than also using their transposes. There are also multiple ways of writing non-symmetric elementary cycles [e.g., $(\mathcal{AACAC})_{ii} = (\mathcal{CACAA})_{ii}$].

We adopt a convention in which we transpose all elementary cycles so that we select the one in which the first element is $\mathcal{A}$ rather than $\mathcal{C}$ when comparing the two versions of the term from left to right. That is, for two equivalent terms, we choose the one that comes first in alphabetical order. To calculate the clustering coefficients that we defined in the appendix (see B), we also need to include elementary cycles that start and end in an inter-layer step. The set of elementary 3-cycles is thus $\mathscr{E} = \{\mathcal{AAA}$, $\mathcal{AACAC}$, $\mathcal{ACAAC}$, $\mathcal{ACACA}$, $\mathcal{ACACAC}$, $\mathcal{CAAAC}$, $\mathcal{CAACAC}$, $\mathcal{CACACAC}\}$.

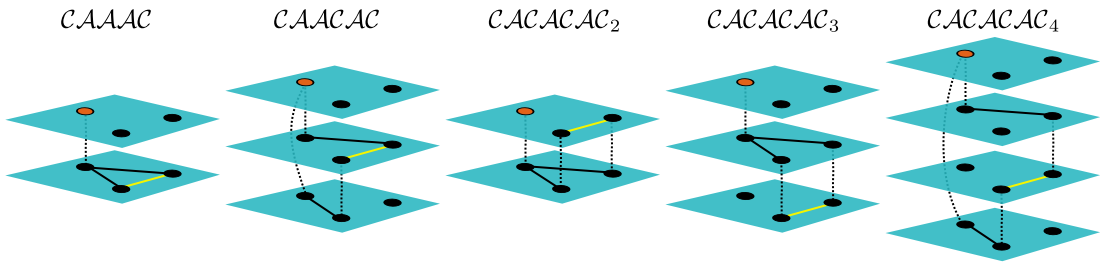

Figure 2.2: Sketches of elementary cycles for which both the first and the last step are allowed to be an inter-layer step. These elementary cycles are $\mathcal{CAAAC}$, $\mathcal{CAACAC}$, and $\mathcal{CACACAC}$. The orange node is the starting point of the cycle. The intra-layer edges are the solid lines, and the intra-layer edges are the dotted curves. In each case, the yellow line represents the second intra-layer step. Note that the elementary cycle $\mathcal{CACACAC}$ also includes three "degenerate" versions in which the 3-cycle returns to a previously-visited layer.

We now write our clustering coefficients using elementary 3-cycles. We obtain the normalization formulas by using the elementary 3-cycles and then replacing the second $\mathcal{A}$ term with $\mathcal{F}$. This yields a standard form for any of our local multiplex clustering coefficients:

$$c_{*,i} = \frac{t_{*,i}}{d_{*,i}}\,, \tag{2.10}$$

where

$$\begin{aligned} t_{*,i} = [&w_{\mathcal{AAA}}\mathcal{AAA} + w_{\mathcal{AACAC}}\mathcal{AACAC} + w_{\mathcal{ACAAC}}\mathcal{ACAAC} \\ &+ w_{\mathcal{ACACA}}\mathcal{ACACA} + w_{\mathcal{ACACAC}}\mathcal{ACACAC} \\ &+ w_{\mathcal{CAAAC}}\mathcal{CAAAC} + w_{\mathcal{CAACAC}}\mathcal{CAACAC} \\ &+ w_{\mathcal{CACACAC}}\mathcal{CACACAC}]_{ii} \end{aligned} \tag{2.11}$$

$$\begin{aligned} d_{*,i} = [&w_{\mathcal{AAA}}\mathcal{AFA} + w_{\mathcal{AACAC}}\mathcal{AFCAC} + w_{\mathcal{ACAAC}}\mathcal{ACFAC} \\ &+ w_{\mathcal{ACACA}}\mathcal{ACFCA} + w_{\mathcal{ACACAC}}\mathcal{ACFCAC} \\ &+ w_{\mathcal{CAAAC}}\mathcal{CAFAC} + w_{\mathcal{CAACAC}}\mathcal{CAFCAC} \\ &+ w_{\mathcal{CACACAC}}\mathcal{CACFCAC}]_{ii}\,, \end{aligned} \tag{2.12}$$

where i is a node-layer pair and the $w_{\mathcal{E}}$ coefficients are scalars that correspond to the weights for each type of elementary cycle. (These weights are different for different types of clustering coefficients; one can choose whatever is appropriate for a given problem.) Note that we have absorbed the parameters β and γ into these coefficients (see below and Table 2.1). We illustrate the possible elementary cycles in Fig. 2.1 and in Fig. 2.2.

One can even express the cycles that include two consecutive inter-layer steps in the standard form of Eqs. 2.11–2.12 for node-aligned multiplex networks, because $\mathcal{CC} = (m-1)\mathcal{I} + (m-2)\mathcal{C}$ in this case. Without the assumption that $\beta = \gamma = 1$, the expansion for the coefficient c_{SM} is cumbersome because it includes coefficients $\beta^k \gamma^h$ with all possible combinations of k and h such that $k+h = 6$ and $h \neq 1$. Furthermore, in the general case, it is also not possible to infer the number of layers in which a walk traverses an intra-layer edge based on the exponents of β and γ for c_{SM} and $c_{SM'}$. For example, in $c_{SM'}$, the intra-layer elementary triangle $\mathcal{AAA}$ includes a contribution from both β^3 (i.e., the walk stays in the original layer) and $\beta\gamma^2$ (i.e., the walk visits some other layer but then comes back to the original layer without traversing any intra-layer edges while it was gone). Moreover, all of the terms with m arise from a walk moving to a new layer and then coming right back to the original layer in the next step. Because there are $m-1$ other layers from which to choose, the influence of cycles with such transient layer visits is amplified by the total number of layers in a network. That is, adding more layers (even ones that do not contain any edges) changes the relative importance of different types of elementary cycles.

In Table 2.1, we show the values of the coefficients $w_{\mathbf{E}}$ for the different ways that we define 3-cycles in multiplex networks. In Table 2.2, we show their corresponding expansions in terms of elementary cycles for the case $\beta = \gamma = 1$. These cycle decompositions illuminate the difference between $c_{M,i}$, $c_{M',i}$, $c_{SM,i}$, and $c_{SM',i}$. The clustering coefficient $c_{M,i}$ gives equal weight to each elementary cycle, whereas $c_{M',i}$ gives half of the weight to $\mathcal{AAA}$ and $\mathcal{ACACA}$ cycles (i.e., the cycles that include an implicit double-counting of cycles) as compared to the other cycles.

2.1.3 Clustering Coefficients for Aggregated Networks

A common way to study multiplex networks is to aggregate layers to obtain either multi-graphs or weighted networks, where the number of edges or the weight of an edge is the number of different types of edges between a pair of nodes [1]. One can then use any of the numerous ways to define clustering coefficients for weighted monoplex networks [84, 68] to calculate clustering coefficients for the aggregated network.

One of the weighted clustering coefficients is a special case of our multiplex clustering coefficient (for others, see References [102, 3, 42] calculated a weighted clustering coefficient as

$$C_{Z,u} = \frac{\sum_{vw} W_{uv} W_{vw} W_{wu}}{w_{\max} \sum_{v \neq w} W_{uv} W_{uw}} = \frac{(\mathbf{W}^3)_{uu}}{((\mathbf{W}(w_{\max}\mathbf{F})\mathbf{W})_{uu}}\,, \tag{2.13}$$

C.C.	$\beta^h\gamma^k$	$\mathcal{AAA}$	$\mathcal{AACAC}$	$\mathcal{ACAAC}$	$\mathcal{ACACA}$	$\mathcal{ACACAC}$	$\mathcal{CAAAC}$	$\mathcal{CAACAC}$	$\mathcal{CACACAC}$
M	β^3	2							
	$\beta\gamma^2$		2	2	2				
	γ^3					2			
M'	β^3	1							
	$\beta\gamma^2$		2	2	1				
	γ^3					2			
SM'	β^3	1							
	$\beta\gamma^2$	$2(m-1)$	2	4	3		1		
	γ^3			$2(m-2)$	$2(m-2)$	2		2	
SM	β^6	1							
	$\beta^4\gamma^2$	$2(m-1)$	4	4	4		1		
	$\beta^3\gamma^3$		$2(m-2)$	$2(m-2)$	$4(m-2)$	8		4	
	$\beta^2\gamma^4$	$(m-1)^2$	$4(m-1)$	$4(m-1)$	$(m-2)^2$	$8(m-2)$	$2(m-1)$	$2(m-2)$	4
	$\beta^1\gamma^5$		$2(m-2)(m-1)$	$2(m-2)(m-1)$		$2(m-2)^2$		$4(m-1)$	$4(m-2)$
	γ^6						$(m-1)^2$	$2(m-2)(m-1)$	$(m-2)^2$

Table 2.1: Coefficients of elementary multiplex 3-cycle terms $w_{\mathcal{E}}$ (see Eqs. 2.11 and 2.12) for different multiplex clustering coefficients. For example, $w_{\mathcal{AAA}}$ for type-M clustering coefficients (i.e., C_M, $C_{M,u}$, and $c_{M,i}$) is equal to $2\beta^3$. For type-SM' and type-SM clustering coefficients, we calculate the expansions only for node-aligned multiplex networks.

C. C.	$\mathcal{AAA}$	$\mathcal{AACAC}$	$\mathcal{ACAAC}$	$\mathcal{ACACA}$	$\mathcal{ACACAC}$	$\mathcal{CAAAC}$	$\mathcal{CAACAC}$	$\mathcal{CACACAC}$
M	2	2	2	2	2	0	0	0
M'	1	2	2	1	2	0	0	0
SM	$1m^2$	$2m^2$	$2m^2$	m^2	$2m^2$	m^2	$2m^2$	m^2
SM'	$2m-1$	2	$2m$	$2m-1$	2	1	2	0

Table 2.2: Coefficients of the elementary multiplex 3-cycle terms $w_{\mathcal{E}}$ (see Eqs. 2.11 and 2.12) for different multiplex clustering coefficients when $\beta = \gamma = 1$. For type-SM' and type-SM clustering coefficients, we calculate the expansions only for node-aligned multiplex networks.

where $\mathbf{W}$ is the sum aggregate adjacency matrix as defined before, the quantity $w_{\max} = \max_{u,v} \mathbf{W}_{uv}$ is the maximum weight in $\mathbf{W}$, and $\mathbf{F}$ is the adjacency matrix of the complete unweighted graph. We can define the global version C_Z of $C_{Z,u}$ by summing over all of the nodes in the numerator and the denominator of Eq. 2.13 (analogously to Eq. 2.5).

For node-aligned multiplex networks, the clustering coefficients $C_{Z,u}$ and C_Z are related to our multiplex clustering coefficients $C_{M,u}$ and C_M. Letting $\beta = \gamma = 1$ and summing over all layers yields $\sum_{i \in l(u)} ((\mathcal{A}\widehat{\mathcal{C}})^3)_{ii} = (\mathbf{W}^3)_{uu}$ (see section 1.4). That is, in this special case, the weighted clustering coefficients $C_{Z,u}$ and C_Z are equivalent to the corresponding multiplex clustering coefficients $C_{M,u}$ and C_M. That is, $C_{M,u}(\beta = \gamma) = w_{\max} C_{Z,u}$ and $C_M(\beta = \gamma) = w_{\max} C_Z$.

Note that this relationship between our multiplex clustering coefficient and the weighted clustering coefficient in Eq. 2.13 is only true for node-aligned multiplex networks. If some nodes are not shared among all layers, then the normalization of our multiplex clustering coefficient depends on how many nodes are present in the local neighborhood of the focal node. This contrasts with the "global" normalization by $w_{\max}$ used by the weighted clustering coefficient in Eq. 2.13.

2.1.4 Clustering Coefficients in Erdős-Rényi (ER) networks

Almost all real networks contain some amount of transitivity, and it is often desirable to know if a network contains more transitivity than would be expected by chance. In order to examine this question, one typically compares clustering-coefficient values of a network to what would be expected from some random network that acts as a null model. The simplest random network to use is an Erdős-Rényi (ER) network. In this section, we give formulas for expected clustering coefficients in node-aligned multiplex networks in which each intra-layer network is an ER network that is created independently of other intra-layer networks and the inter-layer connections are created as described in chapter 1.

The expected value of the local clustering coefficient in an unweighted monoplex ER network is equal to the probability p of an edge to exist. That is, the density of the neighborhood of a node, measured by the local clustering coefficient, has the same expectation as the density of the entire network for an ensemble of ER networks. In multiplex networks with ER intra-layer graphs with connection probabilities p_α, the same result holds only when all of the layers are statistically identical (i.e., $p_\alpha = p$ for all α). Note that this is true even if the network is not node-aligned. However, heterogeneity among layers complicates the behavior of clustering coefficients. If

the layers have different connection probabilities, then the expected value of the mean clustering coefficient is a nontrivial function of the connection probabilities. In particular, it is not always equal to the mean of the connection probabilities. For example, the formulas for the expected global layer-decomposed clustering coefficients are

$$\langle C_M^{(1)} \rangle = \frac{\sum_\alpha p_\alpha^3}{\sum_\alpha p_\alpha^2} \equiv \frac{\overline{p^3}}{\overline{p^2}}\,, \tag{2.14}$$

$$\langle C_M^{(2)} \rangle = \frac{3 \sum_{\alpha \neq \kappa} p_\alpha p_\kappa^2}{(b-1) \sum_\alpha p_\alpha^2 + 2 \sum_{\alpha \neq \kappa} p_\alpha p_\kappa}\,, \tag{2.15}$$

$$\langle C_M^{(3)} \rangle = \frac{\sum_{\alpha \neq \kappa, \kappa \neq \mu, \mu \neq \alpha} p_\alpha p_\kappa p_\mu}{(b-2) \sum_{\alpha \neq \kappa} p_\alpha p_\kappa}\,. \tag{2.16}$$

The expected values of the local clustering coefficients in node-aligned ER multiplex networks are

$$\langle c_{\mathcal{AAA},i} \rangle = \frac{1}{b} \sum_{\alpha \in L} p_\alpha \equiv \overline{p}\,, \tag{2.17}$$

$$\langle c_{\mathcal{AACAC},i} \rangle = \frac{1}{b} \sum_{\alpha \in L} p_\alpha \equiv \overline{p}\,, \tag{2.18}$$

$$\langle c_{\mathcal{ACAAC},i} \rangle = \frac{1}{b} \sum_{\alpha \in L} \frac{\sum_{\kappa \neq \alpha} p_\kappa^2}{\sum_{\kappa \neq \alpha} p_\kappa}\,, \tag{2.19}$$

$$\langle c_{\mathcal{ACACA},i} \rangle = \frac{1}{b} \sum_{\alpha \in L} p_\alpha \equiv \overline{p}\,, \tag{2.20}$$

$$\langle c_{\mathcal{ACACAC},i} \rangle = \frac{1}{b(b-1)} \sum_{\alpha \in L} \frac{\sum_{\kappa \neq \alpha; \mu \neq \kappa, \alpha} p_\kappa p_\mu}{\sum_{\kappa \neq \alpha} p_\kappa}. \tag{2.21}$$

Note that $c_{M,i}^{(1)} = c_{\mathcal{AAA},i}$ and $c_{M,i}^{(3)} = c_{\mathcal{ACACAC},i}$, but the 2-layer clustering coefficient $c_{M,i}^{(2)}$ arises from a weighted sum of contributions from three different elementary cycles.

In Fig. 2.3, we illustrate the behavior of the global and local clustering coefficients in multiplex networks in which the layers consist of ER networks with varying amounts of heterogeneity in the intra-layer edge densities. Although the global and mean local clustering coefficients are equal to each other when averaged over ensembles of monoplex ER networks, we do not obtain a similar result for multiplex networks with ER layers unless the layers have the same value of the parameter p. The global clustering coefficients give more weight than the mean local clustering coefficients to denser layers. This is evident for the intra-layer clustering coefficients $c_{M,i}^{(1)}$ and $C_M^{(1)}$, for which the ensemble average of the mean of the local clustering coefficient $c_{M,i}^{(1)}$ is always equal to the mean edge density, whereas the ensemble average

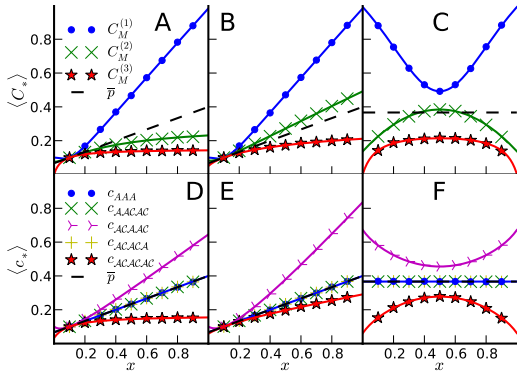

Figure 2.3: (A, B, C) Global and (D, E, F) local multiplex clustering coefficients in multiplex networks that consist of ER layers. The markers give the results of simulations of 100-node ER node-aligned multiplex networks that we average over 10 realizations. The solid curves are theoretical approximations (see Eqs. 2.14–2.16 of the main text). Panels (A, C, D, F) show the results for three-layer networks, and panels (B, E) show the results for six-layer networks. The ER edge probabilities of the layers are (A, D) $\{0.1, 0.1, x\}$, (B, E) $\{0.1, 0.1, 0.1, 0.1, x, x\}$, and (C, F) $\{0.1, x, 1-x\}$.

of the global clustering coefficient $C_M^{(1)}$ has values that are greater than or equal to the mean edge density. This effect is a good example of a case in which the situation in multiplex networks differs from the results and intuition from monoplex networks. In particular, failing to take into account the heterogeneity of edge densities in multiplex networks can lead to incorrect or misleading results when trying to distinguish among values of a clustering coefficient that are what one would expect from an ER random network versus those that are a signature of a triadic-closure process (see Fig. 2.3).

2.2 Transitivity in empirical multiplex networks

We investigate transitivity in empirical multiplex networks by calculating clustering coefficients. In Table 2.3, we give the values of layer-decomposed global clustering coefficients for multiplex networks (four social networks and two transportation networks) constructed from real data. Note that the two transportation networks have different numbers of nodes in different layers (i.e., they are not "node-aligned" [1]). To help give context to the values, the table also includes the clustering-coefficient values that we obtain for ER networks with matching edge densities in each layer. See C for a similar table that uses an alternative null model in which we shuffle the inter-layer connections.

As we will now discuss, multiplex clustering coefficients give insights that are impossible to infer by calculating weighted clustering coefficients for aggregated networks or even by calculating them separately for each layer of a multiplex network.

For each social network in Table 2.3, note that $C_M < C_M^{(1)}$ and $C_M^{(1)} > C_M^{(2)} > C_M^{(3)}$. Consequently, the primary contribution to the triadic structure of these multiplex networks arises from 3-cycles that stay within a given layer. To check that the ordering of the different clustering coefficients is not an artifact of the heterogeneity of densities of the different layers, we also calculate the expected values of the clustering coefficients in ER networks with identical edge densities to the data. We observe that all clustering coefficients exhibit larger inter-layer transitivities than would be expected in a ER networks with identical edge densities, and that the same ordering relationship (i.e.,$C_M^{(1)} > C_M^{(2)} > C_M^{(3)}$) holds. This observation suggests that triadic-closure mechanisms in social networks cannot be considered purely at the aggregated network level, because these mechanisms appear to be more effective inside of layers than between layers. For example, if there is a connection between individuals u and v and also a connection between v and w in the same layer, then it is more likely that u and w "meet" in the same layer than in some other layer.
The transportation networks that we examine exhibit the opposite pattern from the social networks. For example, for the London Underground ("Tube") network, in which each layer corresponds to a line, we observe that $C_M^{(3)} > C_M^{(2)} > C_M^{(1)}$. This reflects the fact that single lines in the Tube are designed to avoid redundant connections. A single-layer triangle would require a line to make a loop among 3 stations. Two-layer triangles, which are a bit more frequent than single-layer ones, entail that two lines run in almost parallel directions and that one line jumps over a single station. For 3-layer triangles, the geographical constraints do not matter because one can construct a triangle with three straight lines.

We also analyze the local triadic closure of the Kapferer tailor-shop social network by examining the local clustering-coefficient values. In Fig. **??**A, we show a comparison of the layer-decomposed local clustering coefficients (also see Fig. 6a of [8]). Observe that the condition $c_{M,i}^{(1)} > c_{M,i}^{2} > c_{M,i}^{(3)}$ holds for most of the nodes. In Fig. **??**B, we subtract the expected values of the clustering coefficients of nodes in a network generated with the configuration model[3] from the corresponding clustering-coefficient values observed in the data to discern whether we should also expect to

[3]We use the configuration model instead of an ER network as a null model because the local clustering-coefficient values are typically correlated with node degree in monoplex networks [65], and an ER-network null model would not preserve degree sequence.

		Tailor Shop	Management	Families	Bank	Tube	Airline
C_M	orig.	0.319**	0.206**	0.223'	0.293**	0.056	0.101**
	ER	0.186 ± 0.003	0.124 ± 0.001	0.138 ± 0.035	0.195 ± 0.009	0.053 ± 0.011	0.038 ± 0.000
$C_M^{(1)}$	orig.	0.406**	0.436**	0.289'	0.537**	0.013"	0.100**
	ER	0.244 ± 0.010	0.196 ± 0.015	0.135 ± 0.066	0.227 ± 0.038	0.053 ± 0.013	0.064 ± 0.001
$C_M^{(2)}$	orig.	0.327**	0.273**	0.198	0.349**	0.043*	0.150**
	ER	0.191 ± 0.004	0.147 ± 0.002	0.138 ± 0.040	0.203 ± 0.011	0.053 ± 0.020	0.041 ± 0.000
$C_M^{(3)}$	orig.	0.288**	0.192**	-	0.227**	0.314**	0.086**
	ER	0.165 ± 0.004	0.120 ± 0.001	-	0.186 ± 0.010	0.051 ± 0.043	0.037 ± 0.000

Table 2.3: Clustering coefficients C_M, $C_M^{(1)}$, $C_M^{(2)}$, and $C_M^{(3)}$ that correspond, respectively, to the global, one-layer, two-layer, and three-layer clustering coefficients for various multiplex networks. "Tailor Shop": Kapferer tailor-shop network ($n = 39$, $m = 4$) [46]. "Management": Krackhardt office cognitive social structure ($n = 21$, $m = 21$) [53]. "Families": Padgett Florentine families social network ($n = 16$, $m = 2$) [14]. "Bank": Roethlisberger and Dickson bank wiring-room social network ($n = 14$, $m = 6$) [79]. "Tube": The London Underground (i.e., "The Tube") transportation network ($n = 314$, $m = 14$) [81]. "Airline": Network of flights between cities, in which each layer corresponds to a single airline ($n = 3108$, $m = 530$) [67]. The rows labeled "orig." give the clustering coefficients for the original networks, and the rows labeled "ER" give the expected value and the standard deviation of the clustering coefficient in an ER random network with exactly as many edges in each layer as in the original network. For the original values, we perform a two-tailed Z-test to examine whether the observed clustering coefficients could have been produced by the ER networks. We designate the p-values as follows: *: $p < 0.05$, **: $p < 0.01$ for Bonferroni-corrected tests with 24 hypothesis; ': $p < 0.05$, ": $p < 0.01$ for uncorrected tests. We do not use any symbols for values that are not significant. We symmetrize directed networks by considering two nodes to be adjacent if there is at least one edge between them. The social networks in this table are node-aligned multiplex graphs, but the transport networks are not node-aligned. We report values that are means over different numbers of realizations: 1.5×10^5 for Tailor Shop, 1.5×10^3 for Airline, 1.5×10^4 for Management, 1.5×10^5 for Families, 1.5×10^4 for Tube, and 1.5×10^5 for Bank.

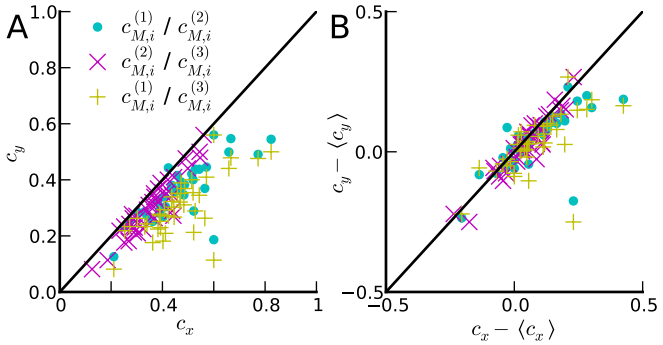

Figure 2.4: Comparison of different local clustering coefficients in the Kapferer tailor-shop network. Each point corresponds to a node. (A) The raw values of the clustering coefficient. (B) The value of the clustering coefficients minus the expected value of the clustering coefficient for the corresponding node from a mean over 1000 realizations of a configuration model with the same degree sequence in each layer as in the original network. In a realization of the multiplex configuration model, each intra-layer network is an independent realization of the monoplex configuration model.

observe the relative order of the local clustering coefficients in an associated random network (with the same layer densities and degree sequences as the data). Similar to our results for global clustering coefficients, we see that taking a null model into account lessens—but does not remove—the difference between the coefficients that count different numbers of layers.

We investigate the dependence of local triadic structure on degree for one social network and one transportation network. In Fig. 2.5A, we show how the different multiplex clustering coefficients depend on the unweighted degrees of the nodes in the aggregated network for the Kapferer tailor shop. Note that the relative order of the mean clustering coefficients is independent of the degree. In Fig. 2.5B, we illustrate that the aggregated network for the airline transportation network exhibits a non-constant difference between the curves of $C_{M,u}$ and the weighted clustering coefficient $C_{Z,u}$. Using a global normalization (see the discussion in Section 2.1.3) reduces the clustering coefficient for the small airports much more than it does for the large airports. That, in turn, introduces a bias.

The airline network is organized differently from the London Tube network. When comparing these networks, note that each layer in the former encompasses flights from a single airline. For the airline network (see Fig. 2.5B), we observe that the two-layer local clustering coefficient is larger than the single-layer one for hubs (i.e., high-degree nodes), but it is smaller for small airports (i.e., low-degree nodes). However, the global clustering coefficient counts the total number of 3-cycles and connected

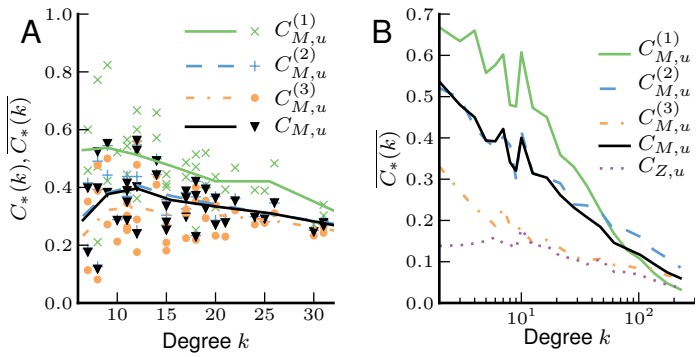

Figure 2.5: Local clustering coefficients versus unweighted degree of the aggregated network for (A) the Kapferer tailor-shop network and (B) the airline network. The curves give the mean values of the clustering coefficients for a degree range (i.e., we bin similar degrees). Note that the horizontal axis in panel (B) is on a logarithmic scale.

triplets and it thus gives more weight to high-degree nodes than to low-degree nodes, and we thus find that the global clustering coefficients for the airline network satisfies $C_M^{(2)} > C_M^{(1)} > C_M^{(3)}$. The intra-airline clustering coefficients have small values, presumably because it is not in the interest of an airline to introduce new flights between two airports that can already be reached by two flights via the same airline through some major airport. The two-layer cycles correspond to cases in which an airline has a connection from an airport to two other airports and a second airline has a direct connection between those two airports. Completing a three-layer cycle requires using three distinct airlines, and this type of congregation of airlines to the same area is not frequent in the data. Three-layer cycles are more likely than single-layer cycles only for a few of the largest airports.

We derived measurements of transitivity for multiplex networks by developing multiplex generalizations of triadic relationships and clustering coefficients. By using examples from empirical data in diverse settings, we showed that different notions of multiplex transitivity are important in different situations. For example, the balance between intra-layer versus inter-layer clustering is different in social networks versus transportation networks (and even in different types of networks within each category, as we illustrated explicitly for transportation networks), reflecting the fact that multilayer transitivity can arise from different mechanisms. Such differences are rooted in the new degrees of freedom that arise from inter-layer connections and are invisible to calculations of clustering coefficients on single-layer networks obtained via aggregation. In other words, transitivity is inherently a multilayer phenomenon: all

of these diverse flavors of transitivity reduce to the same description when one throws away the multilayer information. Generalizing clustering coefficients for multiplex networks makes it possible to explore such phenomena and to gain deeper insights into different types of transitivity in networks. The existence of multiple types of transitivity also has important implications for multiplex network motifs and multiplex community structure. In particular, our work on multiplex clustering coefficients demonstrates that the definition of any clustering notion for multiplex networks needs to be able to handle such features.
The case of social multiplex networks is of particular interest, since our measures point to the fact that triadic closure mechanism is context dependent.

2.3 Subgraph centrality

In this section we scale up the topological scale at which we consider the system and we will look at cycles of all lengths. In monoplex networks subgraph centrality is a well established metric to measure the connectedness of a node at all scales as a generalisation of the clustering coefficient that looks at a local scale. Having established the parallelism between walks in monoplex networks and supra-walks in multiplex networks, we can generalise the definition of subgraph centrality in a direct and standardised way.

2.3.1 Subgraph centrality and Estrada index in monoplex network

Estrada and Rodríguez-Velázquez [32] defined the subgraph centrality of a node i in a complex network as the infinite weighted sum of closed walks of different lengths in the network starting and ending at vertex i, where the weights are the factorial of the length of each walk, i.e.

$$SC_i = \sum_l \frac{\mu_i(l)}{l!} \tag{2.22}$$

where the number of cycles of length l attached to i is $\mu_i(l) = (\mathbf{A}^l)_{ii}$.
It is easy to recognize that the subgraph centrality has the following functional form:

$$SC_i = (\exp(\mathbf{A}))_{ii} \tag{2.23}$$

The Estrada index of a network is defined as

$$SC = \sum_i SC_i = Tr \exp(\mathbf{A}) \tag{2.24}$$

2.3.2 Supra-walks and subgraph centrality for multiplex networks

As done for the clustering coefficient, we generalize the subgraph centrality to multiplex networks constructing on the notion of supra-walk. Thus:

$$sc_{M,i} = \sum_{l} \frac{(\mathcal{A}\widehat{\mathcal{C}})^l}{m^{l-1} l!} \tag{2.25}$$

$$SC_{M,u} = \frac{1}{\kappa_u} \sum_{i \in l(u)} sc_i \tag{2.26}$$

A slight modification of the same functional form 2.23 applies, that is

$$sc_{M,i} = m(\exp(m^{-1}\mathcal{A}\widehat{\mathcal{C}}))_{ii}. \tag{2.27}$$

Note that, while in the case of monoplex networks the off-diagonal element $(\exp(\mathbf{A}))_{ij}$ is the communicability between node i and node j , this is not the case for multiplex networks. This is because, while $(\mathcal{A}\widehat{\mathcal{C}})^l$ exactly count the number of closed walks (cycles) of length l, it is not true for open walks (see section 1.4). Note, additionally, that we need the factor m^{l-1} in the normalization in order to take into account redundant cycles. In other words, the number of cycles attached to i is given by $\mathcal{A}\widehat{\mathcal{C}}^l + \widehat{\mathcal{C}}\mathcal{A}^l = 2\mathcal{A}\widehat{\mathcal{C}}^l$. The possible number of different cycles that touch the same set on nodes in the same order (i.e.,they touch different representatives of the same nodes in different layers in the same order) is exactly $2m^{l-1}$. Normalized in this way, the subgraph centrality is intensive in the number of layers and takes the same value as the standard single layer one one when layers are identical and there is no cost to change layer. Besides, for identical layers, we have:

$$sc_{M,i} = sc_{M,u}, \forall i \in l(u) \tag{2.28}$$

Finally, accordingly to the traditional definition for single layer networks, we define the supra-walk Estrada index of a multiplex network as

$$SC = \frac{1}{m} \sum_{i} sc_{M,i} = Tr(\exp(m^{-1}\mathcal{A}\widehat{\mathcal{C}})) \tag{2.29}$$

It results that:

$$SC = \sum_{u} sc_u \tag{2.30}$$

2.3.3 Subgraph centrality on aggregate network

The subgraph centrality in a weighted network with weighted adjacency matrix $\mathbf{W}$ is defined as [31]

$$sc_u = \exp(\mathbf{W})_{uu}. \tag{2.31}$$

For node-aligned multiplex networks, we have that $\frac{1}{m^l}\sum_{i\in l(u)}\frac{(\mathcal{A}\widehat{\mathcal{C}})_{ii}}{m^l} = (\tilde{\mathbf{W}})^l_{uu}$ (see section 1.4). That is, in this special case, the weighted subgraph centrality measured on the aggregate loopless network is equals to the subgraph centrality measured on the multiplex network,

$$SC_u = SC_{M,u} \tag{2.32}$$

For the Estrada index we also have

$$SC(\tilde{\mathbf{W}}) = SC_M \tag{2.33}$$

Chapter 3

Spectra

Important information on the topological properties of a graph can be extracted from the eigenvalues of the associated adjacency, Laplacian or any other type of graph related matrix. Thus, like spectroscopy for condensed matter physics, graph spectra are central in the study of the structural properties of a complex network.
An $N \times N$ adjacency matrix $\mathbf{A}$ is a real symmetric matrix. As such, has N real eigenvalues, which we order as $\lambda_1 \leq \lambda_2 \leq \cdots \leq \lambda_N$. The set of eigenvalues with corresponding eigenvectors is unique apart from a similarity transformation, i.e.,a relabelling of the nodes in the graph that obviously does not alter the structure of the graph but merely expresses the eigenvectors in a different base.
Accordingly to that, $\mathbf{A}$ can be written as

$$\mathbf{A} = \mathbf{X}\mathbf{\Lambda}\mathbf{X}^T \tag{3.1}$$

where the $N \times N$ orthogonal matrix $\mathbf{X}$ contains, as columns, the eigenvectors $\mathbf{x}_1, \mathbf{x}_2, \ldots,$ $\mathbf{x}_N$ of $\mathbf{A}$ belonging to the real eigenvalues $\lambda_1 \leq \lambda_2 \leq \cdots \leq \lambda_N$ and where the matrix $\mathbf{\Lambda} = diag(\lambda_i)$. The eigendecomposition 3.1 is the basic relation that equates the topology (structural) domain of a network, represented by the adjacency matrix, to the spectral domain of its graph, represented by the orthogonal matrix $\mathbf{X}$ and the diagonal matrix of the eigenvalues $\mathbf{\Lambda}$.
A core subject in network theory is the connection between structure and dynamic, especially the way in which the structure affects critical phenomena. The eigendecomposition 3.1 allows to explain this connection in terms of the spectra of the adjacency matrix thus giving the basic relation that relates the topology a network, to the critical properties of the dynamics occurring on it.

3.1 The largest eigenvalue of supra-adjacency matrix

Consider the adjacency matrix $\mathbf{A}$ of a graph. The Perron Frobenius Theorem for non negative square matrices states that λ_N is simple and non negative, and that its associated eigenvector is the only eigenvector of $\mathbf{A}$ with non negative components. The largest eigenvalue λ_N is also called the spectral radius of the graph. Since $\bar{\mathcal{A}}$ is symmetric and non-negative, we have that the largest eigenvalue $\bar{\lambda}_N$ is simple and non negative possessing the only eigenvector of $\bar{\mathcal{A}}$ with non negative components.
The largest eigenvalue of the adjacency matrix associated to a network has emerged as a key quantity for the study of a variety of different dynamical processes [65], as well as a variety of structural properties, as the entropy density per step of the ensemble of walks in a network.
In order to study the effect of the multiplexity on the spectral radius of a multiplex network, in the following we will interpret $\bar{\mathcal{A}}$ as a perturbed version of $\mathcal{A}$, $\mathcal{C}$ being the perturbation. This choice is reasonable whenever

$$|| \mathcal{C} ||<|| \mathcal{A} ||, \tag{3.2}$$

where $|| \dot{|} ||$ is some matrix metric.
Consider the largest eigenvalue λ of $\mathcal{A}$. Since $\mathcal{A}$ is a block diagonal matrix, the spectrum of $\mathcal{A}$, $\sigma(\mathcal{A})$, is

$$\sigma(\mathcal{A}) = \bigcup_{\alpha} \sigma(\mathbf{A}^{\alpha}), \tag{3.3}$$

$\sigma(\mathbf{A}^{\alpha})$ being the spectrum of the layer-adjacency matrix $\mathbf{A}^{\alpha}$. So, the largest eigenvalue λ of $\mathcal{A}$ is

$$\lambda = \max_{\alpha} \lambda_{\alpha} \tag{3.4}$$

with λ_{α} being the largest eigenvalue of $\mathbf{A}^{\alpha}$. We will look for the largest eigenvalue $\bar{\lambda}$ of $\bar{\mathcal{A}}$ as

$$\bar{\lambda} = \lambda + \Delta\lambda, \tag{3.5}$$

where $\Delta\lambda$ is the perturbation to λ due to the coupling C. For this reason, we call the layer δ for which $\lambda_{\delta} = \lambda$ the dominant layer. Consider a node-aligned multiplex network. Let $\mathbf{1}_{\alpha}$ be a vector of size m with all entries equal to 0 except for the δ-th entry. If ϕ_{δ} is the eigenvector of $\mathbf{A}^{\delta}$ associated to λ_{δ}, we have that

$$\phi = \phi_{\delta} \otimes \mathbf{1}_{\alpha} \tag{3.6}$$

is the eigenvector associated to λ. Observe that ϕ has dimension n, while $\mathbf{1}_\alpha$ has dimension m, where n is the number of nodes, yielding to a product of dimension $N = n \times m$. In the case in which the multiplex is not node-aligned, we must construct the vector ϕ with zeros on all positions, except on the position of the leading eigenvector of the dominant layer.
We can approximate $\Delta\lambda$ as

$$\Delta\lambda \approx \frac{\phi^T \mathcal{C}\phi}{\phi^T\phi} + \frac{1}{\lambda}\frac{\phi^T\mathcal{C}^2\phi}{\phi^T\phi}. \tag{3.7}$$

Because of the structure of ϕ and $\mathcal{C}$, the first term on the *r.h.s.* is zero, while only the diagonal blocks of $\mathcal{C}^2$ take part in the product $\phi^T C^2 \phi$. The diagonal blocks of $\mathcal{C}^2$ are diagonals and

$$(\mathcal{C}^2)_{ii} = \sum_{i'} \mathcal{C}_{ii'}\mathcal{C}_{i'i} = c_i. \tag{3.8}$$

Thus, we have that the perturbation is

$$\Delta\lambda \approx \frac{z}{\lambda}, \tag{3.9}$$

where we have defined the *effective multiplexity* z as the weighted mean of the coupling degree with the weight given by the squares of the entries of the leading eigenvector of $\mathcal{A}$:

$$z = \sum_i c_i \frac{\phi_i^2}{\phi^T\phi}, \tag{3.10}$$

where $z = 0$ in a monoplex network and $z = m - 1$ in a node-aligned multiplex. Summing up, we have that the largest eigenvalue of the supra-adjacency matrix is equal to the largest eigenvalue of the adjacency matrix of the dominant layer at a first order approximation. As a consequence, for example, we will see in chapter 5 that the critical point for an epidemic outbreak in a multiplex network is settled by that of the dominant layer at a first order approximation.
At second order, the deviation of $\bar{\lambda}$ from λ depends on the effective multiplexity and goes to zero with λ. See figure 3.1 and 3.2. Moreover, the approximation given in Eq. (3.9) can fail when the largest eigenvalue is near degenerated. We have two cases in which this can happen:

- the dominant layer is near degenerated,
- there is one (or more) layers with the largest eigenvalue near that of the dominant layer.

The accuracy of the approximation is related to the formula

$$\Delta\lambda \approx \phi^T \mathcal{C} \phi + \sum_i \frac{(\phi^{(i)T} \mathcal{C} \phi)}{\lambda - \lambda^{(i)}}, \tag{3.11}$$

where $\lambda^{(i)}$ and $\phi^{(i)}$ are the non-dominant eigenvalues and the associated eigenvectors. In the first case it is evident that the second term on the *r.h.s.* will diverge, while in the latter, because of the structure of $\mathcal{C}$, ϕ, and $\phi^{(i)}$, it is zero. In that case, we say that the multiplex network is near degenerated and we call the layers with the largest eigenvalues *co-dominant layers*.

When the multiplex network is near degenerated, the ϕ used in the approximation of equation (3.9) has a different structure. Consider that we have l co-dominant layers $\delta_i,\ i = 1, \ldots, l$. If ϕ_{δ_i} is the eigenvector of A^{δ_i} associated to λ_{δ_i}, we have that

$$\phi = \sum_{i=1}^{l} \phi_{\delta_i} \otimes \mathbf{1}_{\delta_i}. \tag{3.12}$$

Note that the same comment on Eq. (3.6) also applies here. The term linear in $\mathcal{C}$ in the approximation of equation (3.9) is no more zero. We have

$$z_c = \frac{\phi^T \mathcal{C} \phi}{\phi^T \phi} = \frac{1}{\phi^T \phi} \sum_{l,m:l \neq m} \phi_{\delta_l}^T \phi_{\delta_m} \tag{3.13}$$

and we name z_c the *correlated multiplexity*. We can decompose z_c in the contribution of each single node-layer pair

$$z_{ci} = \frac{1}{\phi^T \phi} \sum_{m:m \neq l} \sum_j \phi_{\delta_l i} C_{ij} \phi_{\delta_m j}. \tag{3.14}$$

and we call z_{ci} the *correlated multiplexity degree* of node-layer i. By definition, coupled node-layer pairs have the same correlated multiplexity degree. So, if we have m_d co-dominant layers in the multiplex, we get

$$\Delta\lambda \approx z_c + \frac{z}{\lambda} = m_d \sum_{i \in \delta} z_{ci} + \frac{\sum_{i \in \delta} z_i}{\lambda}. \tag{3.15}$$

3.1.1 Statistics of walks

Given a network with adjacency matrix $\mathbf{A}$, the number of walks of length l is given by

$$N_{ij}(l) = (\mathbf{A}^l)_{ij} = \sum_r x_{ri} x_{rj} \lambda_r^l \tag{3.16}$$

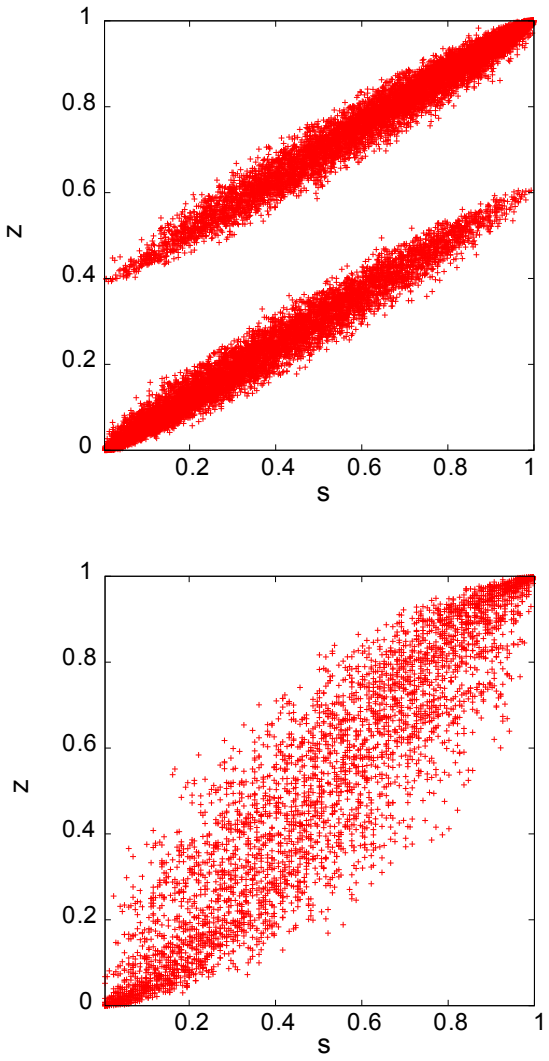

Figure 3.1: Effective multiplexity z as a function of the fraction of nodes coupled s for a two layers multiplex with 800 nodes with a power law distribution with $\gamma = 2.3$ in each layer. For each value of s, 40 different realizations of the coupling are shown while the intra-layer structure is fixed. In the panel on the top the z shows a two band structure, while in the panel on the bottom, it is continuous. The difference is due to the structure of the eigenvector.

where x_{ri} indicates the $i-th$ entry of the normalized eigenvector $\mathbf{x}_r$ belonging to the eigenvalue λ_r. Define the entropy $H_{ij}(l)$ of the ensemble of paths $\{\pi_{ij}(l)\}$ of length l between nodes i and j as

$$H_{ij}(l) = lnN_{ij}(l). \tag{3.17}$$

For large walks $l \longrightarrow \infty$, it results

$$H_{ij}(l) = ln\lambda_N + ln(x_{Ni}x_{Nj}) \tag{3.18}$$

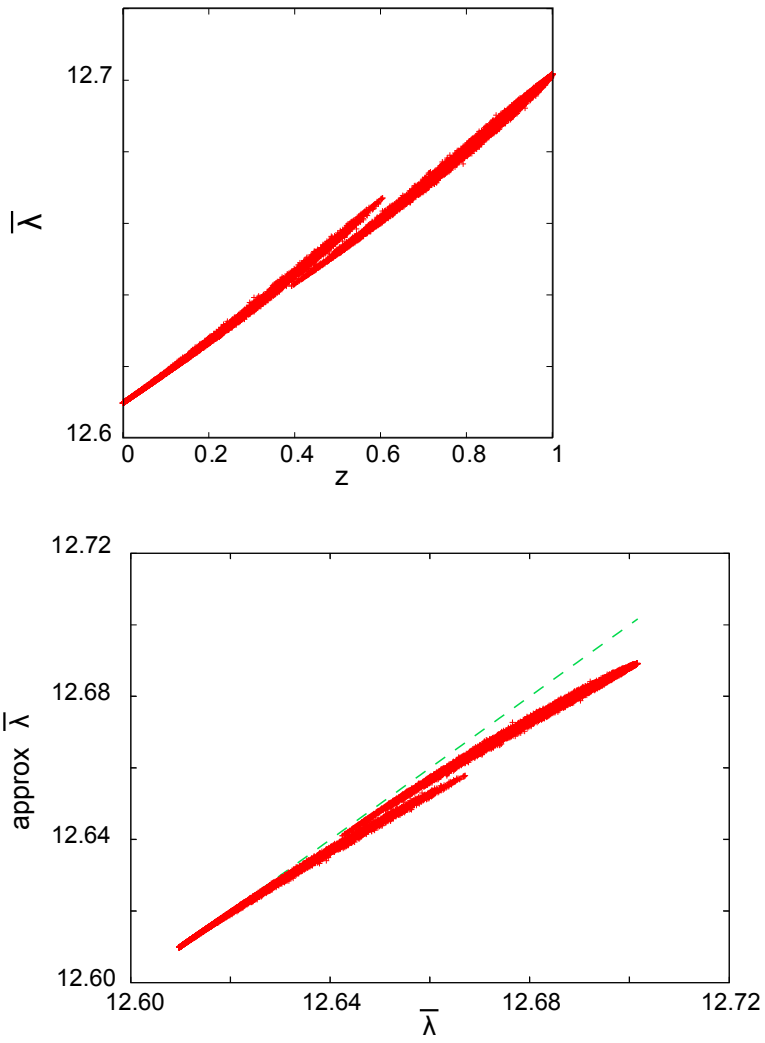

Figure 3.2: Same setting of top panel of previous figure. On the top: calculated $\bar{\lambda}$. We can see two branches corresponding to the two branches of the previous figure. Bottom: calculated vs approximated $\bar{\lambda}$

The leading term is independent of the positions of the endpoints. So, for large l, the entropy production rate is

$$h = \lim_{l \leftarrow \infty} \frac{H_{ij}(l)}{l} = ln\lambda_N. \tag{3.19}$$

That is, h only depends on the largest eigenvalue of the adjacency matrix.
Now, consider walks on multiplex networks that treat in the same way inter- and intra- layer steps, thus we have the supra-adjacency matrix as the supra walk matrix. From the perturbative approximation above, we have that the entropy production

rate on a multiplex network is:

$$\bar{h} = \ln \bar{\lambda}_N \sim ln(\lambda + \frac{z}{\lambda}) \tag{3.20}$$

That is, large walks on a multiplex are dominated by walks on the dominant layer plus a term due to the entropy production needed to reach the dominant layer from non-dominant ones.

3.2 Dimensionality reduction and spectral properties

In this section, we relate the adjacency and Laplacian eigenvalues of a multiplex network to the two quotient networks we have defined in Chapter 1. The main theoretical result that we will exploit is that the eigenvalues of a quotient interlace the eigenvalues of its parent network. Let $m < n$ and consider two sets of real numbers

$$\mu_1 \leq \cdots \leq \mu_m \; and \; \lambda_1 \leq \ldots \lambda_n.$$

We say that the first set *interlaces* the second if

$$\lambda_i \leq \mu_i \leq \lambda_{i+(n-m)}, \;\; for \; i = 1, \ldots, m. \tag{3.21}$$

The key spectral result is that the adjacency eigenvalues of a quotient network interlace the adjacency eigenvalues of the parent network. The same result applies for Laplacian eigenvalues, if the Laplacian matrix of the quotient is defined appropriately, i.e., as we have defined it in chapter 1.

3.2.1 Interlacing Eigenvalues

All the interlacing results we refer to are a consequence of the theorem below, which in turn follows from the Courant-Fisher max-min theorem

Theorem. *([43], Thm. 2.1(i)). Let* $\mathbf{A}$ *be a symmetric matrix of order* n*, and let* $\mathbf{U}$ *be an* $n \times m$ *matrix such that* $\mathbf{U}^T\mathbf{U} = \mathbf{I}$*. Then the eigenvalues of* $\mathbf{U}^T\mathbf{A}\mathbf{U}$ *interlace those of* $\mathbf{A}$*.*

Observe that the matrix $\mathbf{U}^T\mathbf{A}\mathbf{U}$ is symmetric, and hence it has real eigenvalues. If $\mathbf{U}$ is the characteristic matrix of a subset $\alpha \subset \{1, 2 \ldots, n\}$, that is, $\mathbf{U} = (u_{ij})$ of size $n \times \mid \alpha \mid$ and non-zero entries $u_{i\alpha} = 1$ if $i \in \alpha$, then $\mathbf{U}^T\mathbf{A}\mathbf{U}$ equals the principal submatrix of $\mathbf{A}$ with respect to α. As $\mathbf{U}^T\mathbf{U}$ is the identity, we conclude from the theorem above:

Corollary. *([43], Cor. 2.2). Let* $\mathbf{B}$ *be a principal submatrix of* $\mathbf{A}$*. Then the eigenvalues of* $\mathbf{B}$ *interlace the eigenvalues of* $\mathbf{A}$*.*

On the other hand, if $\mathbf{S}$ is the characteristic matrix of the partition, then $\mathbf{S}^T S = \Lambda$ is a diagonal non-singular matrix, and hence $\mathbf{U} = \mathbf{S}\Lambda^{-1/2}$ satisfies the hypothesis of the theorem. We conclude that the eigenvalues of $\mathbf{U}^T\mathbf{A}\mathbf{U} = \Lambda^{-1/2}\mathbf{S}^T\mathbf{A}\mathbf{S}\Lambda^{-172}$ interlace those of $\mathbf{A}$. Using the Lemma 1.3.1.1, we conclude:

Corollary. *([11], Cor. 2.3(i)). Let* $\mathbf{B}$ *be a quotient matrix of* $\mathbf{A}$ *with respect to some partition. Then the eigenvalues of* $\mathbf{B}$ *interlace the eigenvalues of* $\mathbf{A}$*.*

3.2.2 Equitable partitions

Equation 1.22 defines equitable partitions. This can be expressed in matrix form as

$$\mathbf{A}\mathbf{S} = \mathbf{S}Q(\mathbf{A}).$$

We call the matrix $Q(\mathbf{A})$ a regular quotient if it is the quotient of an equitable partition. If the quotient is regular, then the eigenvalues of $Q(\mathbf{A})$ not only interlace but are a subset of the eigenvalues of $\mathbf{A}$. In fact, there is a *lifting* relating both sets of eigenvalues, as we explain now.
If $\mathbf{v}, \mathbf{w}$ are column vectors of size m and n, we say that $\mathbf{S}\mathbf{v}$ represents the vector $\mathbf{v}$ lifted to $\mathbf{A}$, and $\mathbf{S}^T\mathbf{w}$ the vector w projected to $Q(\mathbf{A})$. The vector $\mathbf{S}\mathbf{v}$ has constant coordinates on each $\mathbf{X}_i$, while the vector $\mathbf{S}^T\mathbf{w}$ is created by adding the coordinates on each X_i. The vector $\mathbf{w}$ is called orthogonal to the partition if $\mathbf{S}^T\mathbf{w} = 0$, that is, the sum of the coordinates over each $\mathbf{X}_i$ is zero. If the quotient is regular, the spectrum of $\mathbf{A}$ decomposes into the spectrum of $\mathbf{B}$ lifted to $\mathbf{A}$ (i.e.,eigenvectors constant on each X_i), and the remaining spectrum is orthogonal to the partition (i.e.,eigenvectors with coordinates adding to zero on each X_i):

Theorem. *Let* $\mathbf{B}$ *be the quotient matrix of* $\mathbf{A}$ *with respect to an equitable partition with characteristic matrix* $\mathbf{S}$*. Then the spectrum of* $\mathbf{B}$ *is a subset of the spectrum of* $\mathbf{A}$*. More precisely,* $(\lambda, \mathbf{v})$ *is an eigenpair of* $\mathbf{B}$ *if and only if* $(\lambda, \mathbf{S}\mathbf{v})$ *is an eigenpair of* $\mathbf{A}$*.*
Moreover, there is an eigenbasis of $\mathbf{A}$ *of the form* $\{\mathbf{S}\mathbf{v}_1, \ldots, \mathbf{S}\mathbf{v}_m, \mathbf{w}_1, \ldots, \mathbf{w}_{(n-m)}\}$ *such that* $\{\mathbf{v}_1, \ldots, \mathbf{v}_m\}$ *is any eigenbasis of* $\mathbf{B}$*, and* $\mathbf{S}^T\mathbf{w}_i = 0$ *for all* i*.*

Proof. The first part follows easily from the identity $\mathbf{A}\mathbf{S} = \mathbf{S}\mathbf{B}$ (note that $\mathbf{S}\mathbf{v} \neq 0$ as $\mathrm{Ker}(\mathbf{S}) = 0$). For the second part, note that $\mathbf{S}$ is an isomorphism onto $\mathrm{Im}(\mathbf{S})$,

as it has trivial kernel, so $\{\mathbf{S}\mathbf{v}_1, \ldots, \mathbf{S}\mathbf{v}_m\}$ is a basis of $\mathrm{Im}(\mathbf{S})$. It is easy to show that the orthogonal complement $\mathrm{Im}(\mathbf{S})^\perp$ equals $\mathrm{Ker}(\mathbf{S}^T)$, hence we can complete the linearly independent set of eigenvectors $\{\mathbf{S}\mathbf{v}_1, \ldots, \mathbf{S}\mathbf{v}_m\}$ to an eigenbasis of $\mathbb{R}^n = \mathrm{Im}(\mathbf{S}) + \mathrm{Im}(\mathbf{S})^\perp$ □

3.2.3 Laplacian Eigenvalues

We want to show that the Laplacian of a quotient graph is the quotient of the Laplacian matrix, as this will allow us to extend the interlacing results to the Laplacian eigenvalues. First, we need to clarify what we mean by the Laplacian of a non-symmetric matrix.

If $\mathbf{A} = (a_{ij})$ is a real symmetric (adjacency) matrix, define the *node out-degrees* as

$$d_i^{out} = \sum_j a_{ij} \text{ (row sum)}. \tag{3.22}$$

The *out-degree Laplacian* is the matrix

$$\mathbf{L}^{out} = \mathbf{D}^{out} - \mathbf{A} \tag{3.23}$$

where $\mathbf{D}^{out}$ is the diagonal matrix of the out-degrees.

We define d_i^{in}, $\mathbf{D}^{in}$, and the in-degree Laplacian $\mathbf{L}^{in}$ analogously. Note that both Laplacian matrices ignore the diagonal values of $\mathbf{A}$. If $\mathbf{A}$ is the adjacency matrix of a graph, we say that the Laplacian ignores self-loops. Consider the left and right quotients of $\mathbf{A}$ with respect to a given partition. Observe that the row sums of $Q_l(\mathbf{A})$ are

$$\bar{d}_i = \frac{1}{n_i} \sum_{k \in V_i} d_k \tag{3.24}$$

the average node degree in V_i.

Let $\bar{D}$ be the diagonal matrix of the average node degrees. Then we define the *quotient Laplacian* as the matrix

$$\mathbf{L}_Q = \bar{D} - Q_l(\mathbf{A}) \tag{3.25}$$

that is, the out-degree Laplacian of the left quotient matrix. Alternatively, we could have defined L_Q as the in-degree Laplacian of the right quotient matrix, giving a transpose matrix with the same eigenvalues. (Note that there is no obvious way of interpreting the symmetric quotient $Q_s(\mathbf{L})$ as the Laplacian of a graph.)

Now we can prove that the Laplacian of the quotient is the quotient of the Laplacian, in the following sense.

Theorem. *Let G be a graph with adjacency matrix $\mathbf{A}$ and Laplacian matrix $\mathbf{L}$. Then:*

$$\mathbf{L}^{out}(Q_l(\mathbf{A})) = Q_l(\mathbf{L})$$

.

The analogous result holds for the right quotients and the in-degree Laplacian.

Proof. By definition (see):

$$Q_l(\mathbf{L}) = \Lambda^{-1}\mathbf{S}^T\mathbf{L}\mathbf{S} = \Lambda^{-1}\mathbf{S}^T(\mathbf{D}-\mathbf{A})\mathbf{S} = \Lambda^{-1}\mathbf{S}^T\mathbf{D}\mathbf{S} - \Lambda^{-1}\mathbf{S}^T\mathbf{A}\mathbf{S} = \bar{\mathbf{D}} - \mathbf{A}$$

The second statement follows by transposing the equation above. □

This theorem allows us to use the interlacing results of 3.2.1 for Laplacian eigenvalues. We finish by studying equitable partitions in the context of Laplacian matrices. We demonstrate that a partition being regular for the Laplacian matrix is equivalent to the partition being almost regular for the adjacency matrix. In particular, the spectral results of subsection 3.2.2 will hold for almost regular quotients and Laplacian eigenvalues.

Theorem. *Let G be a graph with adjacency matrix $\mathbf{A}$ and Laplacian matrix $\mathbf{L}$. Then a partition is equitable with respect to $\mathbf{L}$ if and only if it is almost equitable with respect to $\mathbf{A}$.*

Proof. By relabelling the nodes if necessary, we can assume the block decomposition

$$A = \begin{pmatrix} A_{11} & \dots & A_{1m} \\ \vdots & \ddots & \vdots \\ A_{m1} & \dots & A_{mm} \end{pmatrix}, \tag{3.26}$$

where the $n_i \times n_j$ submatrix A_{ij} represents the edges from V_i to V_j. The matrix $\mathbf{L}$ has then a similar block decomposition into submatrices L_{ij}. As $\mathbf{L} = \mathbf{D} - \mathbf{A}$ and $\mathbf{D}$ is diagonal, we have $L_{ij} = -A_{ij}$ for all $i \neq j$. In particular, the row sums of L_{ij} are constant if and only if the row sums of A_{ij} is constant, for all $i \neq j$. On the other hand, as the row sums in $\mathbf{L}$ are zero, the row sums in L_{ii} equals the sum of the row sums of the matrices L_{ij} for $j \neq i$, and the result follows. □

3.3 Network of layers and Aggregate Network

Applying the spectral results we have already presented, we conclude that the adjacency, respectively Laplacian, eigenvalues of the network of layers interlace the adjacency, respectively Laplacian, eigenvalues of the multiplex network. Namely, if $\mu_1, \dots, \mu_m$ are the (adjacency resp. Laplacian) eigenvalues of the network of layers, then

$$\lambda_i \leq \mu_i \leq \lambda_{i+(N-m)} \quad \text{for } i = 1, \dots, m, \tag{3.27}$$

where $\lambda_1, \dots, \lambda_N$ are the (adjacency resp. Laplacian) eigenvalues of the multilayer network.

The network of layers, ignoring weights and self-loops, simply represents the layer connection configuration (Fig. 1.2). The connectivity of this reduced representation, measured in terms of the eigenvalues, thus relates to the connectivity of the entire multiplex network via the interlacing results.

We turn to the question of when the layer partition is equitable. This requires, in particular, that the intra-layer degrees are constant, that is, each layer must be a d^α-regular graph, a very strong condition unlikely to be satisfied in real-world multiplex networks. Instead, we call a multilayer network *regular* if the layer partition is almost equitable, that is, the inter-layer connections are independent of the chosen vertices. This is a more natural condition, and in particular it is equivalent to require the multiplex being node-aligned.

If the multiplex network is regular, i.e.,node aligned, then, in addition to the interlacing, the Laplacian eigenvalues of the network of layers are a subset of the Laplacian eigenvalues of the multiplex, and we can lift a Laplacian eigenbasis of the quotient, as described in Section 3.2.3. This latter result has also been derived in [89] without referring to the theory of quotient graphs.

Finally, using the spectral results, we conclude that the adjacency (respectively Laplacian) eigenvalues of the aggregate network interlace the adjacency (respectively Laplacian) eigenvalues of the multiplex. Namely, in a multiplex network with N node-layer pairs and n nodes, the (adjacency resp. Laplacian) eigenvalues of the aggregate network quotient $\mu_1, \dots, \mu_n$ satisfy

$$\lambda_i \leq \mu_i \leq \lambda_{i+(n-\widetilde{n})} \quad \text{for } i = 1, \dots, \widetilde{n}, \tag{3.28}$$

where $\lambda_1, \dots, \lambda_N$ are the (adjacency resp. Laplacian) eigenvalues of the multiplex network.

Observe that requiring the aggregate network to be regular, or almost regular, is in

this case very restrictive, as it would require that every pair of nodes connects in the same uniform way on every layer, and thus it is not likely to occur on real-world multiplex networks.
The results obtained in this section will be crucial in studying structural transitions as we will show in the next chapter[1].

3.4 Layer subnetworks

Evidently, the layers of a multiplex form subnetworks, and it is natural to relate the eigenvalues of each layer to the eigenvalues of the multiplex. The interlacing result applies to the adjacency eigenvalues of an induced subnetwork, such as the layers, and partial interlacing also holds for the Laplacian eigenvalues. More precisely, if a layer-graph G_α has n_α nodes and adjacency (resp. Laplacian) eigenvalues $\mu_1, \ldots, \mu_\alpha$, and $\lambda_1, \ldots, \lambda_N$ are the adjacency (resp. Laplacian) eigenvalues of the whole multilayer network, then

$$\lambda_i \leq \mu_i \leq \lambda_{i+(N-n_\alpha)} \qquad \text{for } i = 1, \ldots, n_\alpha, \quad \text{resp.} \tag{3.29}$$

$$\mu_i \leq \lambda_{i+(N-n_\alpha)} \qquad \text{for } i = 1, \ldots, n_\alpha. \tag{3.30}$$

3.5 Discussion and some Applications

From a physical point of view, the adjacency and Laplacian spectra of a network encode information on structural properties of the system represented by the network related to different dynamical processes occurring upon it. We now discuss some consequences and applications of the spectral results derived in the previous sections. In the following, let us write $\lambda_i(A)$ for the ith smallest eigenvalue of a matrix A.

3.5.1 Adjacency spectrum

The spectrum of the adjacency matrix is directly related to different dynamical processes that take place on the system, such as spreading processes, for which it has been shown that critical properties are related to the inverse of the largest eigenvalue of this matrix. As an example, consider a contact process on the multilayer network $\mathcal{M}$ whose dynamic is described by the equation

$$p_i(t+1) = \beta \sum_j \bar{a}_{ij} p_j(t) - \mu\, p_i(t) \tag{3.31}$$

[1] Although here we deal only with multiplex network, the spectral theory of quotient graphs also applies to the more general framework of multilayer networks

in which $p_i(t)$ is the probability of node i to be infected at time t, β is the infection rate, μ is the recovery rate and $\bar{a}_{ij}$ are the elements of the supra-adjacency matrix $\bar{\mathcal{A}}$. This model is a special case of the more general one introduced in Chapter 5. In this model, each infected node contacts its neighbours with probability 1, and tries to infect them. The contact between two instances of the same object in different layers is modelled in the same way as the contact between any two other nodes.
The critical value of the infection rate for which the infection survives is given by

$$\beta_c = \frac{\mu}{\lambda_N(\bar{\mathcal{A}})}. \tag{3.32}$$

From the interlacing result for the layer subnetworks we have that

$$\lambda_{n_\alpha}(\mathbf{A}_\alpha) \leq \lambda_N(\bar{\mathcal{A}}), \tag{3.33}$$

where $\mathbf{A}_\alpha$ is the adjacency matrix of the layer α. This means that the critical point for the multiplex network β_c is bounded from above by the corresponding critical points of the independent layers. This implies that the multiplex network is more efficient as far as a spreading processes are concerned than the most efficient of its layers on its own.
On the other hand, if λ_m is the largest adjacency eigenvalue of the network of layers, then

$$\lambda_m \leq \lambda_N(\mathcal{A}), \tag{3.34}$$

which means that the connections between layers also impose constraints to the dynamics on the multilayer network. In particular, the critical point of the spreading dynamics on the multilayer network is bounded from above by the corresponding critical point of the network of layers. Interestingly, the existence of this bound explain the existence of a *mixed phase* [28].
Consider now the same process (3.31), this time defined on the aggregate network

$$p_u(t+1) = \beta \sum_v a_{uv} p_v(t) - \mu\, p_u(t). \tag{3.35}$$

Here a_{uv} are the elements of $Q(\bar{\mathcal{A}})$, the adjacency matrix of the aggregate graph. The critical value is given by

$$\widetilde{\beta}_c = \frac{\mu}{\lambda_n(Q(\bar{\mathcal{A}}))} \tag{3.36}$$

where n is the number of nodes in $\mathcal{M}$ (the size of the aggregate network). From the interlacing result we have that

$$\widetilde{\beta}_c \geq \beta_c.$$

Therefore the spreading process on $\mathcal{M}$ is at least as efficient as the same spreading process on the aggregate network.It is important to note that Equations 3.31 and 3.35 describe two rather different processes, that is, two different strategies that actors can adopt in order to spread information across the multiplex network. In the former, a node can infect any other node on any layer, while in the latter, each supra-node chooses at each time step with uniform probability a layer in which an instance representing it is present and then contacts all its neighbours in that layer. Our results show that the former strategy is more effective than the latter, as expressed by the relation between the critical points.

3.5.2 Laplacian spectrum

The Laplacian of a network $\mathbf{L} = (l_{ij})$ is the operator of the dynamical process described by

$$\dot{p}_{ij}(t) = -\sum_k p_{ik}(t)\, l_{ki} \tag{3.37}$$

where $p_{ij}(t)$ represents the transition probability of a particle from node i to node j at time t.

The second smallest eigenvalue of the Laplacian matrix sets the time scale of the process. From the interlacing results applied to the Laplacian matrix we have that for any quotient

$$\lambda_2(\bar{\mathcal{L}}) \leq \lambda_2(Q(\bar{\mathcal{L}})). \tag{3.38}$$

That is, the relaxation time on the multiplex is at most the relaxation time on any quotient, in particular the network of layers or the aggregate network. If we interpret λ_2 of the Laplacian of a network as algebraic connectivity [17], Eq. 3.38 means that the algebraic connectivity of the multiplex network is always bounded above by the algebraic connectivity of any of its quotients.

On the other hand, the Laplacian of the aggregated network is the operator corresponding to the dynamical process described by

$$\dot{p}_{uv}(t) = \sum_w p_{uw}(t)\, a_{wv} - d_u\, p_{uv}(t) = \sum_w p_{uw}(t)\, \tilde{l}_{wu} \tag{3.39}$$

where $p_{uv}(t)$ is the transition probability of a particle from supra-node u to supra-node v at time t, a_{uw} are the elements of the adjacency matrix of the aggregated contact network, $\tilde{L} = (\tilde{l}_{ij})$ is the Laplacian matrix of the aggregate contact network

(i.e. $\tilde{L} = Q(\bar{\mathcal{L}})$) and $d_u = \sum_v a_{uv}$ is the strength or degree of a node in the aggregate network). Note that if we define the overlapping degree [8] of a node as

$$o_u = \sum_v a_{uv}$$

then we have that

$$d_u = \frac{1}{\kappa_u} o_u.$$

From the interlacing result for the Laplacian we have that

$$\lambda_2(\bar{\mathcal{L}}) \leq \lambda_2(Q(\bar{\mathcal{L}})). \tag{3.40}$$

That is, the diffusion process on the aggregate network (Eq. 3.39) is faster than the diffusion process on the entire multiplex network (Eq. 3.37). Note that in [89], in a setting in which the multiplex is node-aligned, the authors obtained by means of a perturbative analysis that $\lambda_2(\bar{\mathcal{L}}) \sim \lambda_2(Q(\bar{\mathcal{L}}))$ when the diffusion parameter between layers is large enough. In [2] this result is generalized (in a different framework, since they are interested in structural properties of interdependent networks) to all almost regular multilayer networks. In the framework of quotient networks that we have presented here those results arise in a very natural way. Besides, eigenvalue interlacing between multilayer and quotient eigenvalues holds for every possible inter-layer connection scheme. In the next chapter we will discuss the existence and location of an abrupt transition in the structure of a multiplex network by constructing on the interlacing results for the Laplacian. We finally note that, in the context of synchronization, the smallest non-zero Laplacian eigenvalue λ_2 is also related to the stability of a synchronized state [5], and indeed the larger λ_2 is, the more stable is the synchronized state. Considering a multiplex network, the bound in (3.38) means that the synchronized state of a system supported on the multiplex network is at most as stable as the synchronized state on any of its quotients.

3.6 The algebraic connectivity

The algebraic connectivity of a graph G is the second-smallest eigenvalue of the Laplacian matrix of G [100]. We naturally define the algebraic connectivity of a multiplex as the second-smallest eigenvalue of its the supra-Laplacian matrix.
From the interlacing results of the previous section, we know that

$$\bar{\mu}_2 \leq \tilde{\mu}_{a2} \tag{3.41}$$

$$\bar{\mu}_2 \leq m \tag{3.42}$$

We also know that m is always an eigenvalue of the supra-Laplacian, so, we can look for the condition under which $\bar{\mu}_2 = m$ holds. By combining equations 3.41 and 3.42, we arrive to the conclusion that

$$if\ m \geq \tilde{\mu}_{a2},\ \text{then}\ \bar{\mu}_2 \neq m.$$

On the other hand, we can approximate $\bar{\mu}_2$ as

$$\bar{\mu}_2 \sim \mu_2 + \triangle\mu_2 \tag{3.43}$$

where μ_2 is the second-smallest eigenvalue of L and

$$\triangle\mu_2 = \sum_{i<j} c_{ij}(x_i - x_j)^2 \tag{3.44}$$

where $\mathbf{x}$ is the unity norm eigenvector associated to μ_2 and x_i its $i-th$ entry. Because of the structure of $\mathcal{C}$ and $\mathbf{x}$, it results

$$\triangle\mu_2 = m - 1 \tag{3.45}$$

for a node-aligned multiplex network. Thus, since m is always an eigenvalue of $\bar{L}$, for that approximation to be correct, the following condition must hold

$$\mu_2 + m - 1 < m \tag{3.46}$$

from which we can conclude that

$$if\ \mu_2 < 1\ then\ \bar{\mu}_2 \neq m.$$

In summary, we have that

$$if\ \tilde{\mu}_{a2} < m\ or\ \mu_2 > 1\ then\ \bar{\mu}_2 \neq m,$$

the converse not being true in general.

Chapter 4

Structural organization and transitions

Complex networks show non-traditional critical effects due to their extreme compactness (small-world property) together with their *complex organization* [30]. The introduction of multilayer networks in general, and multiplex in particular, as a more natural substrate for a plethora of phenomena, poses the central theoretical question of whether critical phenomena will behave differently on such networks with respect to traditional networks. So far theoretical studies have pointed out that such differences in the critical behaviours indeed exists [70, 90]. In [2] and in [76] it has be showed that a multiplex network can exists in different *structural phases*, the transition among them being abrupt under some conditions.
The main observation is that three different topological scales can be naturally identified in a multiplex: that of the individual layers, that of the network of layers, and that of the aggregate network. The notion of quotient graph that we have introduced in Chapter 1 gives the connection between those scales in therms of spectral properties of the parent multiplex network an its aggregate representation.
In the rest of this chapter we will focus on the spectra of the supra-Laplacian in order to show how the interplay between those scales affect the whole structural organization of the multiplex network. The spectrum of the Laplacian is a natural choice to address this problem, since it reveals a number of structural properties. In particular, eigengaps are known to unveil a number of structural and dynamical properties of the network related to the presence of different topological scales in it, from communities at different topological scales to synchronization patterns [6, 87]. Thus, the emerging of an eigengap points to structural changes going on, that will result in qualitatively different dynamical patterns. For this reason, we will introduce a weight parameter p for the coupling. This parameter will allow us to tune the relative strength of the

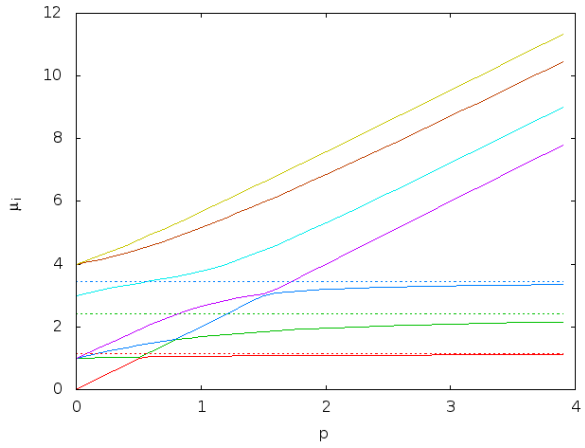

Figure 4.1: Eigenvaluse of a toy multiplex with 4 nodes per layers. Continuous lines are the eigenvalues of the multiplex networks; dashed lines are the eigenvalues of the aggregate network

coupling with respect to intra-layer connectivity [1].
The supra-Laplacian 1.14 with the weight parameter p reads as:

$$\bar{\mathcal{L}} = \bigoplus_{\alpha} \mathbf{L}^{\alpha} + p\mathcal{L}_C, \tag{4.1}$$

and in the special case of node-aligned multiplex networks it takes the simple form:

$$\bar{\mathcal{L}} = \bigoplus_{\alpha} (\mathbf{L}^{(\alpha)} + p(m-1)\mathbf{I_n}) - p\mathbf{K_m} \otimes \mathbf{I}_n. \tag{4.2}$$

Remember that, in this special case, the spectrum of the Laplacian of the network of layers is a subset of the spectrum of the parent supra-Laplacian. In figure 4.1 the full spectrum of a toy multiplex of 4 nodes and 2 layers (then 8 node-layer pairs) is showed. The first thing to note - as already observed in [39] and [89]- is that the spectrum splits in two groups: one made up by eigenvalues that stay bounded while increasing p, and one group of eigenvalues that diverge by increasing p. The whole characterization of the structural changes in a multiplex network basically depends on that splitting, i.e. on the emerging of gaps in the spectrum.

4.1 Eigengap and structural transitions

The Laplacian spectrum of the network of layers is composed of just two eigenvalues: 0 with multiplicity 1, and mp with multiplicity $(m-1)$. Because of the inclusion

[1] The weight p may have a physical meaning, like the (inverse of) the commuting time in a transportation multiplex network, however it can be always intended as a tuning parameter.

relation between the cross-grained and the parent spectra, mp will be always an eigenvalue of the supra-Laplacian. It results that, for low enough values of p, mp will be the smallest non-zero eigenvalue of $\bar{\mathcal{L}}$. On the other hand, each eigenvalue $\bar{\mu}_i$, with $i = 1 \dots n$, will be bounded by the respective Laplacian eigenvalue $\tilde{\mu}_i^{(a)}$ of the aggregate network because of the interlace.

It is evident that, by increasing p, at some value $p = p^*$, it will happen that $\bar{\mu}_2 \neq mp$ and that it will approach its bound $\tilde{\mu}_2^{(a)}$. For continuity, at p^*, $\bar{\mu}_3 = mp$ must hold, since mp is always an eigenvalue of the supra-Laplacian. $p = p^*$ is the point at which the structural transition described in [2, 59] occurs, as already noted by Darabi Sahneh et al. [83]. Each eigenvalue up to $\bar{\mu}_n$ will follow the same pattern, following the line $\bar{\mu}_i = mp$ and leaving it to approach its bound $\tilde{\mu}_i^{(a)}$ when it hits the next eigenvalue $\bar{\mu}_i = mp$ (see Fig.:4.1). At the point $p = p^\diamond$ at which $\bar{\mu}_n \neq mp$, $\bar{\mu}_{n+1} = mp$ must hold and it will hold forever, since $\bar{\mu}_{n+1}$ is not bounded.

Following this reasoning, we realize that the supra-Laplacian spectrum for $p > p^\diamond$ can be divided into two groups: one of n bounded eigenvalues that will approach the aggregated Laplacian eigenvalues as p increases, and one of $N - n = n(m-1)$ eigenvalues diverging with p. Because of that, the system can be characterized by an eigengap emerging at $p^\diamond$.Moreover, while the splitting of the eigenvalues in those two groups is always present (because of the interlacing), the crossing of the eigenvalues at p^* and at $p^\diamond$ (and between those points) only happens when the multiplex is node-aligned, this is because the inclusion relation only holds in that case.

In order to quantify an eigengap, we introduce the following metric:

$$g_k = \frac{\log(\bar{\mu}_{k+1}) - \log(\bar{\mu}_k)}{\log(\bar{\mu}_{k+1})} \tag{4.3}$$

and we will focus on $g_n(p)$, i.e. the gap emerging between the last bounded eigenvalue and the first unbounded at $p^\diamond$.

By construction

$$g_n(p^\diamond) = 0. \tag{4.4}$$

For $p > p^\diamond$, $\log(\bar{\mu}_{n+1})$ will diverge while $\log(\bar{\mu}_n)$ will remain bounded by $\tilde{\mu}_n^{(a)}$, so g_n will approach 1. For $p < p^\diamond$, in general both $\bar{\mu}_{n+1}$ and $\bar{\mu}_n$ will be in the continuous part of the spectrum, so g_n will be 0 in the large size limit. That is,

$$\begin{aligned} g_n &= 0, p \leq p^\diamond \\ g_n &\neq 0, p > p^\diamond. \end{aligned} \tag{4.5}$$

This phenomenology is confirmed by our numerical experiment (see Fig. 4.2), and

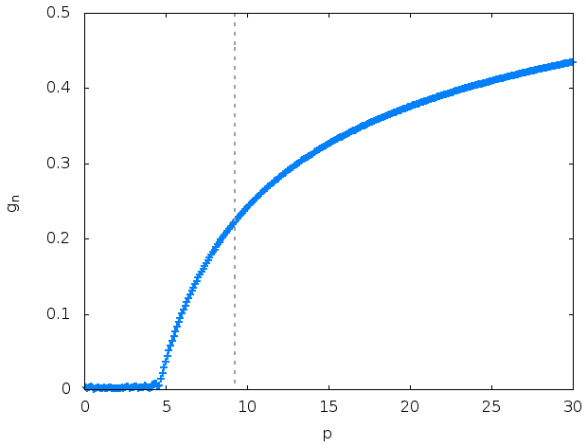

Figure 4.2: Eigengap between the last bounded and the first unbounded eigenvalue for a multiplex network of two Erdosh-Reniy of 200 nodes and $< k >= 5$. Dashed line is the bound given in the text

it describes a structural transition occurring at $p^{\diamond}$. In the case of a non node-aligned multiplex network, where $p^{\diamond}$ is not defined since there is no crossing, $g_n(p)$ can be used to operationally define it.

An upper bound for $p^{\diamond}$ can be given in terms of the structural properties of the layers. If $\omega_i^{(\alpha)}$ is the strength of node u in layer α, its strength in the aggregate network is $\tilde{\omega}_i = \frac{1}{m}\sum_\alpha \omega_i^{(\alpha)}$ Next define

$$\tilde{\omega}_{ij} = \tilde{\omega}_i + \tilde{\omega}_j, \forall i \sim j \tag{4.6}$$

where $i \sim j$ indicates a link between i and j in the aggregate network. We have that [25]

$$\tilde{\mu}_n^{(a)} \leq max_{i\sim j}\{\tilde{\omega}_{ij}\}, \tag{4.7}$$

and we can give the following bound for $p^{\diamond}$

$$p^{\diamond} \leq \frac{max_{i\sim j}\{\tilde{\omega}_{ij}\}}{m}, \tag{4.8}$$

and

$$p^{\diamond} \leq \frac{max_{i\sim j}\{\sum_\alpha \omega_{ij}^{\alpha}\}}{m^2} \tag{4.9}$$

The exact value of $p^{\diamond}$ can be derived following [83] to be

$$p^{\diamond} = \frac{1}{2}\lambda_n(\mathbf{Q}) \tag{4.10}$$

being, for the case of two layers, $\mathbf{Q} = \mathbf{L}^{+} - \mathbf{L}^{-}\mathbf{L}^{+\dagger}L^{-}$, $L^{\pm} = \frac{1}{2}(L_1 \pm L_2)$, and $A^{\dagger}$ the Moore-Penrose pseudoinverse of A.

4.2 The Aggregate-Equivalent Multiplex and the structural organization of a multiplex network

In order to characterize this transition, we want to compare a multiplex network $\mathcal{M}$ with the coarse-grained networks associated to it. However, a direct comparison is not possible, since those structures have different dimensionality. To overcome this problem, we define an auxiliary structure that has the same properties of the aggregate network and the network of layers, but also the same dimensionality of $\mathcal{M}$. We call it the Aggregate-Equivalent Multiplex (AEM). The AEM of a parent multiplex network $\mathcal{M}$ is a multiplex network with the same number of layers of $\mathcal{M}$, each layer being identical to the aggregate network of $\mathcal{M}$. Additionally, node-layer pairs representing the same nodes are connected with a connection pattern identical to the network of layers. Formally speaking, the AEM is given by the Cartesian product between the aggregate network and the network of layers. Thus, its adjacency matrix is given by

$$\mathbf{A} = \mathbf{I}_m \otimes \tilde{\mathbf{A}} + p\mathbf{K}_m \otimes \mathbf{I}_n, \tag{4.11}$$

and its Laplacian matrix is given by

$$\mathbf{L} = \mathbf{I}_m \otimes \tilde{\mathbf{L}}_a + p\tilde{\mathbf{L}}_l \otimes \mathbf{I}_n. \tag{4.12}$$

Its Laplacian spectrum is completely determined in terms of the spectra of $\tilde{\mathbf{L}}_a$ and of the spectra of $\tilde{\mathbf{L}}_l$. In particular, we have

$$\sigma(\mathbf{L}) = \{\tilde{\mu}_a + \tilde{\mu}_l \mid \tilde{\mu}_a \in \sigma(\tilde{L}_a), \tilde{\mu}_l \in \sigma(\tilde{L}_l)\}. \tag{4.13}$$

In words, each eigenvalue of $\mathbf{L}$ is the sum of an eigenvalue of $\tilde{\mathbf{L}}_a$ and an eigenvalue of $\tilde{\mathbf{L}}_l$. We can note that, since 0 is an eigenvalue of both coarse-grained Laplacians, the spectrum of both $\tilde{\mathbf{L}}_a$ and $\tilde{\mathbf{L}}_l$ are included in the spectrum of $\tilde{\mathbf{L}}_a$.
To compare the parent multiplex network with its AEM, we compute the quantum relative entropies between the former and the latter. The quantum entropy (or Von-Neumann entropy) of $\mathcal{M}$ being defined as

$$S_q(\mathcal{M}) = Tr(\rho \log \rho) \tag{4.14}$$

where $\rho = \frac{\bar{\mathbf{L}}}{2E+N(m-1)p}$, with E being the number of intra-layer links in $\mathcal{M}$ [71], i.e., ρ is the supra-Laplacian normalized by the degree sum. Thus, the quantum relative entropy of the multiplex network $\mathcal{M}$ with its associated AEM is defined as

$$R_q(\mathcal{M} \mid\mid AEM(\mathcal{M})) = Tr\rho(\log \rho - \log \sigma), \tag{4.15}$$

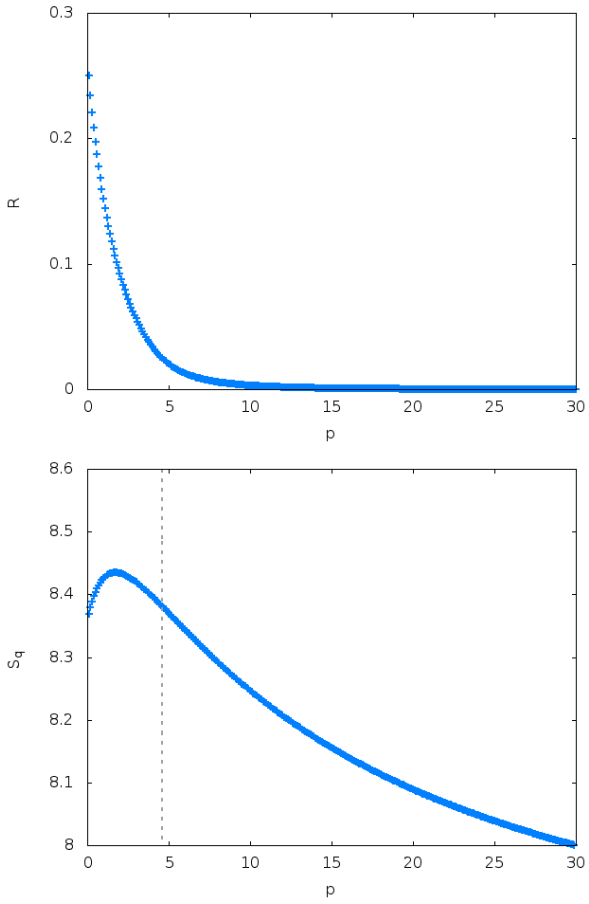

Figure 4.3: Relative entropy ($\times 10$) (top), and Quantum Entropy (bottom) for the same system of figure 4.2. The vertical line indicates the exact transition point $p^{\diamond}$.

with σ being the supra-Laplacian of the AEM normalized by its degree sum. In Fig.:4.3 we show the quantum relative entropy between the parent multiplex and its AEM: it goes to 0 by increasing p, meaning that the parent multiplex will be indistinguishable from the AEM.

Finally, it is informative to look at the quantum entropy. $S(\mathcal{M})$ shows a clear peak after p^* and before $p^{\diamond}$ (see Fig.:4.3), i.e. in the region after the transition observed in [2, 59] and before that one we have introduced here. By studying the sign of the derivative of S_q at p^* and at $p^{\diamond}$, it can be proven that the quantum entropy must have a peak between those two points.

4.3 Dynamical consequences and discussions

To gain intuition on the phenomenology, it is enlightening to look at it in terms of diffusion dynamic. The large time scale is dominated by the bounded group of eigenvalues for $p \geq p^{\diamond}$. Those eigenvalues are close to that of the aggregate network, meaning that each layer shows practically the same behaviour of the aggregate network. This is because the fast time scale is dominated by the diverging group of eigenvalues that are close to those of the aggregate network plus those of the network of layers. In summary, the network of layers determines how each node-layer pair accommodates with its replica on a fast time scale, being always "at equilibrium", while the aggregate network determines how and on what time scale the global equilibrium is attained. From that point of view, the "world" will look the same from each layer and it will look like in the aggregate network. From a random walk point of view, we can look at the average commute time $c(i, j)$, i.e. the mean time needed by a walker starting in i to hit node j for the first time and coming back. It can be expressed in terms of the eigenvalue of $\bar{L}^{\dagger}$, the pseudoinverse of the supra-laplacian. Since the eigenvalues of $\bar{L}^{\dagger}$ are the reciprocal of the eigenvalues of $\bar{L}$, the aggregate network mean commute time $\tilde{c}(i, j)$ is a good approximation of $c(i, j)$ after $p^{\diamond}$[82]:

$$\| c(i,j) - \tilde{c}(i,j) \| \leq E \frac{n(m-1)}{2p}. \tag{4.16}$$

It is interesting to note that the eigenvalues of the aggregate network do not depend on p.

Summarizing, before p^{*} the system is structurally dominated by the network of layers, whereas after $p^{\diamond}$ it is structurally dominated by the aggregate network. Between those two points the system is in an effective multiplex state, i.e., neither of the coarse-grained structures dominate. In this region the VN-entropy -a measure of structural complexity - shows a peak. Finally, we observe that the relative entropy between the parent multiplex and its AEM varies smoothly with p, meaning that the two transition are smooth from a global point of view.

Chapter 5

Dynamical Processes on Multiplex Networks

5.1 Contact-based Social Contagion

In this chapter we develop a theoretical framework for the study of epidemic-like social contagion in large scale social systems by considering the most general setting in which different communication platforms or categories form multiplex networks. Specifically, we propose a contact-based information spreading model, and show that the critical point of the multiplex system associated to the active phase is determined by the dominant layer. The framework is applied to a number of different situations, including a real multiplex system. Finally, we also show that when the system through which information is disseminating is inherently multiplex, working with the aggregate network is inaccurate.

5.1.1 Social contagion processes

Social contagion processes such as the adoption of a belief, the propagation of opinions and behaviors, and the massive social movements that have recently unfolded worldwide [20, 101, 92, 80, 22, 11, 40] are determined by many factors, among which the structure of the underlying topology and the dynamics of information spreading [94]. The advent of new communication platforms such as online social networks (OSN), has made the study of social contagion more challenging. Today, individuals are increasingly exposed to many diverse sources of information, all of which they value differently [34], giving raise to new communication patterns that directly impact both the dynamics of information spreading and the structure of the social networks [66, 48, 44, 63]. One way to address the latter is to consider that the process of contagion occurs in a system made up of different layers, i.e., in a multiplex network.

The dynamics of this kind of processes can be modeled using different classes of approaches. Threshold models [41, 96, 61, 10] assume that individuals enroll in the process being modeled if a given intrinsic propensity level, the threshold, is surpassed. Although this class of models is useful to address the emergence of collective behavior, they are generally designed to simulate a single contagion process and therefore individuals, once they are active, remain so forever. This is not convenient in many situations that are characterized by self-sustained activity patterns [11, 40]. For instance, think of an online social network in which tags are used to identify the topic of the information being transmitted (like *hashtags* in Twitter): individuals can use the same tag many times, but they can also decide not to use it after a number of times, thus being again susceptible to the contagion or in the language of threshold models, inactive. The latter features can be captured if one uses epidemic-like models of social contagion [78, 37]. In particular, the Susceptible-Infected-Susceptible (SIS) model [64], a classical approach to the study of disease spreading, allows individuals to cyclically change their dynamical state from susceptible (i.e., exposed to the tag) to infected (actively participating in the spreading process) and back to susceptible. Here, we propose a *contact-based Markov chain approach* [38] to study epidemic-like social contagion in multiplex networks. We derive the conditions under which the dynamics reaches a steady state with active (infected) individuals coexisting with non-adopters. Our results show that the dynamics of the multiplex system is characterized by a critical point that depends solely on the dominant layer 3. We also show how our modeling framework can be applied to different scenarios and that working with the aggregated network is not accurate.

5.1.2 The model

Let us consider a multiplex system made up of N nodes and M layers (see Figure 5.1), and let the supra-contact probability matrix $\bar{R} = \{R_{ij}\}$ be

$$\bar{R} = \bigoplus_{\alpha} R_{\alpha} + \left(\frac{\vec{\gamma}}{\beta}\right)^{T} C \tag{5.1}$$

where the R_{α}'s are the contact probability matrices of each layer α and $\mathcal{C}$ is the interlayer coupling matrix 1. Moreover, for a given layer α, R_{α} is defined as in the single-layer scenario [38], i.e.,

$$(R_{\alpha})_{ij} = 1 - \left(1 - \frac{(A_{\alpha})_{ij}}{k_{\alpha i}}\right)^{\lambda_{\alpha i}}, \tag{5.2}$$

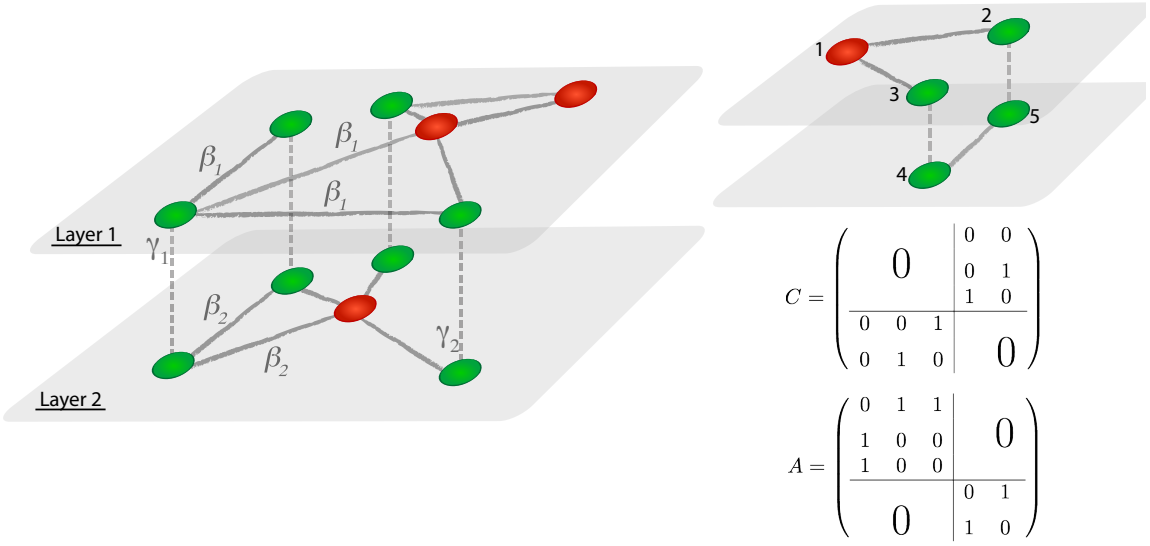

Figure 5.1: (color online) Schematic of a 2-layer multiplex system where the contagion dynamics takes place. There are actors that take part in more than one layer (green nodes connected by the dotted edges), whereas others are present only in one layer (red nodes). $\beta_{1,2}$ is the contagion rate within the same layer whereas $\gamma_{1,2}$ represents the probability that the contagion occurs between layers. The right panel shows a small network and its associated C and $A = \bigoplus_\alpha A_\alpha$.

being A_α the adjacency matrix of layer α and k_{α_i} the degree of node i in layer α. In addition, all vectors are column vectors of the form $\vec{x}^T = (x_1\vec{1}_1^T, \ldots, x_M\vec{1}_m^T)$, and $\vec{1}_\alpha$ are the vectors of all 1s whose size is equal to the number of nodes N_α in layer α. Thus, $\bar{R}$ is a block matrix with the R_α on the diagonal blocks and $\frac{\gamma_{l_i}}{\beta_{l_i}} C_{l_i l_j}$ on the off-diagonal block (l_i, l_j).

As in the simplex network, in each layer, the parameter $\lambda_{\alpha i}$ determines the number of contacts that are made, so that one may go from a contact process (one contact per unit time) when $\lambda_{\alpha i} = 1$ to a fully reactive process (all neighbors within the layer are contacted) in the limit $\lambda_{\alpha i} \longrightarrow \infty$. Moreover, the contagion between the layers is characterized by the ratio $\frac{\gamma_\alpha}{\beta_\alpha}$, where β_α is the rate at which the contagion spreads in layer α. Finally, γ_α has the same meaning of β but characterizes how contagion spreads from other layers to layer α (see Fig. 5.1), i.e., it is the rate at which a node in layer α gets infected if its counterparts in others layers are infected.

With the above ingredients, it is easy to see that the discrete-time evolution equation for the probability of contagion of a node i of the multiplex system has the

same functional form as in the single-layer case [38], namely,

$$\begin{aligned}\vec{p}(t+1) &= (\vec{1}-\vec{p}(t))*(\vec{1}-\vec{q}(t))+(\vec{1}-\vec{\mu})*\vec{p}(t) \\ &+ \vec{\mu}*(\vec{1}-\vec{q}(t))*\vec{p}(t),\end{aligned} \tag{5.3}$$

where $*$ stands for elements' wise multiplication of two vectors, i.e., $(\vec{p}*\vec{q})_i = p_i q_i$ and $\vec{\mu}$ is a vector whose components are the rates at which adopters are again susceptible. Moreover, $q_i(t)$ is the probability that node i will not be infected by any neighbor

$$q_i(t) = \prod_j (1-\beta R_{ij} p_j(t)). \tag{5.4}$$

5.1.3 Critical condition

Let us now assume that $\frac{\gamma_\alpha}{\beta_\alpha} = \frac{\gamma}{\beta}$ and $\frac{\mu_\alpha}{\beta_\alpha} = \frac{\mu}{\beta}, \forall \alpha = 1, \ldots, M$. The phase diagram can be studied by solving Eq. (5.3) at the stationary state

$$\vec{p} = (1-\vec{q}) + (1-\vec{\mu})\vec{p}*\vec{q} \tag{5.5}$$

This equation has always the trivial solution $p_i = 0$, $\forall i = 1, \ldots, N$. Other non-trivial solutions are given by non zero fixed points of Eq. (5.5) and can be easily computed numerically by iteration. Linearizing q_i around 0, at first order we get

$$[\bar{R} - \frac{\mu}{\beta} I]p = 0 \tag{5.6}$$

that has non-trivial solutions if and only if $\frac{\mu}{\beta}$ is an eigenvalue of $\bar{R}$. Since we are looking for the onset of the macroscopic social contagion, namely, the critical point, the lowest value of $\frac{\beta}{\mu}$ satisfying Eq. (5.6) is

$$\left(\frac{\beta}{\mu}\right)_c = \frac{1}{\bar{\Lambda}_{max}}, \tag{5.7}$$

where $\bar{\Lambda}_{max}$ is the largest eigenvalue of the matrix $\bar{R}$.
It is worth analyzing this result by means of a perturbative analysis. Let $\bar{\Lambda}_{max} \simeq \Lambda + \epsilon \triangle \Lambda$, where Λ is the largest eigenvalue of $R = \bigoplus_\alpha R_\alpha$ and consider $\bar{R} = R + \epsilon C$, with $\epsilon = \frac{\gamma}{\beta} \ll 1$. Since R is a block diagonal matrix, it has the same set of eigenvalues of $\{R_\alpha\}$ and thus we can analyze the system in terms of the largest eigenvalues of the contact matrices R_α of the layers α. For simplicity, we take the calculation in the case of two layers (i.e., $\alpha = 1, 2$), but generalization to any number of layers is

straightforward. The change in the eigenvalue (eigenvector) can be estimated using a first order approximation [62]

$$\triangle\Lambda_{max} = \frac{\vec{v}^T C \vec{v}}{\vec{v}^T \vec{v}}, \tag{5.8}$$

$$\triangle\vec{v} = \frac{C}{\Lambda}\vec{v}, \tag{5.9}$$

where $\vec{v}$ is the eigenvector associated to the largest eigenvalue Λ of the unperturbed matrix R.

Two cases are possible: *i)* $\Lambda_1 \gg \Lambda_2$ ($\Lambda_2 \gg \Lambda_1$ is completely equivalent), and *ii)* $\Lambda_1 \simeq \Lambda_2$, where Λ_1 (Λ_2) is the largest eigenvalue of R_1 (R_2). In the first case, the eigenvector associated to the largest eigenvalue $\Lambda = \Lambda_1$ is

$$\vec{v} = \begin{pmatrix} \vec{v}_{(1)} \\ 0 \end{pmatrix}. \tag{5.10}$$

Hence, $\triangle\Lambda = 0$ and

$$\triangle\vec{v} = \begin{pmatrix} 0 \\ \frac{\epsilon}{\Lambda}\vec{v}_{(1)} \end{pmatrix}. \tag{5.11}$$

Therefore, at first order approximation, we have that the largest eigenvalue of $\bar{R}$ is $\bar{\Lambda}_{max} = \max_\alpha\{\Lambda_\alpha\}$, and hence the emergence of a macroscopic steady state for the dynamics is determined by the layer with the largest eigenvalue. We call that layer the dominant layer. Besides, the probability of a node to catch the contagion at the critical point in a non-dominant layer is also specified by the probability of being infected in the dominant one.

In the second case *(ii)*, the eigenvector associated with the largest eigenvalue $\Lambda = \Lambda_1 = \Lambda_2$ is

$$\vec{v} = \begin{pmatrix} \vec{v}_{(1)} \\ \vec{v}_{(2)} \end{pmatrix}, \tag{5.12}$$

where $\vec{v}_{(1)}$ ($\vec{v}_{(2)}$) is the eigenvector associated to Λ_1 (Λ_2). Thus, at first order we have

$$\triangle\Lambda = \frac{\vec{v}_{(1)} C_{12} \vec{v}_{(2)} + \vec{v}_{(2)} C_{21} \vec{v}_{(1)}}{\vec{v}_{(1)}^T \vec{v}_{(1)} + \vec{v}_{(2)}^T \vec{v}_{(2)}}, \tag{5.13}$$

and

$$\triangle\vec{v} = \begin{pmatrix} \frac{\epsilon}{\Lambda}\vec{v}_{(2)} \\ \frac{\epsilon}{\Lambda}\vec{v}_{(1)} \end{pmatrix}. \tag{5.14}$$

The previous expression indicates that in this scenario, the critical point is smaller and that the correction depends on the relation between the eigenvector centralities of the nodes in both layers. To further analyze the dynamical features of the contagion process, we numerically solve the system of equations given by Eqs. (5.4) and (5.5)

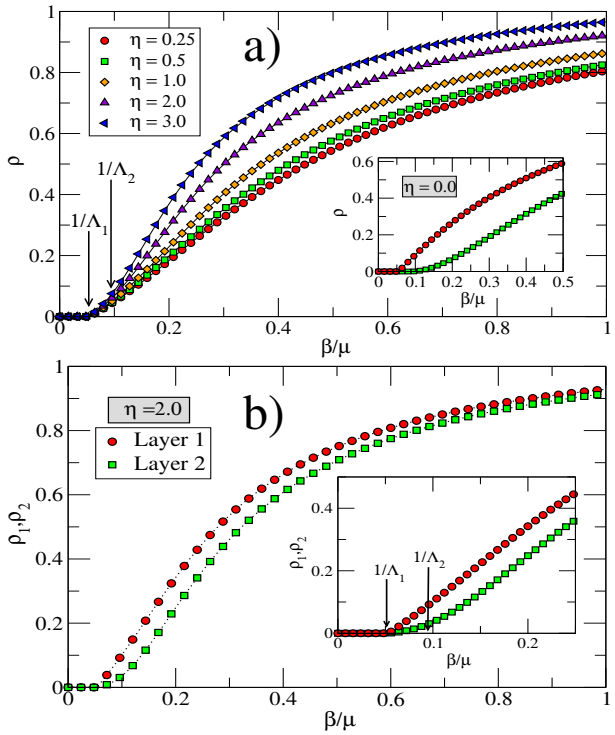

Figure 5.2: Panel (a): Density of adopters (ρ) at the steady state against the rescaled contagion probability $\frac{\beta}{\mu}$ for a multiplex system composed of two layers with $N = 10^4$ nodes each for different values of the ratio $\eta = \frac{\gamma}{\beta}$. The arrows represent the inverse of the largest eigenvalues of the two layers, whereas the inset shows the case in which both layers are completely disconnected. Panel (b): the same quantity of panel (a), for $\eta = 2.0$, is represented but computed at each layer. The inset is a zoom around the critical point. See the text for further details.

for the different scenarios considered above. In the first case, when $\Lambda_1 \gg \Lambda_2$, the dynamics of the multiplex system is completely dominated by the layer with the largest eigenvalue of R_α. Thus, we expect that the contagion threshold coincides with the one of the dominant layer and no effect of the inter-layer diffusion parameter $\epsilon = \frac{\gamma}{\beta}$ near the threshold.

Figure 5.2a depicts the fraction of infectees, $\rho = \frac{1}{N}\sum_i p_i$, at the steady state against the rescaled contagion probability $\frac{\beta}{\mu}$ for a multiplex composed by two layers of $N_1 = N_2 = 10^4$ nodes (thus $N = N_1 + N_2 = 2 \cdot 10^4$). Both layers have been obtained using the uncorrelated configuration model with degree distribution $P(k) \sim k^{-g}$ with $g = 2.3$ for the first layer and $g = 3.0$ for the second one. Furthermore, we have assumed a fully reactive scenario in both layers of the system (i.e., $\lambda_1 = \lambda_2 \to \infty$ in Eq. (5.2)). As seen in panel (a), where arrows represent the inverse of the largest eigenvalues, the contagion threshold is set by $1/\Lambda_1$. It is worth noticing that the perturbative result still hold even for $\frac{\gamma}{\beta} = 1$. This is due to the fact that the number of links added to the multiplex is small compared to the number of intra-layer links and the perturbation can still be considered small [62]. On the other hand, the inset shows the results one would obtain if both layers were disconnected. In this case, each one would have their independent contagion thresholds determined by their largest eigenvalues.

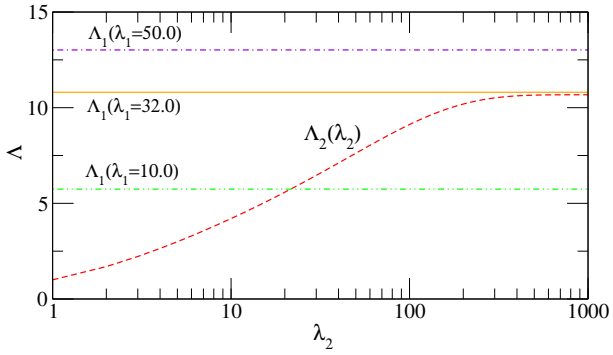

Figure 5.3: Dependence of the largest eigenvalues of the contact probability matrices, R_α's, on λ_α for the system in Fig. 5.2. As it can be seen, there might be a crossover signaling that the dominant layer changes. This crossover occurs only if the activity of the topologically dominant layer is small enough: in the example, it should be smaller than $\lambda_1 = 32$.

It is also of interest to inspect the phase diagrams of the two layers separately. This is what is shown in Fig. 5.2b, where we represent the fraction of infectees at the steady state of each layer. As already discussed, the dominant layer fixes the contagion threshold of the multiplex network. However, it also induces a shift of the critical point of the second layer to smaller values. In other words, the multiplex nature of the system leads to an earlier transition to an active phase also in the non-dominant layer, as its critical point is now smaller than the expected value for the isolated system, i.e., $(\frac{\beta}{\mu})_{c_2} < \frac{1}{\Lambda_2}$.

Furthermore, a unique feature of the model directly linked to the multiplex nature of the system is worth stressing. As the largest eigenvalues involved in the calculations are those associated to the matrices R_α, they depend not only on the adjacency matrices A_α, but also on λ_{α_i} (see Eq. (5.2)). This dependency has an interesting and novel effect as shown in Fig. 5.3: as the λ_α's characterize the number of effective contacts per unit time, a layer that does not prevail in the contagion dynamics because it is not topologically dominant (in terms of its A_α) can compensate its lack of structural strength by increasing λ_α so as to eventually become the one with the largest eigenvalue of the multiplex network. The previous feature opens the door to potential applications in which by tuning the activity on one layer, the latter can take over the rest of the system and set its critical properties. Similarly, the above mechanism could explain situations in which the system is in the critical region despite the fact that by observing one layer one would expect the contrary. In other words, to determine whether the system is in a critical regime, one should have access to both the topological and activity features of all layers. This is in line with the findings in [18], however, our model shows that once the dominant layer (if there is one) is detected, the analysis of the system dynamics can be carried out only on that layer.

We have also explored the scenario *ii)*, $\Lambda_1 \simeq \Lambda_2$, for which the largest eigenvalue of the multiplex is given as $\Lambda_{max} = \max_{\{1,2\}}\{\Lambda_1, \Lambda_2\} + O(\epsilon)$. In particular, as one needs two networks with similar (very similar in this case) largest eigenvalues, we have used the same network in each layer and reshuffled the nodes from one layer to another to avoid correlation between the degree and the neighborhood of a node in the two layers. Also in this case (figure not shown), numerical results confirm the theoretical expectation.

5.1.4 The process on the aggregate network

We study the differences in the contagion process when considering the aggregate network (see chapter 1). Since the largest eigenvalue of the aggregate network is larger than that of the multiplex, we expect the contagion threshold of the projected network to be smaller than that of the multiplex system. In addition, the number of infectees at the steady state should also be smaller for the multiplex network, since the correction to the probabilities of being infected, p_i's, is small in this system. Figure 5.4 shows results of numerical calculations for both systems. As it can be seen more clearly in the inset of panel, the contagion thresholds are different. More importantly, the figure provides grounded evidences of why one cannot reduce a system that is inherently multi-level to a projected network − the observed level of prevalence significantly differs from one system to the other. For instance, fixing the ratio $\frac{\beta}{\mu}$ that characterizes the spreading process within one layer, one can get estimates for the contagion incidence as higher as twice the actual value (that of the multiplex network).

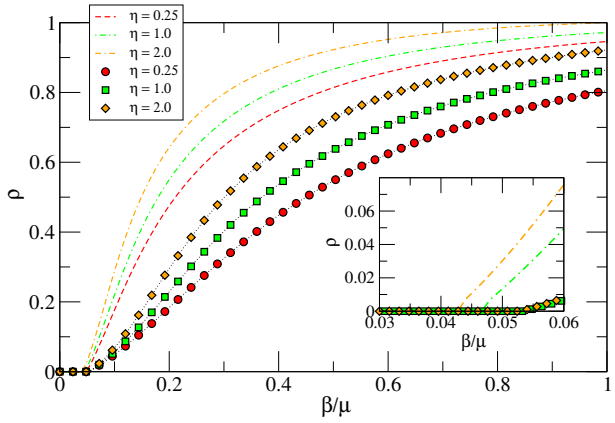

Figure 5.4: Density of adopters (ρ) at the steady state as a function of the rescaled contagion probability $\frac{\beta}{\mu}$ for a multiplex system composed of two layers with $N = 10^4$ nodes each (lines with symbols) and the corresponding aggregated graph (dotted lines). Different curves represent different values of the ratio $\eta = \frac{\gamma}{\beta}$ as indicated. The inset is a zoom of the region around the contagion threshold.

Conclusions

In chapter 1 we have introduced the basic formalism to describe multiplex networks in terms of graphs. In a multiplex network we have different types of interactions among the constituents of the system that we call layers. We have introduced the participation graph $G_P = (V, L, P)$ that models the participation of a node in an interaction network. This graph implicitly defines the notion of node-layer pair, i.e. the representative of a node in a particular layer of interaction. Node-layer pairs are basic objects of the graph model of a multiplex network, since them preserve the identity of the components of a multiplex network, while allowing for differentiation among different interaction networks. If we think in multiplex social networks, we are modelling the fact that individuals have different faces in different contexts, especially online [77]. Yet, despite their involvement in different contexts they are still the same persons. In [77], Lee Rainie and Barry Wellman talk about a *"networked self"*, which resonates well with the concept of supra-node introduced in chapter 1. However, this situation is not specific of social networks, as, for instance, in the biological realm we can think of a chemical species that plays different roles in a variety of signalling channels.

As in traditional monoplex network studies, we represent each layer of interaction as a graph G_α and we next consider the set of all layer graphs $M = \{G_\alpha\}_{\alpha \in L}$. The (disjoint) union of all the graphs in M together with the coupling graph G_C that encodes the relations between different node-layer pairs representing the same node constitutes our proposal for a comprehensive representation of a multiplex network. Once we have defined a graph representation of the multiplex network we can associate matrices to it (section 1.2). The convenience of associating matrices to graph resides in the possibility to use tools from linear algebra and random matrix theory to study the structural properties of complex networks in general and, in particular, multiplex networks.

First we have introduced the supra-adjacency matrix $\bar{\mathcal{A}}$ (section 1.2.1) and the supra-Laplacian matrix $\bar{\mathcal{L}}$ that are direct generalizations of the adjacency and Laplacian matrices of a graph. Due to the peculiar nature of multiplex networks, we have also introduced *multiplex walk matrices* (section 1.2.3) to represent the multiple ways a multiplex can be walked. Such matrices are needed because often it is of interest to treat intra and inter-layer edges differently. On those matrices are based the definitions of the clustering coefficients and of the subgraph centrality we have given in chapter 2.

Finally, we have defined a coarse-grained representation of a multiplex network (section 1.3). This representation is just a network in which the interaction patterns of each layer or among layers are aggregated in a single network somehow. The operation can be performed in a variety of arbitrary ways. Our definition is based on the notion of *quotient graphs* (section 1.3.1), that is intimately related to the partitioning of the node set of a graph. Since we can recognize two natural partitions in multiplex networks -that associated to supra-nodes and that associated to layers-, we have been able to define two coarse-grained networks: the aggregate network, that aggregates interactions across layers, and the network of layers that encodes the pattern of interactions between layers. Having defined the coarse-grained representations of multiplex networks through quotient graphs, we exploited the spectral interlacing results that exists between a quotient and its parent graph. In that sense, we say that the notion of quotient graph underpins the notion of multiplex network, since a number of spectral properties, -and thus structural ones-, of the parent multiplex network can be deduced from its coarse-grained representation, as we have done in chapter 3 and in chapter 4.

We have also explored the relations between supra-walk matrices and the aggregate network (section 1.4). Those relations open up an entirely new line of research that is promising in order to understand the structural organization of multiplex networks and their intimately different nature in comparison to traditional monoplex networks. Armed with the formalism developed in chapter 1, we have been able to define some structural metrics for multiplex networks in terms of its walks matrices (chapter 2). Based on the experience gained during the course of this thesis, we propose a list of requirements that a structural metric should fulfil in order to be properly defined. The aim of this list is to help with the generalization of standard monoplex metrics to multiplex networks in a systematic way, as well as to guide the theoretical

development of new genuinely multiplex metrics. In particular, it is grounded on the relation that exists between multiplex walk matrices and the aggregate network.

In section 2.1 we have studied triadic relations in multiplex networks by defining multiplex generalizations of clustering coefficients. The definition already existing in the literature has different problems, the solution of which aimed our research and guides our list of requirement. The main point is that multiplex networks also contain cycles that can traverse different additional layers but still have 3 intra-layer steps. To take into account this, we based our definition on multiplex walk matrices. Depending on the application, one can define a way to walk the multiplex and hence a walk matrix from which the local and global clustering coefficients derive. It is useful to decompose multiplex clustering coefficients into *elementary cycles*. This decomposition allows, as we discuss in section 2.2, to unveil that multilayer transitivity can arise from different mechanisms. In particular, we show that the *triadic closure* mechanism in social networks is context-dependent, in the sense that triangles in one layer are statistically more abundant than those spanning two o three layers. This claim is based on our analytical derivation for the expected clustering coefficients in node-aligned multiplex networks with Erdős-Rényi layers and on comparisons with randomized versions of the empirical multiplex networks that were studied.

Clustering coefficients characterize the system at a very small topological scale. For larger scales, we have generalized the definition of subgraph centrality of multiplex networks (section 2.3) capitalizing on the notion of supra-walk and walk matrices. Those example show the power of multiplex walk matrices as a general representation of a multiplex network when studying its structural properties. The connection given between supra-walk matrices and coarse-grained representations made it clear the need to deal differently with inter- and intra- layer links in each situation.

In chapter 4 we have discussed the structural transitions that a multiplex network undergoes when changing the coupling parameter p between layers. We have seen that two *critical values* can be defined. Before the first point p^* the multiplex network is structurally dominated by the topological scale of the network of layers, while after the second point $p^\diamond$ the topological scale of the aggregate network dominates. Focusing on the first transition at p^*, that was the first observed in literature [2, 59], the main quantity is the algebraic connectivity, i.e., the first non-zero eigenvalue of

the supra-Laplacian, and its associated eigenvector, named Fiedler eigenvector. Following [59], one can identify the algebraic connectivity with the internal energy of a thermodynamical system, then its first derivative exhibits a discontinuity at p^*, although its second derivative doesn't diverge, as in second order thermodynamical phase transitions.

On the other hand, if one identifies the algebraic connectivity with a thermodynamic potential, its Legendre transform exhibits a discontinuity at p^*, as in first order phase transitions. However, as noted in [59], "despite this interesting parallel, it is worth noting that the Fiedler eigenvalue and its Legendre transform are not extensive quantities and, hence, they cannot be properly regarded as thermodynamic potentials". However, we should note that the algebraic connectivity indeed is extensive in the number of layers, i.e. $\mu_2 = mp$ for a node-aligned multiples network. Let's focus on the Fiedler vector, i.e., the eigenvector associated to the first non-zero eigenvalue of the supra-Laplacian. As a consequence of the inclusion relation (see section 3.3) between the laplacian spectrum of the network of layers an that of the supra-Laplacian for node-aligned multiplex networks, the Fiedler vector of the whole system is a lifting of the Fiedler vector of the network of layers before p^*, i.e., there is a privileged direction defined by the network of layers. Therefore, the Fiedler cut of the graph [1] only intercepts inter-layer links. At p^* the second and third eigenvalues swap and after p^* the Fiedler vector has no privileged direction. As a consequence, the Fiedler cut intercepts intra-layer links. One can interpret the Shannon entropy of the Fielder vector as an *order parameter*: it is zero before p^*, while it is different from zero after p^*.

This observation unveils the role played by symmetries. The non-analyticity of the Fiedler eigenvalue as a function of p is a consequence of the inclusion relation that only holds for node-aligned multiplex networks, i.e., when the partition induced by layers is almost regular and the network of layers is a (weighted) symmetric graph. If the multiplex is not node-aligned, the inclusion relation doesn't hold and the algebraic connectivity is analytic in p. In other words, there is no actual transition. In [59], authors suggest to view p as a coupling parameter of a main-field multiplex

[1] A graph bipartition is defined as a partition of the nodes set in two clusters. Given a bipartition, a cut is the set of edges between nodes in distinct clusters. A minimum cut is that obtained by partitioning the nodes such that the size of the cut is the minimum possible. The Fiedler cut is the cut obtained partitioning the nodes set according to the sign of the entries of the Fiedler vector. It can be shown that it is a good approximation of the minimum cut [75]

network in which a fraction p of node-layer pairs is coupled across all layers. In that case, the mean-field is adding spurious symmetries that the real system does not have. At this point, we are able to propose the Aggregate Equivalent Multiplex network defined in chapter 4 as a mean-field model of the parent multiplex network, where more spurious symmetries are added, since in the AEM all layers are identical. The system will approach the mean-field in the limit of infinite p.

The transition at $p^{\diamond}$ is better characterized in terms of an eigengap. In fact, as observed in chapter 4, at this point a gap appears in the spectrum of the supra-Laplacian. However, a characterization in terms of the non-analyticity of the $(n+1)th$ supra-Laplacian eigenvalue is also possible. Moreover, after $p^{\diamond}$ this eigenvalue has the lifted Fielder vector of the network of layers as its associated eigenvector, because of the inclusion relation. That makes it possible the interpretation of the Shannon entropy of that vector as an order parameter also here. The same considerations done before regarding non node-aligned multiplex networks apply here. The non analyticity in p of the $(n+1)th$ supra-Laplacian eigenvalue and the behavior of the Shannon entropy of its associated eigenvector depend on the inclusion relations of the spectrum that only hold for node-aligned multiplex networks. Node-layer pairs with different couplings destroy the symmetries that characterize the transitions. Because of that, a non node-aligned multiplex networks can not display an actual transition, but only a transition like behavior.

Finally, in Chapter 5, we have developed a theoretical framework for the study of epidemic-like social contagion in large scale social systems. Capitalizing on the perturbative results on the largest eigenvalue of the supra-adjacency matrix obtained in Chapter 3, we showed that the existence of a dominant layer sets the condition for the emergence of a macroscopic steady state for the dynamics. Besides, the probability of a node to catch the contagion at the critical point in a non-dominant layer is also specified by the probability of being infected in the dominant one, making clear the relevance of the effective multiplexity measure we have defined in Chapter 3.

Multiplex networks represent a challenge and an opportunity of innovation for the science of complex networks. The power of complex networks science as an interdisciplinary toolbox resides in its high level of abstraction in representing empirical systems in a common and well established mathematical framework. Thus, the first basic challenge is represented by the need of a common formal language to represent

them. On the other hand, the necessity to reconsider the very foundations of the discipline in order to take into account the new level of complexity represented by multiplexity, is an opportunity to enrich and refine all the mathematical paraphernalia that is at the core of complex networks science. This is the case, for example, of the relation between the Laplacian spectrum and structural transitions going on in the system.

The formal and quantitative study of multiplexity is another key step for the hypothesis that the structure and function are intimately related to one another, thus representing the natural evolution of complex networks science as a mature discipline and the opportunity to enlarge the framework of interactions with other specialized sciences, such as social sciences and systems biology. In the last few years, the bases to face such challenges have been laid, this thesis being intended to be a contribution in that line. Special effort was devoted in setting a formal language and exploring its possibilities in the characterization of multiplex networks. In particular, the notion of quotient graph as underpinning that of multiplex networks has proved to be useful in order to understand the spectra, and thus the structure, of multiplex networks. In the same way, the representation of multiplex networks in terms of multiplex walk matrices as a base to generalize different structural metrics has proved to be versatile enough to deal with very different empirical systems, as well as in the understanding of the structural organization of multiplex networks and their relation to its natural coarse-grained representation (i.e., the aggregate network).

Constructing on that, there are different possibilities for future work, among which we want to mention a few: the statistical characterization of the Laplacian and adjacency spectra of ensembles of multiplex networks; the generalization of more structural metrics in the common framework settled up by the walk matrix representation; and finally, a deeper understanding of structural transitions in multiplex networks and eventually their dynamical implications, especially with regard to the role played by symmetries and correlations among and across layers.

Appendix A

Multiplex Clustering Coefficient in the Literature

Let $\mathbf{A}^{(\alpha)}$ denote the layer adjacency matrix for layer α. For a weighted multiplex network, we use $\mathbf{W}^{(\alpha)}$ to denote the layer weight matrix (i.e., the weighted layer adjacency matrix) for layer α. We use $\mathbf{W}$ to denote the weight matrix of the aggregated sum network (See Section 1.4). The clustering coefficient that was defined in [7] for node-aligned multiplex networks is

$$C_{Be,u} = \frac{\sum_{v,w} \sum_{\alpha} A_{uv}^{(\alpha)} \sum_{\kappa} A_{uw}^{(\kappa)} \sum_{\mu} A_{uw}^{(\mu)}}{\sum_{v,w} \sum_{\kappa} A_{uv}^{(\kappa)} \sum_{\alpha} \max(A_{uw}^{(\alpha)}, A_{vw}^{(\alpha)})}\,, \tag{A.1}$$

which can be expressed in terms of the aggregated network as

$$C_{Be,u} = \frac{\sum_{v,w} W_{uv} W_{uw} W_{vw}}{\sum_{v,w} W_{uv} \sum_{\alpha} \max\left(A_{uw}^{(\alpha)}, A_{vw}^{(\alpha)}\right)}\,. \tag{A.2}$$

The numerator of Eq. A.2 is the same as the numerator of the weighted clustering coefficient $C_{Z,u}$, but the denominator is different. Because of the denominator in Eq. A.2, the values of the clustering coefficient $C_{Be,u}$ do not have to lie in the interval $[0, 1]$. For example, $C_{Be,u} = (n-2)b/n$ for a complete multiplex network (where n is the number of nodes in the multiplex network), so $C_{Be,u} > 1$ when $b > \frac{n}{n-2}$.

References [16, 15] defined a family of local clustering coefficients for directed and weighted multiplex networks:

$$C_{Br,u,t} = \frac{\sum_{\alpha \in L} \sum_{v,w \in N(u,t)} (W_{wv}^{(\alpha)} + W_{vw}^{(\alpha)})}{2|N(u,t)|m}\,, \tag{A.3}$$

where $N(u,t) = \{v : |\{\alpha : A_{uv}^{(\alpha)} = 1 \quad \text{and} \quad A_{vu}^{(\alpha)} = 1\}| \geq t\}$, t is a threshold, and we recall that $L = \{1, \ldots, m\}$ is the set of layers. The clustering coefficient A.3 does not

yield the ordinary monoplex local clustering coefficient for unweighted (i.e., networks with binary weights) and undirected networks when it is calculated for the special case of a monoplex network (i.e., a multiplex network with $m = 1$ layer). Furthermore, its values are not normalized to lie between 0 and 1. For example, consider a complete multiplex network with n nodes and an arbitrary number of layers. In this case, the clustering coefficient **A.3** takes the value of $n-2$ for each node. If a multiplex network is undirected (and unweighted), then $C_{Br,u,t}$ can always be calculated when one is only given an aggregated network and the total number of layers in the multiplex network. As an example, for the threshold value $t = 1$, one obtains

$$C_{Br,u,1} = \frac{1}{k_u m} \sum_{v,w} \frac{W_{vw}}{2} A_{uv} A_{uw} A_{vw} \,, \tag{A.4}$$

where $\mathbf{A}$ is the binary adjacency matrix corresponding to the weighted adjacency matrix $\mathbf{W}$ and $k_u = \sum_v A_{uv}$ is the degree of node u.

Reference [**?**] defined a clustering coefficient for multiplex networks that are not necessarily node-aligned as

$$C_{Cr,u} = \frac{2 \sum_{\alpha \in L} |\overline{E}_\alpha(u)|}{\sum_\alpha |\Gamma_\alpha(u)|(|\Gamma_\alpha(u)| - 1)} \,, \tag{A.5}$$

where $L = \{1, \ldots, m\}$ is again the set of layers, $\Gamma_\alpha(u) = \Gamma(u) \cap V_\alpha$, the quantity $\Gamma(u)$ is the set of neighbors of node u in the aggregate network, V_α is the set of nodes in layer α, and $\overline{E}_\alpha(u)$ is the set of edges in the subgraph induced by $\Gamma_\alpha(u)$ in the aggregated network. For a node-aligned multiplex network, $V_\alpha = V$ and $\Gamma_\alpha(u) = \Gamma(u)$, so one can write

$$C_{Cr,u} = \frac{\sum_{vw} A_{uv} W_{vw} A_{wu}}{b \sum_{v \neq w} A_{uv} A_{wu}} \,, \tag{A.6}$$

which is a local clustering coefficient for the aggregated network.
Battiston et al. [8] defined two versions of clustering coefficients for node-aligned multiplex networks:

$$C_{Bat1,u} = \frac{\sum_\alpha \sum_{\kappa \neq \alpha} \sum_{v \neq u, w \neq u} A^{(\alpha)}_{uv} A^{(\kappa)}_{vw} A^{(\alpha)}_{wu}}{(m-1) \sum_\alpha \sum_{v \neq u, w \neq u} A^{(\alpha)}_{uv} A^{(\alpha)}_{wu}} \,, \tag{A.7}$$

$$C_{Bat2,u} = \frac{\sum_\alpha \sum_{\kappa \neq \alpha} \sum_{\mu \neq \alpha, \kappa} \sum_{v \neq u, w \neq u} A^{(\alpha)}_{uv} A^{(\mu)}_{vw} A^{(\kappa)}_{wu}}{(b-2) \sum_\alpha \sum_{\kappa \neq \alpha} \sum_{v \neq u, w \neq u} A^{(\alpha)}_{uv} A^{(\kappa)}_{wu}} \,. \tag{A.8}$$

The first definition, $C_{Bat1,u}$, counts the number of $\mathcal{ACACA}$-type elementary cycles; and the second definition, $C_{Bat2,u}$, counts the 3-layer elementary cycles $\mathcal{ACACAC}$.

Property	$C_{M(,u)}$	$C_{Be,u}$	$C_{Z(,u)}$	$C_{Ba,u}$	$C_{O,u}$	$C_{Br,u}$	$C_{Cr,u}$	$C_{Bat(1,2),u}$
(1) Reduces to monoplex c	✓	✓	✓	✓	✓		✓	
(2) $C_* \leq 1$	✓		✓	✓	✓		✓	✓
(3) $C_* = p$ in multiplex ER	✓						✓	
(4) Monoplex C for copied layers	✓		✓	✓	✓		✓	
(5) Defined for node-layer pairs	✓							
(6) Defined for non-node-aligned	✓						✓	

Table A.1: Summary of the properties of the different multiplex clustering coefficients. The notation $C_{*(,u)}$ means that the property holds for both the global version and the local version of the associated clustering coefficient.

In both of these definitions, note that the sums in the denominators allow terms in which $v = w$, so a complete multiplex network has a local clustering coefficient of $(n-1)/(n-2)$ for every node.

Reference [27] proposed definitions for global clustering coefficients using a tensorial formalism for multilayer networks; when representing a multiplex network as a third-order tensor, the formulas in [27] reduce to the clustering coefficients that we propose (See Eq. 2.5). Parshani et al. [70] defined an "inter-clustering coefficient" for two-layer interdependent networks that can be interpreted as multiplex networks [1]. Their definition is similar to edge "overlap" [8]; in our framework, it corresponds to counting 2-cycles of type $(\mathcal{AC})^2$. A few other scholars [29, 73] have also defined generalizations of clustering coefficients for multilayer networks that cannot be interpreted as multiplex networks [1].

In Table A.1, we show a summary of the properties satisfied by several different (local and global) multiplex clustering coefficients. In particular, we check the following properties. (1) The value of the clustering coefficient reduces to the values of the associated monoplex clustering coefficient for a single-layer network. (2) The value of the clustering coefficient is normalized so that it takes values that are less than or equal to 1. (All of the clustering coefficients are nonnegative.) (3) The clustering coefficient has a value of p in a large (i.e., when the number of nodes $n \to \infty$) node-aligned multiplex network in which each layer is an independent ER network with an edge probability of p in each layer. (4) Suppose that we construct a multiplex network by replicating the same given monoplex network in each layer. We indicate whether the clustering coefficient for the multiplex network has the same value as for the monoplex network. (5) There exists a version of the clustering coefficient that is defined for each node-layer pair separately. (6) The clustering coefficient is defined for multiplex networks that are not node-aligned.

Appendix B

Other Possible Definitions of Cycles

There are many possible ways to define cycles in multiplex networks. If we relax the condition of disallowing two consecutive inter-layer steps, then we can write

$$t_{SM,i} = [(\widehat{\mathcal{C}}\mathcal{A}\widehat{\mathcal{C}})^3]_{ii}\,, \tag{B.1}$$

$$t_{SM',i} = [(\widehat{\mathcal{C}}'\mathcal{A} + \mathcal{A}\widehat{\mathcal{C}}')^3]_{ii}\,, \tag{B.2}$$

where $\widehat{\mathcal{C}}' = \frac{1}{2}\beta\mathcal{I} + \gamma\mathcal{C}$. Unlike the matrices in definition Eq. 2.1 in section 2.1.1, the matrices $\widehat{\mathcal{C}}\mathcal{A}\widehat{\mathcal{C}}$ and $\widehat{\mathcal{C}}'\mathcal{A} + \mathcal{A}\widehat{\mathcal{C}}'$ are symmetric. We can thus interpret them as weighted adjacency matrices of symmetric supra-graphs, and we can then calculate cycles and clustering coefficients in these supra-graphs.
It is sometimes desirable to forbid the option of staying inside of a layer in the first step of the second term of Eq. B.2. In this case, one can write

$$t_{M',i} = [(\mathcal{A}\widehat{\mathcal{C}})^3 + \gamma\mathcal{C}\mathcal{A}(\widehat{\mathcal{C}}\mathcal{A})^2]_{ii}\,. \tag{B.3}$$

With this restriction, cycles that traverse two adjacent edges to the focal node i are only calculated two times instead of four times.
In this case, we simplify Eq. B.3 to obtain

$$t_{M',i} = [2(\mathcal{A}\widehat{\mathcal{C}})^2\mathcal{A}\widehat{\mathcal{C}}']_{ii}\,, \tag{B.4}$$

which is similar to Eq. 2.2 in section 2.1.1. In Table B.1, we show the values of the clustering coefficients that we calculate using this last definition of cycle for the empirical networks that we studied in the main text.

An elegant way to generalize clustering coefficients for multiplex networks is to define a new (possibly weighted) auxiliary supra-graph G_M as in section 1.2.3 so that

CC	Families	Bank	Tailor Shop	Management	Tube	Airline
$C_{M'}$	0.218	0.289	0.320	0.206	0.070	0.102
$C^{(1)}_{M'}$	0.289	0.537	0.406	0.436	0.013	0.100
$C^{(2)}_{M'}$	0.202	0.368	0.338	0.297	0.041	0.173
$C^{(3)}_{M'}$	-	0.227	0.288	0.192	0.314	0.086
$C_{M'}(\frac{1}{3}, \frac{1}{3}, \frac{1}{3})$	0.164	0.377	0.344	0.309	0.123	0.120
$\overline{C_{Cr,u}}$	0.342	0.254	0.308	0.150	0.038	0.329
$\overline{C_{Ba,u}}$	0.195	0.811	0.612	2.019	-	-
$\overline{C_{Br,u}}$	0.674	1.761	4.289	1.636	-	-
$\overline{C_{O,u}}$	0.303	0.268	0.260	0.133	-	-
$\overline{C_{Be,u}}$	0.486	0.775	0.629	0.715	-	-
$\overline{C_{Bat1,u}}$	0.159	0.199	0.271	0.169	-	-
$\overline{C_{Bat2,u}}$	-	0.190	0.282	0.179	-	-

Table B.1: Clustering coefficients (rows) for the same empirical networks (columns) from Table 1 in the main text. For the Tube and the Airline networks, we only calculate clustering coefficients for non-node-aligned networks. For local clustering coefficients we average over all nodes, $\overline{C_{*,u}} = \frac{1}{n}\sum_u C_{*,u}$.

one can define cycles of interest as weighted 3-cycles in G_M.

Once we have a function that produces the auxiliary supra-adjacency matrix $\mathcal{M} = \mathcal{M}(\mathcal{A}, \mathcal{C})$, we can define the auxiliary complete supra-adjacency matrix $\mathcal{M}^F = \mathcal{M}(\mathcal{F}, \mathcal{C})$. One can then define a local clustering coefficient for node-layer pair i with the formula

$$c_i = \frac{(\mathcal{M}^3)_{ii}}{(\mathcal{M}\mathcal{M}^F\mathcal{M})_{ii}} \,. \tag{B.5}$$

As with a monoplex network, the denominator written in terms of the complete matrix $\mathcal{M}^F$ is equivalent to the usual one written in terms of connectivity. We thereby consider the connectivity of a node in the supra-graph induced by the multiplex walk matrix $\mathcal{M}$.

A key advantage of defining clustering coefficients using an auxiliary supra-graph is that one can then use it to calculate other diagnostics (e.g., degree or strength) for nodes. One can thereby investigate correlations between clustering-coefficient values and the size of the multiplex neighborhood of a node. (The size of the neighborhood is the number of nodes that are reachable in a single step via connections defined by matrix $\mathcal{M}$.)

We can write the symmetric multiplex walk matrices in Eqs. B.1 and B.2 as

$$\mathcal{M}_{SM} = \widehat{\mathcal{C}}\mathcal{A}\widehat{\mathcal{C}}\,, \tag{B.6}$$

$$\mathcal{M}_{SM'} = (\widehat{\mathcal{C}'}\mathcal{A} + \mathcal{A}\widehat{\mathcal{C}'})\,. \tag{B.7}$$

To avoid double-counting intra-layer steps in the definition of $\mathcal{M}_{SM'}$, we need to rescale either the intra-layer weight parameter β (i.e., we can write $\widehat{\mathcal{C}'} = \beta'\mathcal{I} + \gamma\mathcal{C} = \frac{1}{2}\beta\mathcal{I} + \gamma\mathcal{C}$) or the inter-layer weight parameter γ [i.e., we can write $\widehat{\mathcal{C}'} = \beta\mathcal{I} + \gamma'\mathcal{C} = \beta\mathcal{I} + 2\gamma\mathcal{C}$ and also define $\mathcal{M}_{SM'} = \frac{1}{2}(\mathcal{A}\widehat{\mathcal{C}'} + \widehat{\mathcal{C}'}\mathcal{A})$].

Consider a supra-graph induced by a multiplex walk matrix. The distinction between the matrices $\mathcal{M}_{SM}$ and $\mathcal{M}_{SM'}$ is that $\mathcal{M}_{SM}$ also includes terms of the form $\mathcal{C}\mathcal{A}\mathcal{C}$ that take into account walks that have an inter-layer step ($\mathcal{C}$) followed by an intra-layer step ($\mathcal{A}$) and then another inter-layer step ($\mathcal{C}$). Therefore, in the supra-graph induced by $\mathcal{M}_{SM}$, two nodes in the same layer that are not adjacent in that layer are nevertheless adjacent if the same nodes are adjacent in another layer.

The matrix $\widehat{\mathcal{C}}$ sums the contributions of all node-layer pairs that correspond to the same physical node when $\beta = \gamma = 1$. In other words, if we associate a vector of the canonical basis e_i to each node-layer pair i, then

$$\widehat{\mathcal{C}}e_i = \sum_{j \in l^{-1}(i)} e_j \tag{B.8}$$

produces a vector whose entries are equal to 1 for nodes that belong to the basis vector and which are equal to 0 for nodes that do not belong to that vector.

Consequently, $\mathbf{M}_{SM}$ is related to the weighted adjacency matrix of the aggregated graph for $\beta = \gamma = 1$. To be precise, we obtain the following relation:

$$(\widehat{\mathcal{C}}\mathcal{A}\widehat{\mathcal{C}})_{ij} = W_{uv}\,, \qquad i \in l(u), j \in l(v)\,. \tag{B.9}$$

Taking into account the 1.31 in 1.4, the same relation can be written in the compact form:

$$\hat{\mathcal{C}}\mathcal{A}\hat{\mathcal{C}} = \mathcal{S}_n \mathbf{W} \mathcal{S}_n^T \tag{B.10}$$

One can also write the multiplex clustering coefficient induced by Eq. 2.1 in terms of the auxiliary supra-adjacency matrix by considering Eq. 2.2, which is a simplified version of the equation that counts cycles only in one direction. This yields

$$\mathcal{M}_M = \sqrt[3]{2}\mathcal{A}\widehat{\mathcal{C}}\,. \tag{B.11}$$

The matrix $\mathcal{M}_M$ is not symmetric, which implies that the associated graph is a directed supra-graph. Nevertheless, the clustering coefficient induced by $\mathcal{M}_M$ is the same as that induced by its transpose $\mathcal{M}_M^T$ if $\mathcal{A}$ is symmetric.

Appendix C

Null Model for Shuffling Inter-layer Connections

In Table C.1, we compare empirical values of layer-decomposed global clustering coefficients with clustering-coefficient values for a null model in which we preserve the topology of each intra-layer network but for which we independently shuffle the labels of the nodes inside of each layer.

That is, for each intra-layer network $G^\alpha = (V^\alpha, E^\alpha)$ we choose a permutation $\pi : V^\alpha \mapsto V^\alpha$ uniformly at random and construct a new multiplex network starting from $\{\pi(G^\alpha)\}$, where $\pi(G^\alpha) = (\pi(V^\alpha), \pi(E^\alpha))$ and $\pi(E^\alpha) = \{(\pi(u), \pi(v))|(u, v) \in E^\alpha\}$. In this way, we effectively randomize inter-layer edges but preserve both the structure of intra-layer networks and the number of inter-layer edges between each pair of layers. For our comparisons using this null model, most of the clustering coefficients take values that are significant for our data sets (see Table C.1). Because of the way that we construct the null model, the global single-layer clustering coefficients are exactly the same for the original data and the null model.

		Tailor Shop	Management	Families	Bank	Tube	Airline
C_M	orig.	0.319**	0.206**	0.223	0.293**	0.056**	0.101**
	NM	0.218 ± 0.007	0.131 ± 0.003	0.194 ± 0.029	0.223 ± 0.014	0.025 ± 0.008	0.054 ± 0.001
$C_M^{(1)}$	orig.	0.406	0.436	0.289	0.537	0.013	0.100
	NM	0.406	0.436	0.289	0.537	0.013	0.100
$C_M^{(2)}$	orig.	0.327**	0.273**	0.198	0.349**	0.043	0.150**
	NM	0.220 ± 0.009	0.176 ± 0.003	0.158 ± 0.041	0.240 ± 0.018	0.035 ± 0.018	0.082 ± 0.002
$C_M^{(3)}$	orig.	0.288**	0.192**	-	0.227’	0.314**	0.086**
	NM	0.165 ± 0.010	0.120 ± 0.003	-	0.186 ± 0.016	0.053 ± 0.043	0.037 ± 0.002

Table C.1: Clustering coefficients C_M, $C_M^{(1)}$, $C_M^{(2)}$, $C_M^{(3)}$ that correspond, respectively, to the global, one-layer, two-layer, and three-layer clustering coefficients for various multiplex networks. “Tailor Shop”: Kapferer tailor-shop network ($n = 39$, $m = 4$) [46]. “Management”: Krackhardt office cognitive social structure ($n = 21$, $m = 21$) [53]. “Families”: Padgett Florentine families social network ($n = 16$, $m = 2$) [14]. “Bank”: Roethlisberger and Dickson bank wiring-room social network ($n = 14$, $m = 6$) [79]. “Tube”: The London Underground (i.e., “The Tube”) transportation network ($n = 314$, $m = 14$) [**?**]. “Airline”: Network of flights between cities, in which each layer corresponds to a single airline ($n = 3108$, $m = 530$) [67]. The rows labeled “orig.” give the clustering coefficients for the original networks, and the rows labeled “NM” give the expected value and the standard deviation of the clustering coefficient in a null-model network in which we preserve the topology of the intra-layer networks but separately shuffle the node labels for each intra-layer network. For the original values, we perform a two-tailed Z-test to examine whether the observed clustering coefficients could have been produced by the null model. We designate the p-values as follows: *: $p < 0.05$, **: $p < 0.01$ for Bonferroni-corrected tests with 18 hypothesis; ’: $p < 0.05$, ”: $p < 0.01$ for uncorrected tests. We do not use any symbols for values that are not significant. We symmetrize directed networks by considering two nodes to be adjacent if there is at least one edge between them. The social networks above are node-aligned multiplex graphs, but the transportation networks are not node-aligned. We report values that are means over different numbers of realizations: 10^5 for Tailor Shop, 10^3 for Airline, 10^4 for Management, 10^5 for Families, 10^4 for Tube, and 10^5 for Bank.

Appendix D

A Simple Example illustrating differences between different multiplex clustering coefficients

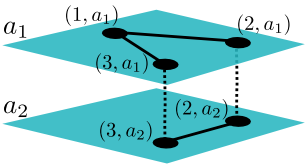

Figure D.1: A simple, illustrative example of a multiplex network.

We now use a simple example (see Fig. D.1) to illustrate the differences between the different notions of a multiplex clustering coefficient. Consider a two-layer multiplex network with three nodes in layer a_1 and two nodes in layer a_2. The three node-layer pairs in layer a_1 form a connected triple, the two node-layer pairs that are not part of this connected triple are adjacent via inter-layer edges to the two node-layer pairs in layer a_2, and these last two node-layer pairs are adjacent to each other.

The adjacency matrix $\mathcal{A}$ for the intra-layer graph is

$$\mathcal{A} = \begin{pmatrix} 0 & 1 & 1 & 0 & 0 \\ 1 & 0 & 0 & 0 & 0 \\ 1 & 0 & 0 & 0 & 0 \\ 0 & 0 & 0 & 0 & 1 \\ 0 & 0 & 0 & 1 & 0 \end{pmatrix}, \tag{D.1}$$

and the adjacency matrix $\mathcal{C}$ of the coupling supra-graph is

$$\mathcal{C} = \begin{pmatrix} 0 & 0 & 0 & 0 & 0 \\ 0 & 0 & 0 & 1 & 0 \\ 0 & 0 & 0 & 0 & 1 \\ 0 & 1 & 0 & 0 & 0 \\ 0 & 0 & 1 & 0 & 0 \end{pmatrix}. \tag{D.2}$$

Therefore, the supra-adjacency matrix is

$$\bar{\mathcal{A}} = \begin{pmatrix} 0 & 1 & 1 & 0 & 0 \\ 1 & 0 & 0 & 1 & 0 \\ 1 & 0 & 0 & 0 & 1 \\ 0 & 1 & 0 & 0 & 1 \\ 0 & 0 & 1 & 1 & 0 \end{pmatrix} . \tag{D.3}$$

The multiplex walk matrix $\mathcal{M}_M$ is

$$\mathcal{M}_M = \sqrt[3]{2} \begin{pmatrix} 0 & 1 & 1 & 1 & 1 \\ 1 & 0 & 0 & 0 & 0 \\ 1 & 0 & 0 & 0 & 0 \\ 0 & 0 & 1 & 0 & 1 \\ 0 & 1 & 0 & 1 & 0 \end{pmatrix} , \tag{D.4}$$

and we note that it is not symmetric. For example, node-layer pair $(2, a_2)$ is reachable from $(1, a_1)$, but node-layer pair $(1, a_1)$ is not reachable from $(2, a_2)$. The edge $[(1, a_1), (2, a_2)]$ in this supra-graph represents the walk $\{(1, a_1), (2, a_1), (2, a_2)\}$ in the multiplex network. The symmetric walk matrix $\mathcal{M}_{SM'}$ is

$$\mathcal{M}_{SM'} = \begin{pmatrix} 0 & 1 & 1 & 1 & 1 \\ 1 & 0 & 0 & 0 & 1 \\ 1 & 0 & 0 & 1 & 0 \\ 1 & 0 & 1 & 0 & 1 \\ 1 & 1 & 0 & 1 & 0 \end{pmatrix} . \tag{D.5}$$

The matrix $\mathcal{M}_{SM'}$ is the sum of $\mathcal{M}_M$ and $\mathcal{M}_M^T$ with rescaled diagonal blocks in order to not double-count the edges $[(1, a_1), (2, a_1)]$ and $[(1, a_1), (3, a_1)]$. Additionally,

$$\mathcal{M}_{SM} = \begin{pmatrix} 0 & 1 & 1 & 1 & 1 \\ 1 & 0 & 1 & 0 & 1 \\ 1 & 1 & 0 & 1 & 0 \\ 1 & 0 & 1 & 0 & 1 \\ 1 & 1 & 0 & 1 & 0 \end{pmatrix} , \tag{D.6}$$

which differs from $\mathcal{M}_{SM'}$ in the fact that node-layer pairs $(2, a_1)$ and $(3, a_1)$ are connected through the multiplex walk $\{(2, a_1), (2, a_2), (3, a_2), (3, a_1)\}$.
The adjacency matrix of the aggregated graph is

$$\mathcal{W} = \begin{pmatrix} 0 & 1 & 1 \\ 1 & 0 & 1 \\ 1 & 1 & 0 \end{pmatrix} . \tag{D.7}$$

That is, it is a complete graph without self-edges.
We now calculate $c_{*,i}$ using different definitions of a multiplex clustering coefficient.

To calculate $c_{M,i}$, we need to compute the auxiliary complete supra-adjacency matrix $\mathcal{M}_M^F$ according to Eq. B.11. We obtain

$$\mathcal{M}_M^F = \sqrt[3]{2}\mathcal{F}\widehat{\mathcal{C}} = \sqrt[3]{2}\begin{pmatrix} 0 & 1 & 1 & 1 & 1 \\ 1 & 0 & 1 & 0 & 1 \\ 1 & 1 & 0 & 1 & 0 \\ 0 & 0 & 1 & 0 & 1 \\ 0 & 1 & 0 & 1 & 0 \end{pmatrix} . \tag{D.8}$$

The clustering coefficient of node-layer pair $(1, a_1)$, which is part of two triangles that are reachable along the directions of the edges, is

$$c_{M,(1,a_1)} = \frac{1}{2} . \tag{D.9}$$

For node-layer pair $(2, a_1)$, we get

$$c_{M,(2,a_1)} = 1 , \tag{D.10}$$

which is the same as the clustering-coefficient values of the remaining node-layer pairs. To calculate $c_{SM',i}$, we need to compute $\mathcal{M}_{\mathcal{SM}'}^{\mathcal{F}}$, which we obtain using Eq. B.7. We thus obtain

$$\mathcal{M}_{SM'}^F = \mathcal{F}\widehat{\mathcal{C}} + \widehat{\mathcal{C}}\mathcal{F} = \begin{pmatrix} 0 & 1 & 1 & 1 & 1 \\ 1 & 0 & 1 & 0 & 1 \\ 1 & 1 & 0 & 1 & 0 \\ 1 & 0 & 1 & 0 & 1 \\ 1 & 1 & 0 & 1 & 0 \end{pmatrix} . \tag{D.11}$$

In the supra-graph associated with the supra-adjacency matrix $\mathcal{F}\widehat{\mathcal{C}} + \widehat{\mathcal{C}}\mathcal{F}$, all node-layer pairs are adjacent to all other node-layer pairs except those that correspond to the same physical nodes.

The clustering coefficient of node-layer pair $(1, a_1)$, which is part of six triangles, is

$$c_{SM',(1,a_1)} = \frac{1}{2} = c_{M,(1,a_1)} . \tag{D.12}$$

The clustering coefficient of node-layer pair $(2, a_1)$, which is part of one triangle, is

$$c_{SM',(2,a_1)} = 1 . \tag{D.13}$$

To calculate $c_{SM,i}$, we compute $\mathcal{M}_{SM}^F$ using Eq. B.6. We thus obtain

$$\mathcal{M}_{SM}^F = \widehat{\mathcal{C}}\mathcal{F}\widehat{\mathcal{C}} = \begin{pmatrix} 0 & 1 & 1 & 1 & 1 \\ 1 & 0 & 2 & 0 & 2 \\ 1 & 2 & 0 & 2 & 0 \\ 1 & 0 & 2 & 0 & 2 \\ 1 & 2 & 0 & 2 & 0 \end{pmatrix} . \tag{D.14}$$

The only difference between the graphs associated with the matrices $\widehat{\mathcal{C}}\widehat{\mathcal{F}}\widehat{\mathcal{C}}$ and $\widehat{\mathcal{F}}\widehat{\mathcal{C}} + \widehat{\mathcal{C}}\widehat{\mathcal{F}}$ is the weight of the edges in $\widehat{\mathcal{C}}\widehat{\mathcal{F}}\widehat{\mathcal{C}}$ that take into account the fact that intra-layer edges might be repeated in the two layers.
The clustering coefficient of node-layer pair $(1, a_1)$, which is part of eight triangles, is

$$c_{SM,(1,a_1)} = \frac{8}{12} = \frac{2}{3}\,. \tag{D.15}$$

The clustering coefficient of node-layer pair $(2, a_1)$, which is part of four triangles, is

$$c_{SM,(2,a_1)} = \frac{4}{6} = \frac{2}{3}\,. \tag{D.16}$$

Because we are weighting edges based on the number of times an edge between two nodes is repeated in different layers among a given pair of physical nodes in the normalization, none of the node-layer pairs has a clustering coefficient equal to 1. By contrast, all nodes have clustering coefficients with the same value in the aggregated network, for which the layer information has been lost. In particular, they each have a clustering-coefficient value of 1, independent of the definition of the multiplex clustering coefficient.

Appendix E

Random Boolean Multilevel Networks

The material presented in this appendix was developed during the very early stage of the investigation reported in this thesis. Partially because of that, it is in a notation and in a formal language slightly different from the rest of the thesis. Although it would have been possible to fit it in the homogeneous framework developed in the first chapter of this thesis, we think that its original formulation is better suited to represent Multilevel Boolean Networks. For these reasons, we present it here in a separate appendix and not in the main text.

Nearly four decades ago, Random Boolean Networks (RBNs) were introduced as a way to describe the dynamics of biochemical networks [49, 12, 4, 13, 52, 51, 26]. RBNs consider that each gene of a genetic regulatory network is a node of a directed graph, the direction corresponding to the effect of one gene on the expression of another. The nodes can be in one of two states: they are either *on* (1) or *off* (0) - i.e. in the case of a gene its target protein is expressed or not. The system so composed evolves at discrete time steps. At each time step nodes are updated according to a boolean rule assigned to each node that is a function of its inputs. Notwithstanding the high simplicity of RBNs models, they can capture the behavior of some real regulatory networks [54] allowing for the study of several dynamical features, above all their critical properties. However, although some coupled Boolean networks have been investigated [86, 85], the vast majority of works has considered RBNs as classical monoplex networks.

The previous description implicitly assumes that all biochemical signals are equivalent and then collapses information from different pathways. Actually, in cellular biochemical networks, many different signaling channels do work in parallel [60, 72], i.e., the same gene or biochemical specie can be involved in a regulatory interaction,

in a metabolic reaction or in another signaling pathway. Considering that different operational levels (pathways) are interconnected layers of interaction is a more accurate set up for the topology of biochemical networks. Thus, this topology is more consistent with a multiplex network in which each level would represent the different signaling pathways or channels the element participates in. On the other hand, accounting for the multilevel nature of the system dynamics also represents a point of interest by itself, as this allows to inspect what are the consequences of new ways of interdependency between the structure and the dynamics. In this sense, a Boolean dynamic is general enough so as to serve as a null model for many other complex dynamical processes.

We inspect a Boolean multiplex network model, in which each node participates in one or more layers of interactions, being its state in a layer constrained by its own state in another layer. Therefore, we focus on the case of canalizing rules as a way to integrate information across layers. Boolean functions are canalizing if whenever the canalizing variable takes a given value, the canalizing one, the function always yields the same output. Capitalizing on a semi-annealed approximation, we analytically and numerically study the conditions defining the stability of the aforementioned system. By doing so, we show that the interdependency between the layers can be enough to either stabilize the different levels or the whole system. Remarkably, this also happens for parameter values where the sub-systems, if isolated, were unstable.

To make thing simple, we use an ad-hoc representation of the multiplex network in that case, which came directly by how boolean rules at different levels integrate. Even if this representation is consistent with that of 1, and can be rewritten in those terms, we prefer to leave it in its original formulation.

We encode the structure of the multiplex in two objects. First, we have the participation matrix $\mathbf{P} = p_{i\alpha}$,as in chapter 1 , whose elements are 1 if node i appears in layer α and 0 otherwise. Secondly, we introduce an adjacency tensor, $A_{ij\alpha}$, whose elements are 1 if there is a link between nodes i and j in layer α and 0 otherwise. The adjacency tensor $A_{ij\alpha}$ is just another way to represent intra-layer connections, more compact then the intra-layer adjacency matrix $\mathcal{A}$. In terms of the adjacency tensor, the *total degree* of node i will be $K_i = \sum_{j\alpha} A_{ij\alpha} = \sum_{\alpha} K_{i\alpha}$, where $K_{i\alpha}$ is the degree of node i in layer α. We remember that the *multiplexity degree* of a node is defined as the number of layers in which it appears as $\kappa_i = \sum_{\alpha} p_{i\alpha}$. Note that the number of different nodes in the multiplex will be then $\tilde{N} = NM - \sum_i (\kappa_i - 1)$.

Next, let us consider a state vector

$$\tilde{\mathbf{x}}(t) = (\tilde{x}_1(t), ..., \tilde{x}_{\tilde{N}(t)}), \tag{E.1}$$

where $\tilde{x}_i(t) \in \{0,1\}$ and a set of update functions such that

$$\tilde{x}_i(t) = \tilde{f}_i(\tilde{x}_{j\in\Gamma_\alpha^{\text{in}}(i)}(t-1)). \tag{E.2}$$

where $\Gamma_\alpha^{\text{in}}(i)$ refers to all the incoming neighbors j of node i at each layer α, with $\alpha = 1 \dots M$.

Equations (E.1-E.2) define a Boolean multiplex network. In addition, due to the multiplex nature of the network, we also define a set of update functions for each layer as

$$x_i^l(t) = f_i^l((\tilde{x}_{j\in\Gamma_l^{\text{in}}(i)}(t-1))). \tag{E.3}$$

where now the arguments of the function are restricted to the specific layer $\alpha = l$. Equation (E.3) governs how each node is updated in each layer. So, Eq. (E.2) can be rewritten as

$$\tilde{x}_i(t) = \tilde{f}_i(f_i^1, \dots f_i^M), \tag{E.4}$$

where $\tilde{f}_i$ is a canalizing function of its inputs. These definitions allow investigating how the stability of the Boolean model is affected by the multiplex structure of the system and by the existence of nodes with different multiplexity degrees.

E.1 The Average Sensitivity

We first inspect the dependency of the average sensitivity s^f, which has been shown to be a useful order parameter in RBNs [88, 56], on the multiplexity degree κ_i. Following [74], we write the activity a_j^f of the variable x_j in a function f of K inputs as $a_j^f = \frac{1}{2^K}\sum_{\mathbf{x}\in\{0,1\}} \frac{\partial f(\mathbf{x})}{\partial x_j}$, where $\frac{\partial f(\mathbf{x})}{\partial x_j} = f(\mathbf{x}_{(j,0)}) \oplus f(\mathbf{x}_{(j,1)})$ and $\mathbf{x}_{(j,R)}$ represents a random vector $\mathbf{x} \in 0,1$ with the jth input fixed to R and $\oplus$ is the arithmetic addition modulo 2.

Similarly, assuming that the inputs are also uniformly distributed, the average sensitivity is equal to the sum of the activities, i.e., $s^f = \sum_{i=1}^K E[\chi[f(\mathbf{x}\oplus e_i) \neq f(\mathbf{x})]] = \sum_{i=1}^K a_j^f$, where e_i is a zeroes vector with 1 in the i-th position, and $\chi[A]$ is an indicator function that is equal to 1 if and only if A is true.

To illustrate how multiplexity affects the sensitivity of a node, without loss of generality, we study analytically and numerically a multiplex network of two layers. Let us denote by p the bias of the Boolean functions, and α and β the two respective layers. A node i in our model depends on the state of its neighbors in layer α and also on the state of its neighbors in β via the auxiliary function $\tilde{f}^\beta$. Suppose that the canalizing state in α and β is 1 (the discussion for 0 would be identical). Then, the

updating function of i can be written as $\tilde{f}_i(f_i^\alpha, f_i^\beta) = f^\alpha \vee f^\beta$, being $\vee$ the Boolean operator OR. From the definition of the activities and the previous relation, it follows that $E[a_j^{\tilde{f}}] = 2^{-(\kappa_i-1)}2p(1-p)$, which is different from the value one would obtain in the case of a simple canalizing function. Similarly, for the sensitivity one gets

$$E[\tilde{s}^{\tilde{f}}] = 2^{-(\kappa_i-1)} \sum_\alpha E[s^{f^\alpha}], \tag{E.5}$$

where $E[s^{f^\alpha}] = 2p(1-p)K_\alpha$ is the expected average sensitivity of a function in layer α if it were isolated.

E.2 Semi-annealed approximation

We study the stability of the Boolean multiplex system using a semi-annealed approximation. This approach considers the network as a static topological object while the update functions f_i^l $(l = \alpha, \beta)$ are assigned randomly at each time step as well as the couplings. Thus, we can write the update function for the components of the difference vector $\tilde{\mathbf{y}}(t) = \langle |\, \tilde{\mathbf{x}}(t) - \hat{\tilde{\mathbf{x}}}(t)\, | \rangle$, where $\hat{\tilde{x}}$ is a perturbed replica of $\tilde{\mathbf{x}}$ in which a (small) fraction of the nodes were flipped, yielding

$$\tilde{y}_i(t) = \tilde{q}_i[1 - \prod_{j \in \Gamma_i}(1 - \tilde{y}_j(t-1))] \tag{E.6}$$

which is equivalent to the expression derived in [74], but also taking into account Eq. (E.5), with $q_i = 2p(1-p)$ for a monoplex network and Γ_i being the set of all neighbors of i in all layers. Considering a small perturbation, linearization of Eq. (E.6) around the fixed point solution $\tilde{\mathbf{y}}(t) = \mathbf{0}$ leads to

$$\tilde{y}_i(t+1) \approx 2^{-(\kappa_i-1)} q_i \sum_{\alpha=1}^{M} \sum_{j=1}^{N} A_{ij\alpha} \tilde{y}_j(t) \tag{E.7}$$

that can be written in matrix form as $\tilde{\mathbf{y}}(t+1) = \sum_\alpha Q_\alpha \tilde{\mathbf{y}}(t)$, with $Q_{ij\alpha} = 2^{-(\kappa_i-1)} q_i A_{ij\alpha}$. The largest eigenvalue, λ_Q, of the matrix $Q = \sum_\alpha Q_\alpha$ governs the stability of the system [74]. It is worth noticing that the latter refers to the stability condition *for the whole system* and, given a fixed topology for each layer, it depends on the multiplexity degree. For the case of nonuniform κ_i we obtain an analogous mean-field approximation to λ_Q in [74],

$$\lambda_Q \approx \frac{\langle 2^{-(\kappa_i-1)} q_i K_i^{\text{in}} K_i^{\text{out}} \rangle}{\langle K \rangle}, \tag{E.8}$$

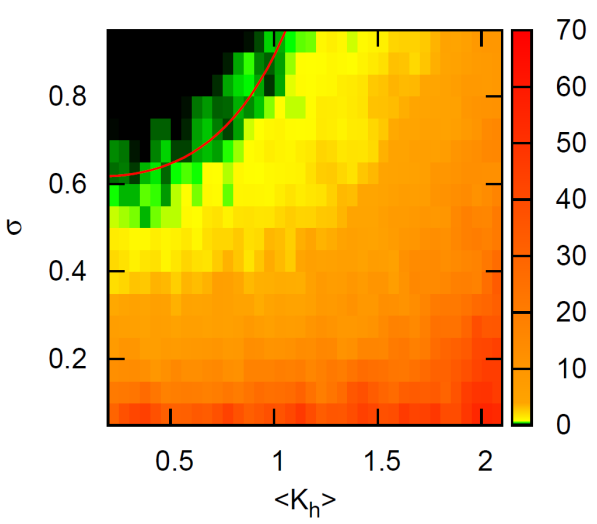

Figure E.1: Color-coded average Hamming distance for the whole system with fixed observed connectivity $\langle K_o \rangle = 2.9$ for different values of the hidden connectivity $\langle K_h \rangle$, and the probability for a node in a layer to be present also in the other layer σ. The network is composed of $N = 10^3$ nodes per layer as explained in Fig **??**. The continuos line is the solution (zeros) of Eq. (E.11). Simulations were performed for an initial Hamming distance of 0.01 and the results are averages over 50 realizations of the network and 300 random initial conditions.

where $\langle K \rangle$ is the average degree of the multiplex. Note that the stability of the multiplex depends on κ_i and $K_i^{\text{in}} K_i^{\text{out}}$, which, in general, are not independent variables – thus, $\tilde{q}_i$ and K_i are anticorrelated. To find the critical condition let $\tilde{P}(\kappa = n)$ be the probability that a node in the whole system has multiplexity degree n. This magnitude depends on the same quantity but at the single layer level as $\tilde{P}(\kappa = n) = \frac{N}{\tilde{N}} \frac{M}{n} P(\kappa = n)$, where $P(\kappa = n)$ is the probability that a randomly chosen node of a layer has multiplexity degree n. For the average degree of the multiplex we have:

$$\langle K \rangle = \sum_n \frac{\binom{M-1}{n-1}}{\binom{M}{n}} \tilde{P}(\kappa = n) \sum_l \langle K_l \rangle = \frac{N}{\tilde{N}} \sum_l \langle K_l \rangle, \tag{E.9}$$

where $\langle K_l \rangle$ is the average degree of layer l.

Inserting the previous expression into Eq. (E.8) and considering the case in which there are no correlations between K^{in} and K^{out}, one gets,

$$\langle \tilde{q} \rangle \sum_l \langle K_l \rangle - \frac{2(M\langle \tilde{q} \rangle - \langle \kappa \tilde{q} \rangle)}{M-1} \frac{\sum_{l_1 < l_2} \langle K_{l_1} \rangle \langle K_{l_2} \rangle}{\sum_l \langle K_l \rangle} = 1, \tag{E.10}$$

with $l_1 = 1 \ldots, M$, $l_2 = 1 \ldots, M$ and $\langle \tilde{q} \rangle = \sum_{n=1}^{M} \tilde{q}(\kappa = n) P(\kappa = n)$ is the average sensitivity on a layer. It is worth noticing that the first term on the l.h.s. of Eq. (E.10) is the expression one would obtain using an annealed approximation. The second term is always positive. Therefore, it captures the stabilizing effects of multiplexity, rightly predicting ordered behavior in regions in which the annealed approximation would not.

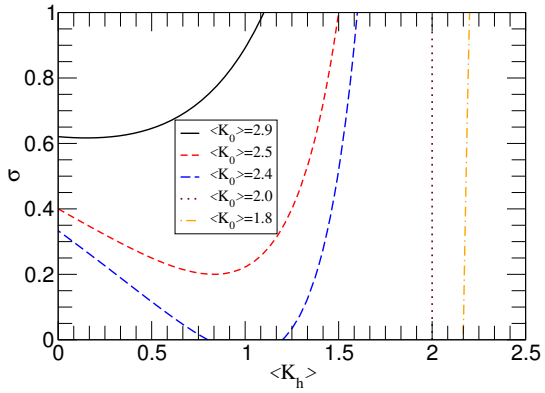

Figure E.2: The lines are the solution (zeros) of Eq. (E.11) for different values of the hidden connectivity $\langle K_{\rm h}\rangle$, the observed connectivity $\langle K_{\rm o}\rangle$ and the probability of a node belongs to both layers σ. We have set $q_i = q = \frac{1}{2}$.

E.3 Numerical Simulations for a two-layers system

Once we have derived the critical condition for a system made up of an arbitrary number of layers, let us compare the analytical results with numerical simulations for a two-layers system with $q_i = q$. Let σ be the probability for a node in a layer to be present also in the other layer, then we have $P(\kappa = 2) = \sigma$ and $P(\kappa = 1) = 1 - \sigma$. Besides, for the sake of simplicity, consider that the average connectivity of one layer is observed, $\langle K_{\rm o}\rangle$, and fixed (for instance, because one measures it), and that the average connectivity of the other layer is unknown or hidden $\langle K_{\rm h}\rangle$. Recalling that the size of the multiplex system is $\tilde{N} = (2-\sigma)N$ −where N is the number of nodes per layer−, the mean connectivity $\langle K\rangle$ can be written as $\langle K\rangle = \frac{\langle K_{\rm h}\rangle + \langle K_{\rm o}\rangle}{(2-\sigma)}$, which leads to the following expression for the critical condition of the two-layers system

$$\frac{2-\sigma}{4}(\langle K_{\rm h}\rangle + \langle K_{\rm o}\rangle) - (1-\sigma)\frac{\langle K_{\rm h}\rangle\langle K_{\rm o}\rangle}{\langle K_{\rm h}\rangle + \langle K_{\rm o}\rangle} = \frac{1}{2q} \tag{E.11}$$

that as a function of σ and $\langle K_{\rm h}\rangle$ gives an hyperbolic critical curve.

To verify that our analytical calculations are valid, we have performed extensive numerical simulations of the Boolean dynamics on a random multiplex network made up of two layers in which N nodes are randomly connected among them and only a fraction σ of them are present on both layers. As it is customarily done, we test the stability of the system by measuring the long-time Hamming distance for different trajectories generated from two close initial states. Figure 3.2 shows the results obtained when the mean connectivity $\langle K_{\rm o}\rangle$ of a layer is fixed and both σ and the mean connectivity of the other layer $\langle K_{\rm h}\rangle$ change (the Hamming distance is color coded as indicated). First, we note that the transition from stability to an unstable regime nicely agrees with the theoretical prediction. Secondly, it is worth highlighting

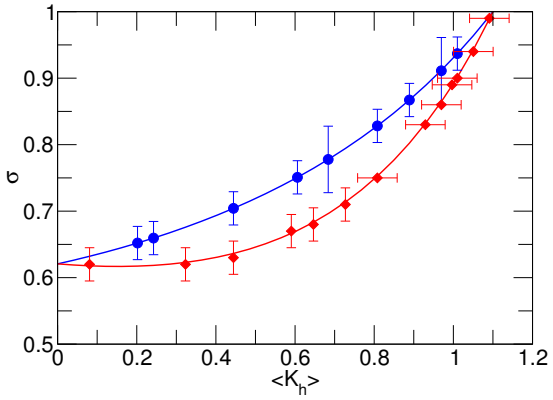

Figure E.3: (color online) Critical curves for a network made up of 10^4 nodes per layer as a function of the probability of a node to be part of both layers σ, and the hidden connectivity $\langle K_{\rm h}\rangle$. The blue line corresponds to the critical curve when a single layer is observed while the red one refers to the whole system. The rest of simulation parameters are the same as for the other figures.

a new effect linked to the multi-level nature of the system: the region of low $\langle K_{\rm h}\rangle$ and low σ is unstable despite the fact that those values of $\langle K_{\rm h}\rangle$ would make the hidden layer, in a *simplex graph* description, stable. However, due to the low coupling (σ), the instability of the multiplex is determined by that of the observed layer, the leading one. Admittedly, when increasing the coupling σ the stable (hidden) layer is able to stabilize the whole system.

We have further explored the dependency between the stability of the multiplex and the average degrees of both layers. Figure E.2 shows the analytical solution of Eq. (E.11) for different values of $\langle K_{\rm h}\rangle$ and $\langle K_{\rm o}\rangle$. The results show a very rich phase diagram. Depending on the values of both connectivities, a double transition from a chaotic regime to an ordered one and again to another chaotic regime is predicted. More interestingly, the transition from the ordered to the disordered regime does not depend on σ only when both layers operate at their respective critical points, namely, when $\langle K_{\rm h}\rangle = \langle K_{\rm o}\rangle = 1/q = 2$.

Up to now, we have analyzed the stability of the multiplex system. In practice, it is more common to have access to only one layer, so that one can measure the stability of that layer given that it is connected to a hidden (inaccessible) one. Therefore, it is also important to inspect the stability condition of a single layer within the multiplex. To this end, we should solve Eq. (E.8) taking into account only the nodes that belong

to the layer whose stability is scrutinized. In this case, the critical condition reads

$$\frac{\sigma}{4}(\langle K_{\rm h}\rangle^2 - \langle K_{\rm o}\rangle^2 + 2\langle K_{\rm h}\rangle\langle K_{\rm o}\rangle) + \frac{\langle K_{\rm o}\rangle^2}{2} = \frac{\langle K_{\rm o}\rangle + \sigma\langle K_{\rm h}\rangle}{2q}. \tag{E.12}$$

Figure E.3 compares results of simulations for a larger network of $N = 10^4$ nodes per layer with the theoretical solution (Eq. (E.12), blue line) showing again a good agreement between analytical and simulation results. Remarkably, the results show that a single ingredient −the multilevel nature of the system − can explain why there are biologically stable systems that are however theoretically expected to operate in the unstable regime (i.e., their average degree is larger than $1/q$). In other words, the sole reason could be that these systems are not isolated, but are coupled to other hidden layers that, if ordered, can stabilize the system. Finally, for the sake of comparisons, we have also represented in Fig. E.3 (red line) the case shown in Fig. 3.2 but for the same larger system size.

Bibliography

[1] Kivela M. Arenas A. Barthelemy M. Gleeson J. P. Moreno Y. Porter M. A. Multilayer networks. *Journal of Complex Networks*, 2(3):203–271, 2014.

[2] Radicchi F. Arenas A. Abrupt transition in the structural formation of interconnected networks. *Nat. Phys.*, 9:717–720, 2013.

[3] Sebastian E Ahnert, Diego Garlaschelli, TMA Fink, and Guido Caldarelli. Ensemble approach to the analysis of weighted networks. *Physical Review E*, 76(1):016101, 2007.

[4] Maximino Aldana, Susan Coppersmith, and Leo P Kadanoff. Boolean dynamics with random couplings. In *Perspectives and Problems in Nolinear Science*, pages 23–89. Springer, 2003.

[5] Juan A Almendral and Albert Díaz-Guilera. Dynamical and spectral properties of complex networks. *New Journal of Physics*, 9(6):187, 2007.

[6] Alex Arenas, Albert Díaz-Guilera, and Conrad J Pérez-Vicente. Synchronization reveals topological scales in complex networks. *Physical review letters*, 96(11):114102, 2006.

[7] Louise Barrett, S Peter Henzi, and David Lusseau. Taking sociality seriously: the structure of multi-dimensional social networks as a source of information for individuals. *Philosophical Transactions of the Royal Society B: Biological Sciences*, 367(1599):2108–2118, 2012.

[8] Federico Battiston, Vincenzo Nicosia, and Vito Latora. Metrics for the analysis of multiplex networks. *Phys. Rev. E*, 89:032804, 2013.

[9] Jay David Bolter and Remediation Grusin. Understanding new media, 1999.

[10] Javier Borge-Holthoefer, Raquel A Baños, Sandra González-Bailón, and Yamir Moreno. Cascading behaviour in complex socio-technical networks. *Journal of Complex Networks*, 1(1):3–24, 2013.

[11] Javier Borge-Holthoefer, Alejandro Rivero, Iñigo García, Elisa Cauhé, Alfredo Ferrer, Darío Ferrer, David Francos, David Iñiguez, María Pilar Pérez, Gonzalo Ruiz, et al. Structural and dynamical patterns on online social networks: the spanish may 15th movement as a case study. *PloS one*, 6(8):e23883, 2011.

[12] Stefan Bornholdt. Less is more in modeling large genetic networks. *SCIENCE-NEW YORK THEN WASHINGTON-*, 310(5747):449, 2005.

[13] Stefan Bornholdt and Thimo Rohlf. Topological evolution of dynamical networks: Global criticality from local dynamics. *Physical Review Letters*, 84(26):6114, 2000.

[14] Ronald L Breiger and Philippa E Pattison. Cumulated social roles: The duality of persons and their algebras. *Social networks*, 8(3):215–256, 1986.

[15] Piotr Bródka, Przemysław Kazienko, Katarzyna Musiał, and Krzysztof Skibicki. Analysis of neighbourhoods in multi-layered dynamic social networks. *International Journal of Computational Intelligence Systems*, 5(3):582–596, 2012.

[16] Piotr Bródka, Katarzyna Musial, and Przemysław Kazienko. A method for group extraction in complex social networks. In *Knowledge Management, Information Systems, E-Learning, and Sustainability Research*, pages 238–247. Spreinger, 2010.

[17] Andries E Brouwer and Willem H Haemers. Spectra of graphs. 2012.

[18] Charles D Brummitt, Kyu-Min Lee, and K-I Goh. Multiplexity-facilitated cascades in networks. *Physical Review E*, 85(4):045102, 2012.

[19] Marcello Buiatti and Marco Buiatti. The living state of matter. In *Rivista di biologia biology forum*, volume 94, pages 59–82. ANICIA SRL, 2001.

[20] Damon Centola. The spread of behavior in an online social network experiment. *science*, 329(5996):1194–1197, 2010.

[21] Stephanie E Chang, Hope A Seligson, and Ronald T Eguchi. Estimation of the economic impact of multiple lifeline disruption: Memphis light, gas and water division case study. 1996.

[22] Nicholas A Christakis and James H Fowler. The spread of obesity in a large social network over 32 years. *New England journal of medicine*, 357(4):370–379, 2007.

[23] L da F Costa, Francisco A Rodrigues, Gonzalo Travieso, and Paulino Ribeiro Villas Boas. Characterization of complex networks: A survey of measurements. *Advances in Physics*, 56(1):167–242, 2007.

[24] Regino Criado, Julio Flores, Alejandro García del Amo, Jesús Gómez-Gardeñes, and Miguel Romance. A mathematical model for networks with structures in the mesoscale. *International Journal of Computer Mathematics*, 89(3):291–309, 2012.

[25] Kinkar Ch Das and RB Bapat. A sharp upper bound on the largest laplacian eigenvalue of weighted graphs. *Linear algebra and its applications*, 409:153–165, 2005.

[26] Maria I Davidich and Stefan Bornholdt. Boolean network model predicts cell cycle sequence of fission yeast. *PloS one*, 3(2):e1672, 2008.

[27] Manlio De Domenico, Albert Solé-Ribalta, Emanuele Cozzo, Mikko Kivelä, Yamir Moreno, Mason A Porter, Sergio Gómez, and Alex Arenas. Mathematical formulation of multilayer networks. *Physical Review X*, 3(4):041022, 2013.

[28] Mark Dickison, Shlomo Havlin, and H Eugene Stanley. Epidemics on interconnected networks. *Physical Review E*, 85(6):066109, 2012.

[29] Jonathan F Donges, Hanna CH Schultz, Norbert Marwan, Yong Zou, and Jürgen Kurths. Investigating the topology of interacting networks. *The European Physical Journal B*, 84(4):635–651, 2011.

[30] Sergey N Dorogovtsev, Alexander V Goltsev, and José FF Mendes. Critical phenomena in complex networks. *Reviews of Modern Physics*, 80(4):1275, 2008.

[31] Ernesto Estrada, Naomichi Hatano, and Michele Benzi. The physics of communicability in complex networks. *Physics reports*, 514(3):89–119, 2012.

[32] Ernesto Estrada and Juan A Rodriguez-Velazquez. Subgraph centrality in complex networks. *Physical Review E*, 71(5):056103, 2005.

[33] Linton C Freeman. Centrality in social networks conceptual clarification. *Social networks*, 1(3):215–239, 1979.

[34] Noah E Friedkin and Eugene C Johnsen. *Social influence network theory: A sociological examination of small group dynamics*, volume 33. Cambridge University Press, 2011.

[35] Riccardo Gallotti and Marc Barthelemy. Anatomy and efficiency of urban multimodal mobility. *Scientific reports*, 4, 2014.

[36] Max Gluckman and Cyril Daryll Forde. *Essays on the ritual of social relations*. Manchester University Press, 1962.

[37] William Goffman and VA Newill. Generalization of epidemic theory. *Nature*, 204(4955):225–228, 1964.

[38] S Gómez, A Arenas, J Borge-Holthoefer, S Meloni, and Y Moreno. Discrete-time markov chain approach to contact-based disease spreading in complex networks. *EPL (Europhysics Letters)*, 89(3):38009, 2010.

[39] Sergio Gomez, Albert Diaz-Guilera, Jesus Gomez-Gardeñes, Conrad J Perez-Vicente, Yamir Moreno, and Alex Arenas. Diffusion dynamics on multiplex networks. *Physical review letters*, 110(2):028701, 2013.

[40] Sandra González-Bailón, Javier Borge-Holthoefer, Alejandro Rivero, and Yamir Moreno. The dynamics of protest recruitment through an online network. *Scientific reports*, 1, 2011.

[41] Mark Granovetter. Threshold models of collective behavior. *American journal of sociology*, pages 1420–1443, 1978.

[42] Peter Grindrod. Range-dependent random graphs and their application to modeling large small-world proteome datasets. *Physical Review E*, 66(6):066702, 2002.

[43] Willem H Haemers. Interlacing eigenvalues and graphs. *Linear Algebra and its applications*, 226:593–616, 1995.

[44] José Luis Iribarren and Esteban Moro. Branching dynamics of viral information spreading. *Physical Review E*, 84(4):046116, 2011.

[45] B. Kapferer. Norms and the manipulation of relationships in a work context. *Social Networks in Urban Situations*, 1969.

[46] Bruce Kapferer. *Strategy and transaction in an African factory: African workers and Indian management in a Zambian town*. Manchester University Press, 1972.

[47] Martin Karlberg. Testing transitivity in graphs. *Social Networks*, 19(4):325–343, 1997.

[48] Márton Karsai, Mikko Kivelä, Raj Kumar Pan, Kimmo Kaski, János Kertész, A-L Barabási, and Jari Saramäki. Small but slow world: How network topology and burstiness slow down spreading. *Physical Review E*, 83(2):025102, 2011.

[49] S Kauffman. Gene regulation networks: a theory for their global structure and behaviors. *Current topics in developmental biology*, 6(6):145, 1971.

[50] Stuart A Kauffman. Metabolic stability and epigenesis in randomly constructed genetic nets. *Journal of theoretical biology*, 22(3):437–467, 1969.

[51] Konstantin Klemm and Stefan Bornholdt. Stable and unstable attractors in boolean networks. *Physical Review E*, 72(5):055101, 2005.

[52] Konstantin Klemm and Stefan Bornholdt. Topology of biological networks and reliability of information processing. *Proceedings of the National Academy of Sciences of the United States of America*, 102(51):18414–18419, 2005.

[53] David Krackhardt. Cognitive social structures. *Social networks*, 9(2):109–134, 1987.

[54] Fangting Li, Tao Long, Ying Lu, Qi Ouyang, and Chao Tang. The yeast cell-cycle network is robustly designed. *Proceedings of the National Academy of Sciences of the United States of America*, 101(14):4781–4786, 2004.

[55] R Duncan Luce and Albert D Perry. A method of matrix analysis of group structure. *Psychometrika*, 14(2):95–116, 1949.

[56] Bartolo Luque and Ricard V Solé. Lyapunov exponents in random boolean networks. *Physica A: Statistical Mechanics and its Applications*, 284(1):33–45, 2000.

[57] Ben D MacArthur and Rubén J Sánchez-García. Spectral characteristics of network redundancy. *Physical Review E*, 80(2):026117, 2009.

[58] Ben D MacArthur, Rubén J Sánchez-García, and James W Anderson. Symmetry in complex networks. *Discrete Applied Mathematics*, 156(18):3525–3531, 2008.

[59] J Martín-Hernández, H Wang, P Van Mieghem, and G DAgostino. Algebraic connectivity of interdependent networks. *Physica A: Statistical Mechanics and its Applications*, 404:92–105, 2014.

[60] Natalia J Martinez and Albertha JM Walhout. The interplay between transcription factors and microrna s in genome-scale regulatory networks. *Bioessays*, 31(4):435–445, 2009.

[61] Sergey Melnik, Jonathan A Ward, James P Gleeson, and Mason A Porter. Multi-stage complex contagions. *Chaos: An Interdisciplinary Journal of Nonlinear Science*, 23(1):013124, 2013.

[62] Attilio Milanese, Jie Sun, and Takashi Nishikawa. Approximating spectral impact of structural perturbations in large networks. *Physical Review E*, 81(4):046112, 2010.

[63] Giovanna Miritello, Rubén Lara, Manuel Cebrian, and Esteban Moro. Limited communication capacity unveils strategies for human interaction. *Scientific reports*, 3, 2013.

[64] J. D. Murray. *Mathematical Biology*. Springer-Verlag, 2002.

[65] Mark Newman. *Networks: an introduction*. Oxford University Press, 2010.

[66] J-P Onnela, Jari Saramäki, Jorkki Hyvönen, György Szabó, David Lazer, Kimmo Kaski, János Kertész, and A-L Barabási. Structure and tie strengths in mobile communication networks. *Proceedings of the National Academy of Sciences*, 104(18):7332–7336, 2007.

[67] openflights.org. http://openflights.org/data.htm.

[68] Tore Opsahl and Pietro Panzarasa. Clustering in weighted networks. *Social networks*, 31(2):155–163, 2009.

[69] Chiara Orsini, Marija M Dankulov, Pol Colomer-de Simón, Almerima Jamakovic, Priya Mahadevan, Amin Vahdat, Kevin E Bassler, Zoltán Toroczkai, Marián Boguñá, Guido Caldarelli, et al. Quantifying randomness in real networks. *Nature communications*, 6, 2015.

[70] Roni Parshani, Sergey V Buldyrev, and Shlomo Havlin. Interdependent networks: Reducing the coupling strength leads to a change from a first to second order percolation transition. *Physical review letters*, 105(4):048701, 2010.

[71] Filippo Passerini and Simone Severini. Quantifying complexity in networks: the von neumann entropy. *International Journal of Agent Technologies and Systems*, 1(4):58–67, 2009.

[72] Nicolás Peláez and Richard W Carthew. Biological robustness and the role of micrornas: a network perspective. *Current topics in developmental biology*, 99:237, 2012.

[73] Boris Podobnik, D Horvatić, Mark Dickison, and H Eugene Stanley. Preferential attachment in the interaction between dynamically generated interdependent networks. *EPL (Europhysics Letters)*, 100(5):50004, 2012.

[74] Andrew Pomerance, Edward Ott, Michelle Girvan, and Wolfgang Losert. The effect of network topology on the stability of discrete state models of genetic control. *Proceedings of the National Academy of Sciences*, 106(20):8209–8214, 2009.

[75] Alex Pothen, Horst D Simon, and Kang-Pu Liou. Partitioning sparse matrices with eigenvectors of graphs. *SIAM journal on matrix analysis and applications*, 11(3):430–452, 1990.

[76] Filippo Radicchi. Driving interconnected networks to supercriticality. *Physical Review X*, 4(2):021014, 2014.

[77] Harrison Rainie and Barry Wellman. *Networked: The new social operating system*. Mit Press Cambridge, MA, 2012.

[78] Anatol Rapoport. Spread of information through a population with socio-structural bias: Ii. various models with partial transitivity. *The bulletin of mathematical biophysics*, 15(4):535–546, 1953.

[79] FJ Roethlisberger and WJ Dickson. Management and the worker. 1939.

[80] Everett M Rogers. *Diffusion of innovations*. Simon and Schuster, 2010.

[81] M Puck Rombach, Mason A Porter, James H Fowler, and Peter J Mucha. Core-periphery structure in networks. *SIAM Journal on Applied mathematics*, 74(1):167–190, 2014.

[82] Marco Saerens, Francois Fouss, Luh Yen, and Pierre Dupont. The principal components analysis of a graph, and its relationships to spectral clustering. In *Machine Learning: ECML 2004*, pages 371–383. 2004.

[83] Faryad Darabi Sahneh, Caterina Scoglio, and Piet Van Mieghem. Exact coupling threshold for structural transition in interconnected networks. *arXiv preprint arXiv:1409.6560*, 2014.

[84] Jari Saramäki, Mikko Kivelä, Jukka-Pekka Onnela, Kimmo Kaski, and Janos Kertesz. Generalizations of the clustering coefficient to weighted complex networks. *Physical Review E*, 75(2):027105, 2007.

[85] Roberto Serra, Marco Villani, Chiara Damiani, Alex Graudenzi, and Annamaria Colacci. The diffusion of perturbations in a model of coupled random boolean networks. In *Cellular automata*, pages 315–322. 2008.

[86] R Serraa, M Villania, C Damiania, A Graudenzia, A Colaccib, and SA Kauffmanc. Interacting random boolean networks. 2007.

[87] Hua-Wei Shen, Xue-Qi Cheng, and Bin-Xing Fang. Covariance, correlation matrix, and the multiscale community structure of networks. *Physical Review E*, 82(1):016114, 2010.

[88] Ilya Shmulevich and Stuart A Kauffman. Activities and sensitivities in boolean network models. *Physical review letters*, 93(4):048701, 2004.

[89] Albert Sole-Ribalta, Manlio De Domenico, Nikos E Kouvaris, Albert Diaz-Guilera, Sergio Gomez, and Alex Arenas. Spectral properties of the laplacian of multiplex networks. *Physical Review E*, 88(3):032807, 2013.

[90] Seung-Woo Son, Golnoosh Bizhani, Claire Christensen, Peter Grassberger, and Maya Paczuski. Percolation theory on interdependent networks based on epidemic spreading. *EPL (Europhysics Letters)*, 97(1):16006, 2012.

[91] Michael Szell, Renaud Lambiotte, and Stefan Thurner. Multirelational organization of large-scale social networks in an online world. *Proceedings of the National Academy of Sciences*, 107(31):13636–13641, 2010.

[92] Thomas W Valente. Social network thresholds in the diffusion of innovations. *Social networks*, 18(1):69–89, 1996.

[93] Lois M Verbrugge. Multiplexity in adult friendships. *Social Forces*, 57(4):1286–1309, 1979.

[94] Alessandro Vespignani. Modelling dynamical processes in complex socio-technical systems. *Nature Physics*, 8(1):32–39, 2012.

[95] Stanley Wasserman and Katherine Faust. *Social network analysis: Methods and applications*, volume 8. Cambridge university press, 1994.

[96] Duncan J Watts. A simple model of global cascades on random networks. *Proceedings of the National Academy of Sciences*, 99(9):5766–5771, 2002.

[97] Duncan J Watts and Steven H Strogatz. Collective dynamics of small-worldnetworks. *nature*, 393(6684):440–442, 1998.

[98] Barry Wellman. Physical place and cyberplace: The rise of personalized networking. *International journal of urban and regional research*, 25(2):227–252, 2001.

[99] Barry Wellman and Stephen D Berkowitz. *Social structures: A network approach*, volume 2. CUP Archive, 1988.

[100] Douglas Brent West et al. *Introduction to graph theory*, volume 2. Prentice hall Upper Saddle River, 2001.

[101] H Peyton Young. Innovation diffusion in heterogeneous populations: Contagion, social influence, and social learning. *The American economic review*, pages 1899–1924, 2009.

[102] Bin Zhang and Steve Horvath. A general framework for weighted gene co-expression network analysis. *Statistical applications in genetics and molecular biology*, 4(1), 2005.